15 Tidal Wetlands and Estuaries

Lead Authors

Lisamarie Windham-Myers, U.S. Geological Survey; Wei-Jun Cai, University of Delaware

Contributing Authors

Simone R. Alin, NOAA Pacific Marine Environmental Laboratory; Andreas Andersson, Scripps Institution of Oceanography; Joseph Crosswell, Commonwealth Scientific and Industrial Research Organisation; Kenneth H. Dunton, University of Texas, Austin; Jose Martin Hernandez-Ayon, Autonomous University of Baja California; Maria Herrmann, The Pennsylvania State University; Audra L. Hinson, Texas A&M University; Charles S. Hopkinson, University of Georgia; Jennifer Howard, Conservation International; Xinping Hu, Texas A&M University, Corpus Christi; Sara H. Knox, U.S. Geological Survey; Kevin Kroeger, U.S. Geological Survey; David Lagomasino, University of Maryland; Patrick Megonigal, Smithsonian Environmental Research Center; Raymond G. Najjar, The Pennsylvania State University; May-Linn Paulsen, Scripps Institution of Oceanography; Dorothy Peteet, NASA Goddard Institute for Space Studies; Emily Pidgeon, Conservation International; Karina V. R. Schäfer, Rutgers University; Maria Tzortziou, City University of New York; Zhaohui Aleck Wang, Woods Hole Oceanographic Institution; Elizabeth B. Watson, Drexel University

Acknowledgments

Camille Stagg (Expert Reviewer), U.S. Geological Survey; Raymond G. Najjar (Science Lead), The Pennsylvania State University; Marjorie Friederichs (Review Editor), Virginia Institute of Marine Science; Zhiliang Zhu (Federal Liaison), U.S. Geological Survey. Authors wish to thank their respective funding agencies, including the U.S. Geological Survey LandCarbon Program, NASA Carbon Monitoring System Program (NNH14AY671 for Windham-Myers), and the National Science Foundation Division of Ocean Sciences (OCE 1238212, 1637630, and 1237140 for Hopkinson).

Recommended Citation for Chapter

Windham-Myers, L., W.-J. **Cai**, S. R. Alin, A. Andersson, J. Crosswell, K. H. Dunton, J. M. Hernandez-Ayon, M. Herrmann, A. L. Hinson, C. S. Hopkinson, J. Howard, X. Hu, S. H. Knox, K. Kroeger, D. Lagomasino, P. Megonigal, R. G. Najjar, M.-L. Paulsen, D. Peteet, E. Pidgeon, K. V. R. Schäfer, M. Tzortziou, Z. A. Wang, and E. B. Watson, 2018: Chapter 15: Tidal wetlands and estuaries. In *Second State of the Carbon Cycle Report (SOCCR2): A Sustained Assessment Report* [Cavallaro, N., G. Shrestha, R. Birdsey, M. A. Mayes, R. G. Najjar, S. C. Reed, P. Romero-Lankao, and Z. Zhu (eds.)]. U.S. Global Change Research Program, Washington, DC, USA, pp. 596-648, https://doi.org/10.7930/SOCCR2.2018.Ch15.

KEY FINDINGS

1. The top 1 m of tidal wetland soils and estuarine sediments of North America contains 1,886 ± 1,046 teragrams of carbon (Tg C) (*high confidence, very likely*).
2. Soil carbon accumulation rate (i.e., sediment burial) in North American tidal wetlands is currently 9 ± 5 Tg C per year (*high confidence, likely*), and estuarine carbon burial is 5 ± 3 Tg C per year (*low confidence, likely*).
3. The lateral flux of carbon from tidal wetlands to estuaries is 16 ± 10 Tg C per year for North America (*low confidence, likely*).
4. In North America, tidal wetlands remove 27 ± 13 Tg C per year from the atmosphere, estuaries outgas 10 ± 10 Tg C per year to the atmosphere, and the net uptake by the combined wetland-estuary system is 17 ± 16 Tg C per year (*low confidence, likely*).
5. Research and modeling needs are greatest for understanding responses to accelerated sea level rise; mapping tidal wetland and estuarine extent; and quantifying carbon dioxide and methane exchange with the atmosphere, especially in large, undersampled, and rapidly changing regions (*high confidence, likely*).

Note: Confidence levels are provided as appropriate for quantitative, but not qualitative, Key Findings and statements.

15.1 Introduction

Estuaries and tidal wetlands are dynamic ecosystems that host high biological production and diversity (Bianchi 2006). They receive large amounts of dissolved and particulate carbon and nutrients from rivers and uplands and exchange materials and energy with the ocean. Estuaries and tidal wetlands are often called biogeochemical "reactors" where terrestrial materials are transformed through interactions with the land, ocean, and atmosphere. Work conducted in the past decade has clearly shown that open-water estuaries as a whole can be strong sources of carbon to the atmosphere—both carbon dioxide (CO_2) and methane (CH_4)—despite the fact that how degassing (i.e., gas emissions) rates vary in space and time in many estuaries is unknown (Borges and Abril 2011; Cai 2011). In contrast, tidal wetlands represent a small fraction of the land surface but are among the strongest long-term carbon sinks, per unit area, because of continuous organic carbon accumulation in sediments with rising sea level (Chmura et al., 2003). Estuaries are included here in the *Second State of the Carbon Cycle Report* (SOCCR2) but were not included in the *First State of the Carbon Cycle Report's* (SOCCR1; CCSP 2007) assessment of coastal carbon cycling. Estuaries have been reviewed in recent synthesis activities, particularly the Coastal CARbon Synthesis (CCARS; Benway et al., 2016). Tidal wetlands were included in the wetlands chapter of SOCCR1 but are separated from inland wetlands in this SOCCR2 assessment to reflect their unique connections to estuarine and ocean dynamics. Consistently missing from previous fieldwork and syntheses are important annual carbon exchanges (including CO_2 and CH_4 flux) across boundaries of intertidal (hereafter, wetland) and subtidal ecosystems and deeper waters (hereafter, estuarine). As subsystems of an integrated coastal mixing zone, this lack of information limits understanding of the relative roles of wetlands and estuaries in carbon cycling at the critical land-ocean margin. An updated synthesis of current knowledge and gaps in quantifying the magnitude and direction of carbon fluxes in dynamic estuarine environments is presented herein.

According to Perillo and Picollo (1995) and Pritchard (1967), estuaries are commonly defined as "semi-enclosed coastal bodies of water that extend

to the effective limit of tidal influence, within which seawater entering from one or more free connections with the open sea, or any saline coastal body of water, is significantly diluted with fresh water [sic] derived from land drainage, and can sustain euryhaline biological species from either part or the whole of the life cycle." For the purpose of this report, the landward boundary of estuarine zones is defined as the "head of tide" (i.e., the maximal boundary of tidal expression in surface water elevation) and the shoreward limit of the continental shelf (i.e., the relatively shallow sea that extends to the edge of continental crust). While island coastlines are included in the overall SOCCR2 domain (namely Hawai'i, Puerto Rico, and the Pacific Islands), due to reliance on recent synthesis products for carbon accounting, the focus herein is exclusively on continental coastlines where stocks and fluxes have been quantified and mapped most comprehensively. Section 15.2, this page, provides a brief historical overview of carbon flux in estuaries and tidal wetlands with an emphasis on coastal processes with global applicability. Section 15.3, p. 601, compiles information on carbon fluxes of estuaries and tidal wetlands of North America in the global context and from regional perspectives. Through literature summaries and data syntheses, Section 15.4, p. 609, provides new estimates of selected fluxes and stocks in tidal wetlands and estuaries of North America. Section 15.5, p. 615, discusses new and relevant coastal carbon observations through indicators, trends, and feedbacks, and Section 15.6, p. 619, reports on management and decisions associated with societal drivers and impacts within the carbon cycle context. Finally, Section 15.7, p. 620, provides a synthesis that summarizes conclusions, gaps in knowledge, and near-future outlooks.

15.2 Historical Context, Overview of Carbon Fluxes and Stocks in Tidal Wetlands and Estuaries

Tidal wetlands and estuaries of North America vary in relative area depending on coastal topography, historic rates of sea level rise, and inputs of suspended solids from land. In drowned river valleys (e.g., Chesapeake Bay) and fjords (e.g., Puget Sound) that are topographically steep, estuarine habitat is the dominant subsystem (Dalrymple et al., 1992). In contrast, the ratio of tidal wetland area to estuarine area is relatively high (Day et al., 2013), though still less than one (Najjar et al., 2018) along coastal plains.

The land-sea interface that defines the presence of tidal wetlands and estuaries (i.e., river-sea mixing zones) is itself extremely dynamic over broad spatial and temporal scales. The current configuration of tidal wetlands and estuaries is the result of processes that have been occurring since the last glacial maximum, roughly 18,000 years ago. Over the past 6,000 years, when rates of sea level rise slowed to less than 1 mm per year, tidal wetlands increased in size relative to open-water estuaries, as bay bottoms filled with sediments from uplands and tidal wetlands prograded into shallow open-water regions and transgressed across uplands (see Figure 15.1, p. 599; Redfield 1967). Concomitant with increasing sea levels, tidal wetlands maintained their relative elevation as wetland plants trapped suspended sediments from tidal floodwaters, as well as accumulated organic matter in soils. Factors that affect tidal wetland area and relative elevation, through lateral and vertical erosion and accretion, include 1) rate of sea level rise, 2) land subsidence or isostasy (glacial rebound), 3) delivery and deposition of suspended sediment, 4) balance between wetland gross primary production (GPP) and respiration of all autotrophs and heterotrophs (R_{AH}), 5) sediment compaction, and 6) slope of land at the land-water interface (Cahoon 2006).

Tidal wetlands are among the most productive ecosystems on Earth, continuously accumulating organic carbon that results from environmental conditions that inhibit organic matter decomposition. As a result, intact tidal wetlands are capable of storing vast amounts of *autochthonous* organic carbon (i.e., fixed through photosynthesis on site) as well as intercepting and storing *allochthonous* organic carbon (i.e., produced off site, terrigenous; Canuel et al., 2012). Documented carbon-related

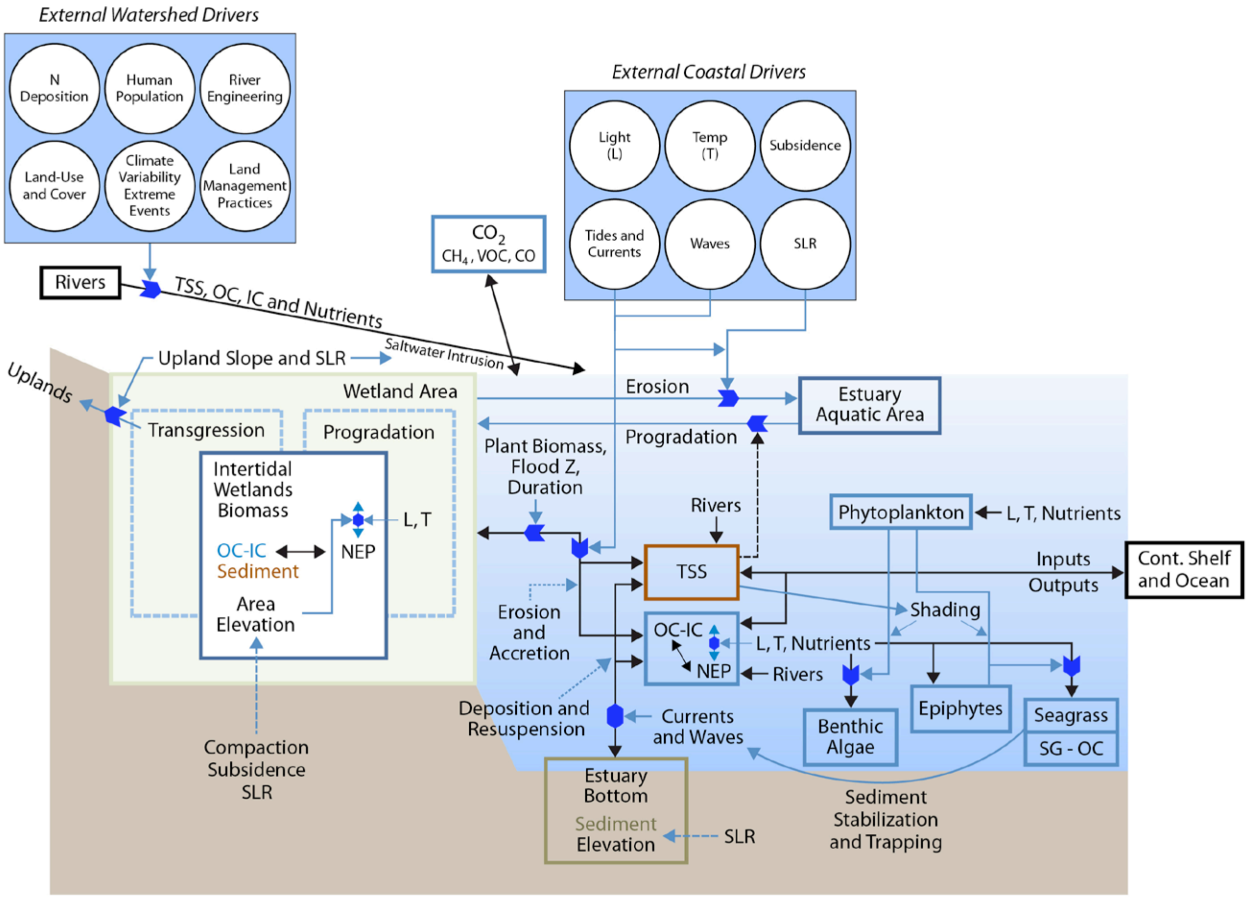

Figure 15.1. Conceptual Model of Coastal Tidal Wetlands and Estuaries and Their Linkages with Adjacent Terrestrial and Oceanic Systems. The drivers, processes, and factors depicted here largely control carbon dynamics in these systems. Net ecosystem production (NEP) is equal to gross primary production minus the sum of heterotrophic and autotropic respiration. [Key: N, nitrogen; CO_2, carbon dioxide; CH_4, methane; VOC, volatile organic compound; CO, carbon monoxide; L, light; T, temperature; TSS, total suspended solids; OC, organic carbon; IC, inorganic carbon; Z, elevation; SG, seagrass; SLR, sea level rise]

ecosystem benefits, referred to as "services," include significant uptake and storage of carbon in wetland soils, as well as export to the ocean of organic matter, which increases the productivity of coastal fisheries (Day et al., 2013). Globally, tidal wetlands are strongly variable in age and structure. Some of today's tidal wetlands have persisted for more than 6,500 years, accumulating to a depth of up to 13 m of tidal peat (Drexler et al., 2009; McKee et al., 2007; Peteet et al., 2006), but some wetlands are young and shallow because of recent human influences that enhanced sediment delivery to nearshore waters. Examples include the colonial-era East Coast (Kirwan et al., 2011) and gold rush in California (Palaima 2012). Because human development is preferentially concentrated on coastlines, tidal wetlands have been subject to active loss through development pressures. While tidal wetland losses have slowed in the United States, global tidal wetland losses are currently estimated at 0.5% to 3% annually (Pendleton et al., 2012), with estimates depending on the ecosystem, time frame, and methods used in evaluation (Hamilton and Casey 2016; Spalding et al., 2010). Loss of carbon stocks through wetland drainage and erosion remains poorly modeled due to limited mapping and quantification of initial carbon stock conditions (Chmura 2013). Further, more subtle rates of wetland loss, through drowning or erosion, may be underestimated by remote-sensing techniques insensitive to small-scale changes observed through aerial photography (e.g., Schepers et al., 2017; Watson et al., 2017).

Estuarine waters are a small but productive fraction of coastal waters (Cloern et al., 2014; Wollast 1991). The role of coastal zones as sinks or sources of atmospheric CO_2 is still poorly understood (Borges 2005; Borges et al., 2005; Smith and Hollibaugh 1997), resulting in a lack of consensus toward their role in global carbon budgets (Cai 2011; Wollast 1991; Borges and Abril 2011; Chen et al., 2013). With poorly characterized boundary conditions, estuarine waters have strong upland and ocean-based drivers, leading to strong seasonality in carbon transport and transformation. Geological records suggest that estuarine carbon storage was enhanced in the past 6,000 years and during recent centuries by watershed activities (Colman et al., 2002), but responses were varied. Human activities initially increased the delivery of organic materials to estuaries (e.g., forest clearing) and thus drove them to support higher net respiration (and likely greater sources of atmospheric CO_2); however, more recent human activities (e.g., dam construction and fertilizer use) have greatly reduced sediment and organic matter delivery but increased nutrient fluxes to many estuaries (Bianchi and Allison 2009; Galloway et al., 2008), driving estuarine waters to be less heterotrophic and, possibly, causing more net carbon burial and export to the ocean (Regnier et al., 2013). While North American estuarine conditions vary along coasts according to upstream land use, the most significant human-induced change to estuarine carbon dynamics over the past century is certainly increased nutrient loading (Schlesinger 2009), which has led to eutrophication and hypoxia in estuaries and continental shelves. Eutrophication promotes carbon uptake and pH increase in surface estuarine waters (Borges and Gypens 2010), but it also may enhance acidification when organic matter fixed by photosynthesis is respired. In stratified estuarine waters, respiration-induced CO_2 and poor buffering capacity could greatly reduce pH and carbonate saturation states to levels much lower than those resulting from the increase of anthropogenic CO_2 in the atmosphere and its subsequent uptake in surface waters (Cai 2011, Cai et al., 2017; Feely et al., 2010). The particularly large pH changes and the difficulty in predicting acidification in estuaries have motivated many scientists to study estuarine acidification in addition to ocean acidification (Duarte et al., 2013).

Estuaries generally have more interannual variability in carbon dynamics than do tidal wetlands, a phenomenon reflecting the balance of exchanges with terrestrial watersheds, tidal wetlands, and the continental shelf (Bauer et al., 2013). Processing of material inputs from land and tidal wetlands determines the autotrophic-heterotrophic balance of the estuary; this processing reflects the biological, chemical, and physical structure of the receiving estuary, as well as the nature of the inputs themselves. The autotrophic-heterotrophic balance of an estuary is especially sensitive to the water residence time (largely a function of freshwater runoff, tidal mixing, and estuarine geometry), the ratio of inputs of organic carbon (primarily from land and tidal wetlands) to inorganic nutrients (primarily from land), the degradability of the organic carbon input (Hopkinson and Vallino 1995; Kemp et al., 1997; Herrmann et al., 2015). The relative abundance of pelagic (i.e., phytoplankton-dominated) versus benthic (i.e., seagrass- or benthic algal–dominated) communities is also a major factor affecting estuarine carbon dynamics. The availability of light is perhaps the major constraint on the distribution of benthic autotrophic communities. Light availability to the benthos depends on estuarine depth and water clarity, which in turn are related to concentrations of suspended solids and phytoplankton in the estuarine water column. In nitrogen-enriched estuarine waters, high-phytoplankton biomass and epiphytic algae decrease light availability to benthic autotrophic communities, sometimes resulting in a complete loss of seagrass habitats (Howarth et al., 2000). In shallow systems, benthic macroalgae often dominate system dynamics. Seagrass, because of its ability to control

wave and current strength, can play a major role in limiting sediment resuspension, thereby maintaining high water clarity (van der Heide et al., 2011). Estuaries typically are heterotrophic and release CO_2 to the atmosphere, largely as a result of their processing of organic carbon inputs from watersheds (Raymond and Bauer 2001) and adjacent tidal wetlands (Bauer et al., 2013; Cai and Wang 1998; Wang and Cai 2004). For example, U.S. Atlantic coastal estuaries as a whole are net heterotrophic (Herrmann et al., 2015); all but three of 42 sites in the U.S. National Estuarine Research Reserve System were net heterotrophic over a year (Caffrey 2004), and a global survey concluded that 66 out of 79 estuaries were net heterotrophic (Borges and Abril 2011). At the same time, estuaries can serve as significant long-term organic carbon sinks through sedimentation of terrestrial inputs and seagrass organic matter burial (Duarte et al., 2005; Hopkinson et al., 2012; McLeod et al., 2011; Nellemann et al., 2009).

15.3 Global, North American, and Regional Context

Similar to the approach used by Benway et al. (2016), this assessment divided the North American coastline into four main subregions (see Figure 15.2, p. 602): the Atlantic Coast (Nova Scotia, Canada, to the southern tip of Florida, United States), the Gulf of Mexico, the Pacific Coast (southernmost Mexico to the Seward Peninsula, United States), and the High-Latitude Coast (the boreal and Arctic coastlines of Alaska and Canada between the Seward Peninsula and Nova Scotia). There are notable differences in carbon cycling among these four major subregions of North America. This section presents a descriptive analysis of those processes by subregion.

15.3.1 Atlantic Coast Estuaries and Tidal Wetlands

Estuaries of the North American Atlantic coast are the most extensive and diverse in structure and function within North America. Relatively shallow and driven primarily by landward influences, they are strongly influenced by freshwater flow and quality from rivers and groundwater. From boreal to subtropical latitudes, a wide range of biotic activity (e.g., photosynthesis and respiration) is seen from Nova Scotia to Florida.

Atlantic Coast Estuaries

South Atlantic Bight. The South Atlantic Bight (SAB: southern tip of Florida to Cape Hatteras, North Carolina) is a passive, western boundary current margin with broad shelf areas, extensive shoals, and a series of barrier islands, behind which are lagoons. Freshwater delivery in the SAB is through rivers that are nearly evenly located along the coast. These rivers carry high loads of dissolved organic carbon (DOC). Because of short transit times through the estuaries, much of the DOC is discharged onto the shelf, supporting respiration, net heterotrophy (Hopkinson 1985, 1988), and CO_2 degassing on the inner-shelf regions (Jiang et al., 2013). Much is known about the export of organic matter from SAB watersheds. The SAB salt marshes are tremendous sinks of CO_2 and organic carbon from uplands, whereas the estuarine waters are strong sources of CO_2 to the atmosphere—sources that are largely supported by organic matter and dissolved inorganic matter (DIC) export from both wetland saltmarshes and from SAB watersheds (Wang and Cai 2004; Cai 2011; Herrmann et al., 2015; Hopkinson 1988).

Mid-Atlantic Bight and Gulf of Maine. The Mid-Atlantic Bight (MAB: Cape Hatteras, North Carolina, to Cape Cod, Massachusetts) and Gulf of Maine (GOM: Cape Cod to Nova Scotia) are characterized by large estuaries. Inorganic carbon from carbonate weathering and organic matter remineralization accounts for the majority of riverine carbon input to the MAB (Hossler and Bauer 2013; Moosdorf et al., 2011). Generally, aqueous organic matter concentrations are higher in southern MAB rivers and can be more than half the riverine carbon load to estuaries (Stets and Striegl 2012; Tian et al., 2015). Lateral exchange with wetlands is an important carbon input to MAB waters and has been linked to net heterotrophy and air-water CO_2 efflux in narrow, marsh-dominated subestuaries (Baumann et al., 2015; Raymond et al., 2000; Wang

Figure 15.2. Map of the Main Coastal Regions and Associated Drainage Basins of North America. In this chapter, the North American coastline is broken up into four main regions: Atlantic Coast, Gulf of Mexico, Pacific Coast (including the Sea of Cortez, Gulf of Alaska, and Bering Sea), and High Latitudes (including the Chukchi Sea, Beaufort Sea, Hudson Bay, Labrador Sea, and Gulf of Saint Lawrence). [Figure source: Redrawn from U.S. Department of Interior]

et al., 2016). However, larger MAB estuaries can be seasonal or annual sinks for atmospheric CO_2 because of stratification and high rates of internal production (Crosswell et al., 2014; Joesoef et al., 2015). Supporting this result, recent carbon budget studies have estimated that MAB estuaries are near metabolic balance and that total organic carbon (TOC) export to the coastal ocean is about equal to riverine TOC input (Herrmann et al., 2015; Crosswell et al., 2017). The GOM shares many of these traits, but its TOC input is low due to its small catchment area (Najjar et al., 2018).

Atlantic Coast Tidal Wetlands

Despite some similarity in vegetation community composition (e.g., estuarine emergent *Spartina* spp., dominant in saline habitats), Atlantic coast tidal marshes are extensive and topographically varied in structure, from the more patchy, organic-rich GOM and MAB soils to the extensive, mineral-rich plains of the SAB. Biomass stocks of the dominant plant species, *Spartina alterniflora,* show a decrease with latitude (Kirwan et al., 2009), with the notably productive SAB marshes (Gallagher et al., 1980; Schubauer and Hopkinson 1984) exporting large amounts of marsh grass–derived organic matter and CO_2 into the estuaries and nearshore ocean where respiration and degassing occur (Jiang et al., 2008; Wang and Cai 2004). Soil carbon burial is not commensurate with productivity, as increased organic matter decomposition (Kirwan and Blum 2011) may negate any latitudinal productivity gradients. More important than latitudinal patterns for carbon flux accounting are within-watershed patterns of marsh elevation (i.e., low marsh versus high marsh), tidal range (e.g., microtidal eastern Florida versus extreme macrotidal Bay of Fundy), and salinity regimes. Freshwater tidal wetlands (both marsh and forest) make up 21% of tidal wetlands of the eastern United States (Hinson et al., 2017). Localized hotspots for soil carbon stock change also occur along the East Coast because of physical drivers such as sea level rise (Sallenger et al., 2012) and storm-induced erosion (Cahoon 2006). Estimated net ecosystem exchange (NEE) of atmospheric CO_2 from chamber and eddy covariance systems illustrates that vertical fluxes dominate carbon inputs to many East Coast tidal wetlands (Forbrich and Giblin 2015; Kathilankal et al., 2008). Much of this NEE is exported to ocean subsystems in particulate and dissolved forms, with lateral exports of DIC and DOC fluxes representing as much as 80% of annual carbon inputs (Wang and Cai 2004; Wang et al., 2016). Further, the role of groundwater flows in driving carbon fluxes, as well as nutrient fluxes that alter estuarine processes, is varied and poorly understood (Kroeger and Charette 2008; Moore 1996).

15.3.2 Gulf of Mexico Estuaries and Tidal Wetlands

Variability of Gulf of Mexico (GMx) estuaries is due, in part, to the variable forcing at their boundaries, including groundwater (dominating the Mexican coastline), rivers (dominating the U.S. coastline), wind, bathymetry, and ocean currents (e.g., the Loop Current). Gulf of Mexico tidal wetlands share many species but notably are experiencing enhanced mangrove encroachment and land subsidence.

Gulf of Mexico Estuaries

Estuarine GMx environments are microtidal with winds and river flows exerting strong control on water levels. On the extensive subtidal carbonate benthos, extensive seagrass meadows (e.g., *Thalassia*) persist and are known to recover rapidly from disturbance (e.g., Thorhaug et al., 2017). There is a paucity of data on air-water CO_2 flux in GMx estuaries. However, the lower-river portion of the two largest rivers, the Mississippi and the Atchafalaya, are strong sources of CO_2 to the atmosphere because the partial pressure of CO_2 (pCO_2) ranges from about 1,000 microatmospheres (μatm: a unit of pressure defined as 101,325 Pascals or 1.01325 bar) in winter to about 2,200 μatm in summer, but some large bays (e.g., Terrebonne Bay) have substantially lower pCO_2 (Huang et al., 2015). In comparison, despite relatively low pCO_2 (about 500 μatm), a semi-arid lagoonal estuary in northwestern GMx has a CO_2 efflux of 149 ± 40 grams of carbon (g C) per m^2 per year due to windy conditions all year

long (Yao and Hu 2017), an amount comparable to other lagoonal estuaries in the world (Laruelle et al., 2014). A strong climatic gradient from northeast to southwest along the northwestern GMx coast leads to riverine freshwater export decreasing by a factor of two (Montagna et al., 2009), with large interannual variability. This hydrological variability exerts strong control on estuarine CO_2 fluxes in this region.

Gulf of Mexico Tidal Wetlands

As of 2017, 52% of conterminous U.S. tidal wetlands are located within GMx, with Louisiana alone containing 40% of all the saltwater wetlands in the United States (Dahl 2011; Edwards and Proffitt 2003). While the GMx U.S. coastline is dominated by emergent marsh vegetation and the Mexican coastline is dominated by mangrove vegetation (see Table 15.1, this page), a wide range of salinity and geomorphic conditions promote structural diversity throughout GMx from tidal freshwater forests to floating peatlands to brackish and saline marshes. For the past two decades, other coastlines have been relatively stable in their tidal wetland extent but GMx is experiencing rapid transitions. Though there is active delta building at the Atchafalaya River outflow, tidal wetland conversion to open water (i.e., wetland loss) is common in GMx as a result of land subsidence, coastal storms, sea level rise, nutrient enrichment, and a lack of sediment delivery to compensate for ongoing compaction. The fate of wetland soil carbon following erosion or conversion to open water is poorly understood but important for conducting carbon accounting, particularly in GMx (DeLaune and White 2011; Lane et al., 2016). Climate shifts are also accelerating changes in wetland cover (Gabler et al., 2017), including mangrove encroachment on salt marshes in Texas, Louisiana, and Florida (Krauss et al., 2011; Saintilan et al., 2014).

Table 15.1. Average Values for Ecosystem Extent (km^2) by Coast (Atlantic, Pacific, Gulf of Mexico, and Arctic) for North America[a] (Includes Combined Mapped Data for Canada, Mexico, and the United States)

Coast	Tidal Freshwater Marsh	Tidal Freshwater Forest	Tidal Brackish and Saline Marsh	Tidal Brackish and Saline Forest	Total Tidal Wetland	Seagrass	Estuarine[b]
Atlantic Coast	539	1,916	7,958	768	11,181	11,889	34,000
Gulf of Mexico	1,612	1,153	9,847	9,899	22,511	20,260	31,900
Pacific Coast	83	188	510	2,642	3,423	1,148	49,000
High Latitudes	ND[c]	ND	1,494	NA[c]	1,494[d]	1,050	238,800
CONUS	2,234	3,257	18,162	3,165	26,818	23,630	75,040
Alaska	ND	ND	948	NA	948[d]	405	ND
Canada	ND	ND	546	NA	546[d]	645	ND
Mexico	ND	ND	153	10,144	10,297[d]	9,667	ND
North America	2,234[d]	3,257[d]	19,809	13,309[d]	38,609[d]	34,347	353,700

Notes

a) Geospatial data sources: CEC 2016; Laruelle et al., 2013; USFWS NWI 2017.

b) All estimates based on MARgins and CATchments Segmentation (MARCATS) data of Laruelle et al. (2013), except the conterminous United States (CONUS), which is from Bricker et al. (2007). Corresponding MARCATS segment numbers are 10 for the Atlantic Coast; 9 for the Gulf of Mexico; 1, 2, and 3 for the Pacific Coast; and 11, 12, and 13 for High Latitudes.

c) ND = no data, NA = not applicable.

d) Indicates missing data from at least one coastal subregion.

Mangroves extend all the way around GMx, with 80% of the total distribution of North American mangroves on the Mexican coastline (50% of which grow on the Campeche, Yucatán, and Quintana Roo coasts). Mangrove carbon sequestration rates can range from 0 to 1,000 g C per m^2 per year, primarily a result of biomass responses to disturbance status and hydrogeomorphic characteristics of the landscape setting (Adame et al., 2013; Breithaupt et al., 2014; Ezcurra et al., 2016; Marchio et al., 2016). Regular tidal flushing and allochthonous input from river and marine sediments generally provide more favorable conditions for above- and belowground productivity. The belowground components of mangrove forests, such as coarse woody debris, soil, and pneumatophores (i.e., aerial roots), can contribute between 45% and 65% of the total ecosystem respiration (Troxler et al., 2015). Mangroves are similar to all tidal wetlands in that soil carbon pools dominate ecosystem carbon stocks, and carbon burial is an important long-term fate of fixed carbon. For example, despite their short stature, dwarf mangroves may generate greater annual increases in belowground carbon pools than might taller mangroves (Adame et al., 2013; Osland et al., 2012).

Coupled stressors from both human and natural drivers, such as groundwater extraction and sea level rise, currently are altering subtropical tidal wetlands. Soil organic carbon (SOC) stocks face increased rates of mineralization and peat collapse with saline intrusion (Neubauer et al., 2013). Still, total carbon stocks may increase as a result of trends in mangrove expansion into salt marsh habitat (Cavanaugh et al., 2014; Doughty et al., 2015; Krauss et al., 2011; Bianchi et al., 2013). This pattern of expansion is expected to continue with current trends in climate change (e.g., the changes in frequency and intensity of hurricanes and freeze events) and with increasing rates of sea level rise (Barr et al., 2012; Lagomasino et al., 2014; Meeder and Parkinson 2017; Dessu et al., 2018). Dwarf and basin mangroves, which generally have shorter canopies, are most affected by freezing temperatures, while hurricane damage has the strongest impact on fringing mangrove forests along the coasts (Zhang et al., 2016). Freeze and cold events drive the poleward advancement of mangroves along the eastern coast of Florida and GMx (Cavanaugh et al., 2014; Giri et al., 2011; Saintilan et al., 2014). Though mangroves in these regions may not currently extend past their historical range limits (Giri and Long 2014), the expansion and contraction of the mangrove forest clearly is documented in field and remotely sensed map products.

15.3.3 Pacific Coast Estuaries and Tidal Wetlands

The Pacific (west) coast of North America is seismically active with subduction zones that create steep topography and narrow continental shelves. As such, seasonal coastal winds drive upwelling and downwelling events that can shape biogeochemical cycling along the Pacific continental margin in estuarine waters and tidal wetlands. A more descriptive approach herein reflects the limited representation of Pacific Coast information presented in Appendix 15A, p. 642, as compared with that for the Atlantic and GMx coastlines.

Pacific Coast Estuaries

Estuaries of the Pacific Coast differ from other North American estuaries in that their carbon cycle dynamics tend to be dominated by ocean-sourced rather than river-borne drivers, predisposing many Pacific Coast estuaries and coastal environments to hypoxia and acidified conditions, largely as a result of natural processes (e.g., Chan et al., 2016, 2017; Feely et al., 2010, 2012; Hales et al., 2016). From the Gulf of Alaska south through Puget Sound, glacially formed estuaries have sills that restrict circulation between estuaries and coastal waters, further predisposing deep estuarine waters to hypoxic or anoxic conditions that form in the deep water of these estuaries. Interannual-to-decadal, basin-scale, ocean-climate oscillations such as the Pacific Decadal Oscillation and El Niño Southern Oscillation drive variations in rainfall along the Pacific Coast, which, in turn, controls material export from land to estuaries and subsequently to the coastal ocean. These oscillating climate drivers, as well as stochastic events such as large marine heatwaves, drive interannual variability in physical and biogeochemical dynamics along the Pacific Coast, with significant effects on estuarine carbon cycle and ecosystem processes (Di Lorenzo and Mantua 2016).

Within spatially large marine ecosystems (LMEs) on the Pacific Coast—Gulf of Alaska, California Current, Gulf of California, and Pacific Central-American Coastal LMEs (lme.noaa.gov)—estuaries represent either globally significant large river systems, such as the Fraser, Columbia, San Joaquin/Sacramento, and Colorado rivers or one of many "small mountainous rivers" (SMRs) with steep watershed terrain and limited continental shelves for delta development. From the Southern California Bight (SCB) south to Panama, lagoons also represent a significant fraction of the semi-enclosed, saline-to-brackish water bodies along the Pacific Coast. Lagoons typically have episodic connection to adjacent coastal ocean areas and lack substantial freshwater input, distinguishing them from estuaries. However, despite the strong along-coast gradients in rainfall and terrestrial input to Pacific Coast lagoons and estuaries, oceanic sources of nutrients and carbon, particularly those delivered via upwelling, play an important or dominant role in carbon cycle dynamics in all systems studied (Camacho-Ibar et al., 2003; Davis et al., 2014; Hernández-Ayón et al., 2007; Steinberg et al., 2010).

Terrestrial inputs to Pacific Coast estuaries vary substantially along the steep rainfall gradient from very wet conditions in the north to arid conditions in southern and Baja California, with precipitation increasing again from central Mexico through Panama. The Global NEWS 2 model estimated terrestrial TOC inputs are approximately 8.5 teragrams of carbon (Tg C) per year to the Gulf of Alaska through northern California, 0.7 Tg C per year to southern and Baja California and the Gulf of California, and 2.8 Tg C per year to Mexico south of Baja California and Central America (Mayorga et al., 2010). The SMRs representing a significant portion of these inputs are similar to the Mississippi River in delivering their freshwater, nutrient, and organic carbon loads directly to the coastal ocean or larger estuarine water bodies such as Puget Sound or the Strait of Georgia (Johannessen et al., 2003; Wheatcroft et al., 2010).

Phytoplankton productivity estimates across Pacific Coast estuaries from San Francisco Bay to British Columbia reflect an order of magnitude variation in median annual primary production rates, from about 50 g C per m^2 per year in the Columbia River estuary to 455 to 609 g C per m^2 per year in the Indian Arm fjord near Vancouver, British Columbia (Cloern et al., 2014). The role of riverborne nutrients is exemplified by the total water column primary production estimate for the Columbia River estuary at 0.030 Tg C per year (Lara-Lara et al., 1990). An air-sea CO_2 exchange study on the Columbia River estuary estimated that the net annual emission is quite small at 12 g C per m^2 per year (Evans et al., 2012). SCB estuaries are also highly productive but most likely act as sources of CO_2 to the atmosphere and net exporters of dissolved inorganic and organic carbon to the coastal ocean owing to input and decomposition of allochthonous carbon from surrounding land areas. All recent studies from lagoons and estuaries in the San Diego area report estuarine pCO_2 levels consistently greater than atmospheric levels (Davidson 2015; Paulsen et al., 2017; see also Southern California Coastal Ocean Observing System: sccoos.org/data/oa). Carbon cycling in lagoons with little or no riverine input is likely to be dominated by upwelling, as in San Quintín Bay, Baja California. Most of San Quintín Bay (85%) acts as a source of CO_2 to the atmosphere (131 g C per m^2 per year) due to the inflow and outgassing of CO_2-rich upwelled waters from the adjacent ocean. The remaining 15%, composed of *Zostera marina* seagrass beds, shows net uptake of CO_2 and bicarbonate (HCO_3^-), with pCO_2 below atmospheric equilibrium, resulting in a net CO_2 sink of 26 g C per m^2 per year (Camacho-Ibar et al., 2003; Hernández-Ayón et al., 2007; Munoz-Anderson et al., 2015; Reimer et al., 2013; Ribas-Ribas et al., 2011). Whereas this Mediterranean climate bay was net autotrophic during the upwelling season in previous decades, it now appears to be net heterotrophic due to import of labile phytoplanktonic carbon generated in the

adjacent ocean during upwelling (Camacho-Ibar et al., 2003). This transition illustrates the potential sensitivity of estuarine, bay, and lagoonal net ecosystem production (NEP) to changes in upwelling intensity and persistence, highlighting the vulnerability to effects of ocean warming or changing coastal stratification on ecosystem metabolism and carbon balance.

Lateral transfers of carbon from estuaries to the coastal ocean are poorly constrained by observations because of the difficulty and expense of making sufficient direct observations to measure this important lateral transfer. Many gaps remain in the understanding of the carbon cycle of Pacific Coast estuaries and lagoons, despite sporadic observations over the last several decades. For example, no systematic information on carbon burial is available and seagrass extent is likely undermapped (CEC 2016). With few exceptions, long-term monitoring time series are inadequate to track changes in terrestrial carbon inputs, primary production, air-sea CO_2 exchange, carbon burial in sediments, and carbon transfers to the coastal ocean that can be expected to result from climate and human-caused environmental changes (Boyer et al., 2006; Canuel et al., 2012). Implementing long-term observations of carbon, oxygen, and nutrient biogeochemistry, along with metrics of ecological response and health, in Pacific Coast estuaries is a priority (Alin et al., 2015).

Pacific Coast Tidal Wetlands

The Pacific Coast is dominated by rocky headlands, broad sand dune complexes, sand beaches, and spits (i.e., sandbars). The area of Pacific Coast tidal wetlands is roughly 628 km^2 in the United States (NOAA 2015) and at least 2,522 km^2 in Mexico, predominantly as mangroves (Valderrama-Landeros et al., 2017), perhaps more if shallow water habitats are included (Contreras-Espinosa and Warner 2004). While small but iconic "low-flow" estuaries are distributed sparsely along the coast (e.g., Elkhorn Slough and Tomales Bay), areas of expansive estuarine wetlands are limited to the larger coastal estuaries, where major rivers enter the sea and where embayments are sheltered by sandbars or headlands (e.g., Coos Bay, Humboldt Bay, and San Diego Bay). San Francisco Bay, which supports the largest extent of coastal wetlands along the Pacific Coast of North America, is a tectonic estuary—a down-dropped graben (i.e., trench) located between parallel north-south trending faults. In Mexico, coastal wetlands are found in association with large barrier-island lagoon complexes where wave energy is reduced by headlands, offshore islands, or the Baja California peninsula, as well as along the Gulf of Tehuantepec, where the continental shelf widens and the winds are intense and offshore (northerly), originating in the Gulf of Campeche across the Isthmus of Tehuantepec. Assuming that published studies of soil carbon accumulation (79 to 300 g C per m^2 per year (Ezcurra et al., 2016) are broadly representative of U.S. and Mexico coastlines, average estimates of soil carbon sequestration by Pacific estuarine wetlands sum to 0.05 Tg C per year for the United States and 2.67 Tg C per year for Mexico.

Although U.S. Atlantic and GMx coastlines are known to support more organic-rich sediments, rates of carbon burial in tidal wetlands on the Pacific Coast tend to be commensurately high due to high rates of volume gain through sediment accretion. Previous studies have reported accretion rates of 0.20 to 1.7 cm per year in natural marshes along the Pacific Coast of North America (Callaway et al., 2012; Thom 1992; Watson 2004), with many values at the higher end of this range. High rates of sediment accretion are a function of the active Pacific Coast margin, because Pacific coastal watersheds tend to have high relief and support elevated erosion rates while providing limited opportunity for deposition of sediments along lowland floodplains (Walling and Webb 1983). This circumstance leads to high water column–suspended sediment concentrations, often exacerbated by anthropogenic land-use activities, such as agriculture, grazing, logging, and development (Meybeck 2003). Although not ubiquitous due to landscape changes (e.g., Skagit River), high rates of sediment accretion are common and known to promote high carbon burial rates when allochthonous organic carbon derived from upland sources is a sediment constituent

(Ember et al., 1987). Additionally, organic carbon produced *in situ* is more quickly buried in the sediment anoxic zone in high-accumulation environments (Watson 2004).

15.3.4 High-Latitude (Alaskan, Canadian, and Arctic) Estuaries and Tidal Wetlands

High-latitude estuaries (boreal and Arctic) are the youngest estuaries (<1,000 years) but the most subject to coastal erosion and hydrological carbon export from thawing permafrost during the current warming climate. Terrigenous inputs of silt and organic carbon are estimated as dominant sources of carbon flux, but inadequate mapping and measurements limit current estimates of carbon fluxes in high-latitude estuaries and tidal wetlands.

High-Latitude (Arctic) Estuaries

Salinity gradients are a defining feature of the estuarine zones of the Arctic Ocean (McClelland et al., 2012). Further, nearshore ice conditions are changing, erosion of coastlines is increasing, and the duration and intensity of estuarine and ocean acidification events are increasing (Fabry et al., 2009), as also discussed in Ch. 16: Coastal Ocean and Continental Shelves and Ch. 17: Biogeochemical Effects of Rising Atmospheric Carbon Dioxide. Lagoons in the Alaskan Beaufort Sea, bounded by barrier islands to the north and Alaska's Arctic slope to the south, span over 50% of the coast. These lagoons link marine and terrestrial ecosystems and support productive biological communities that provide valuable habitat and feeding grounds for many ecologically and culturally important species. Beaufort Sea lagoons are icebound for approximately 9 months of the year; therefore, the brief summer open-water period is an especially important time for resident animals to build energy reserves (i.e., necessary for spawning and surviving winter months) and for migratory animals to feed in preparation for fall migrations. Recent dramatic declines in ice extent have allowed wave heights to reach unprecedented levels as fetch has increased (AMAP 2011).

These studies highlight the climate linkages along coastal margins of the Arctic, especially how changes in sea ice extent can affect terrestrial processes (Bhatt et al., 2010), controlling coastal erosion and the transport of carbon, water, and nutrients to nearshore estuarine environments (Pickart et al., 2013). Nearshore estuarine environments in the Arctic are critical to a vibrant coastal fishery (von Biela et al., 2012) and also serve as habitat for hundreds of thousands of birds representing over 157 species that breed and raise their young over the short summer period (Brown 2006).

High-Latitude (Arctic) Tidal Wetlands

High-latitude ecosystem carbon flux measurements tend to focus on abundant inland peatlands (see Ch. 11: Arctic and Boreal Carbon, p. 428, and Ch. 13: Terrestrial Wetlands, p. 507), and thus less is known about Arctic and subarctic tidal marshes. However, due to high sedimentation rates, Arctic estuarine wetlands are estimated to sequester carbon at rates up to tenfold higher per area than many other wetlands (Bridgham et al., 2006). In a North American survey of published literature, Chmura et al. (2003) accounted for soil carbon stock only to 50 cm in depth, but some brackish marshes, especially in seismically active regions, have much deeper organic sediments. The Hudson Bay Lowlands tidal marshes are a notably understudied region where soil carbon stocks in the nontidal component alone are estimated to contain 20% of the entire North American soil carbon pool (Packalen et al., 2014). Gulf of Alaska marshes are relatively low salinity or freshwater dominated due to the excess of precipitation over evapotranspiration of the Pacific Northwest, as well as the substantial glacial meltwater that characterizes the region. Still, the large impact of melting glaciers, including the Bering and Malaspina piedmont glaciers (each approximating the size of Rhode Island), is expected to contribute to sea level rise locally, as will thawing river deltas, such as the Yukon-Kuskokwim Delta, that are characterized by discontinuous permafrost.

One of the most important coastal Alaskan marsh systems is the Copper River Delta, a critical habitat

for migratory birds along the Pacific Flyway, which extends for more than 75 km and inland as much as 20 km in some places along the Gulf of Alaska (Thilenius 1990). Although carbon storage estimates in these marsh locations are lacking, extensive research on the uplifted (and buried) peats by Plafker (1965) indicate alternating events of extreme subsidence and uplift (i.e., yo-yo tectonics). For example, the 1964 earthquake raised the entire delta from 1.8 to 3.4 m (Reimnitz 1966). Current studies on peat cores reveal marsh vegetation interspersed with intertidal muds, freshwater coastal forest, and moss peat, which extends to depths greater than 7 m (Plafker 1965). Whereas geological drivers clearly are the primary control on carbon storage in these marshes, the dynamic relationship with vegetation illustrates biological feedbacks as well (e.g., nutrient redistribution; Marsh et al., 2000). Highly dynamic sedge- and rush-dominated marshes are notably resilient to extensive sediment deposition from the Copper River, further ensuring growth of willows and shrubs and contributing to the woody component of buried peats. Whether the areal extent of these wetlands will expand or decline with tectonic impact and regional sea level rise is not known.

15.4 Carbon Fluxes and Stocks in Tidal Wetlands and Estuaries of North America

Literature summaries and data compilations discussed in this section enable estimates to be made of carbon stocks and fluxes in North American tidal wetlands and estuaries. Accuracy in quantifying stocks and fluxes in tidal wetlands and estuaries is a function of the accuracy in estimated area (extent) and in estimated stocks and fluxes per unit area. For North America, estimates involve areas, sediment carbon stocks, and the following fluxes: the net change in the carbon stock of tidal wetland soils, tidal wetland exchange of CO_2 with the atmosphere (i.e., NEE), tidal wetland exchange of CH_4 with the atmosphere, tidal wetland carbon burial, lateral exchange of carbon between tidal wetlands and estuaries, and estuarine outgassing of CO_2. Additionally, because the conterminous United States (CONUS) contains a more robust estuarine dataset of most stocks and fluxes, a separate analysis is presented for this region that includes estimates of estuarine NEP, burial, and export of organic carbon to shelf waters.

15.4.1 Tidal Wetland and Estuarine Extent

A synthesis of recent compilation efforts is used to estimate the areas of tidal wetlands and estuaries, and the accuracy of these estimates varies among countries of North America (see Table 15.1, p. 604). In CONUS, a tidal wetland distribution is estimated using the full salinity spectrum of tidal wetland habitats mapped by the U.S. Fish and Wildlife Service National Wetlands Inventory (USFWS NWI; Hinson et al., 2017). However, in Mexico and Canada, only saline wetlands are available at a national scale, as mapped by the Commission for Environmental Cooperation (CEC; CEC 2016). Hence, tidal wetland areas in Mexico and Canada are likely underestimated. Estimates for the estuarine area of North America use a global segmentation of the coastal zone and associated watersheds known as MARCATS (MARgins and CATchments Segmentation; Laruelle et al., 2013). The MARCATS product is available globally at a resolution of 0.5 degrees and delineates a total of 45 coastal regions, or MARCATS segments, eight of which are in North America. Some CONUS-only applications use estuarine areas from the National Estuarine Eutrophication Assessment survey (Bricker et al., 2007), which is based on geospatial data from the National Oceanic and Atmospheric Administration (NOAA) Coastal Assessment Framework (NOAA 1985). The Coastal Assessment Framework includes a high-resolution delineation of the U.S. coastline in this area and delineates 115 individual estuarine subsystems. Seagrasses are considered separately because of their distinct sediment carbon stocks, even though they overlap in area with estuaries. Seagrass area across North America is estimated according to CEC (2016), using web-available map layers.

Table 15.1, p. 604, reveals the relative areas of tidal wetlands, estuaries, and seagrasses of North America, in addition to how these ecosystems are distributed by subregion and country. Estuaries of

North America cover about 10 times the area of tidal wetlands. About half the tidal wetlands of North America are salt marsh, a third are mangrove, and the remainder is split roughly between tidal fresh marsh and tidal fresh forest. The high-latitude region is characterized by a large estuarine area, about 60% of North America's total estuarine area, but has only a few percent of the continent's tidal wetland area and seagrass area. The Gulf of Mexico (GMx), on the other hand, is home to most of North America's tidal wetlands and seagrasses, with 58% of each. The Atlantic Coast and GMx each have about 10% of the total estuarine area, and the Atlantic coast has about half the tidal wetland area and seagrass area of GMx. The Pacific Coast is similar to the high-latitude subregion with a relatively small area of tidal wetlands and seagrasses (although these areas may be undermapped), and it has an estuarine area about 50% greater than that of GMx. Tidal wetlands of North America reside mainly in CONUS (as salt marsh) and Mexico (as mangroves). Similarly, seagrasses are found mainly in coastal waters of CONUS and Mexico. Estuarine area is not available by country, except for CONUS, which is estimated to have 21% of North America's total estuarine area.

15.4.2 Tidal Wetland and Estuarine Stocks

Estimates of tidal wetland and estuarine carbon stock in the upper 1 m of sediment or soil were made by using estimates of the carbon density (mass carbon per unit volume) from large synthetic datasets. Cross-site comparisons of soil carbon stocks in tidal wetlands illustrate very little range in carbon densities in North America both downcore and among tidal wetlands of varied salinity, vegetation structure, and soil types. Hence, for all tidal wetlands except GMx mangroves, a single estimate of carbon density, 27.0 ± 13 kg organic carbon per m^3, was used based on a comprehensive review of the literature (Chmura 2013; Holmquist et al., 2018a; Morris et al., 2016; Nahlik and Fennessy 2016; Ouyang and Lee 2014). For mangroves in GMx, a value of 31.8 ± 1.3 kg organic carbon per m^3 was used (Sanderman et al., 2018). A review of seagrass SOC densities (CEC 2017; Fourqurean et al., 2012; Kennedy et al., 2010; Thorhaug et al., 2017) revealed more variance within and between regions, with some notably high soil carbon densities in GMx. Best estimates (and ranges) of 2.0 ± 1.3 kg organic carbon per m^3 were used for the Atlantic Coast and high-latitude subregions, 3.1 ± 2.4 kg organic carbon per m^3 for GMx, and 1.4 ± 1.2 kg organic carbon per m^3 for the Pacific Coast. For organic carbon density in estuarine sediments, a carbon density of 1.0 ± 1.2 kg organic carbon per m^3 was used based on a mean value of organic carbon mass fraction (0.4% organic carbon in waters shallower than 50 m; Premuzic et al., 1982; Kennedy et al., 2010) and a dry bulk density average of 2.6 g per cm^3 from Muller and Suess (1979). The assumed carbon densities and areas led to carbon stocks in the upper 1 m of 1,410, 354, and 122 Tg C for tidal wetlands, estuaries, and seagrasses, respectively, with a total carbon stock of 1,886 ± 1,046 Tg C.

Net Change in Tidal Wetland Soil Carbon Stock

An estimate of tidal wetland carbon stock loss could only be made using the loss rate for saltwater wetlands in CONUS, as loss rates in other parts of North America and for tidal fresh wetlands are not available. However, CONUS saltwater wetlands make up the overwhelming majority of North American tidal wetlands (see Table 15.1, p. 604), so applying the CONUS saltwater wetland loss rate to all North American tidal wetlands is not unreasonable. The use of a loss rate of CONUS vegetated saltwater wetlands of 0.18% per year between 1996 and 2010 (Couvillion et al., 2017) and estimated mass of carbon in the upper meter of tidal wetland soils (i.e., 1,362 Tg C) resulted in an overall annualized loss rate of 2.4 Tg C per year. For CONUS only, which holds 1,019 Tg C, the loss rate is 1.8 Tg C per year. Expert judgement assigned 100% errors to these losses because they are deeply uncertain due to annualized episodic events (e.g., Couvillion et al., 2017), difficulty in mapping loss, and difficulty in assessing the rate and fate of carbon from disturbed tidal wetlands (Ward et al., 2017; Lane et al., 2016).

15.4.3 Tidal Wetland and Estuarine Fluxes

Tidal Wetland Net Ecosystem Exchange

Presented in Table 15A.1, p. 642, are annual estimates of NEE in North America based on

continuous measurements, focusing primarily on eddy covariance approaches and high-frequency datasets from static chamber deployments to reduce uncertainty. A total of 16 sites were compiled, including restored wetlands, all of which are in CONUS and mostly along the Atlantic Coast. This limited dataset indicates that NEE varies greatly within and among sites, ranging from the highest annual uptakes in a mangrove ecosystem (–1,200 g C per m^2 per year) to the greatest annual losses in a mudflat (1,000 g C per m^2 per year) and in a sequence of tidal marshes in Alabama (400 to 900 g C per m^2 per year; Wilson et al., 2015). Excluding the restored sites and mudflats from the Hudson-Raritan estuary in New Jersey, as well as the static chamber data from Alabama, the mean NEE at the continuously monitored sites (n = 11 of 16) was negative, indicating uptake of atmospheric CO_2 by tidal wetlands. Comparing annual values from the 11 sites (comprising 22 annual datasets) yields coast-specific estimates of NEE: –133 ± 148 g C per m^2 per year on the Pacific (one site, 3 years), –231 ± 79 g C per m^2 per year on the Atlantic (seven sites, 1 to 3 years), and –724 ± 367 g C per m^2 per year in GMx (three sites, 1 to 5 years). Integrating these estimates by area of tidal wetlands on each of North America's three coasts, the NEE estimate is –27 ± 13 Tg C per year. For CONUS only, NEE is –19 ± 10 Tg C per year.

Tidal Wetland Carbon Burial

Rates of carbon burial in wetland soils and sediments are associated with specific temporal scales depending on calculation methods. Typically, carbon burial is calculated as the product of *soil carbon density* (i.e., the mass of carbon stored in soil per unit volume) multiplied by *accretion rate* (i.e., the vertical rate of soil accrual and thus change in volume), which is measured by a variety of dating techniques that span multiple time frames (e.g., marker horizons; radioactive isotopes including those of cesium (^{137}Cs), lead (^{210}Pb), and carbon (^{14}C); pollution chronologies; and pollen stratigraphy). Carbon burial is thus a rate of carbon accumulation in tidal wetland soils over a specific time period (typical units are g C per m^2 per year). This measure integrates all carbon pools present, both "old" and "new," and both autochthonous and allochthonous sources.

Table 15.2 lists carbon burial estimates for salt marshes summarized by Ouyang and Lee (2014), excluding short-term accretion cores (e.g., marker horizons). Identified were 125 cores in North America, about half of which are along the Atlantic Coast and the rest roughly spread evenly among the three other subregions. Mean carbon burial estimates vary considerably among the four subregions, with the lowest rates along the Atlantic Coast, intermediate rates along the Pacific Coast, and the highest rates in the high-latitude subregion and GMx. The spatially integrated burial rate was computed for each subregion by multiplying its mean burial rate by its tidal wetland area, thus using an assumption that the salt marsh burial rate applies to tidal freshwater and mangrove systems. The spatially integrated burial rate (±2 standard errors) across North America is 9.1 ± 4.8 Tg C per year, with more than 75% in GMx, owing to its large tidal wetland area (see Table 15.1, p. 604) and high carbon burial rate (see Table 15.2, p. 612). For CONUS alone, assuming equivalent distributions of rates among coasts and vegetation types, carbon burial is estimated to be 5.5 ± 3.6 Tg C.

Tidal Wetland CH_4 Fluxes

While CH_4 fluxes tend to be negligible from tidal wetlands with high soil salinities, emissions can increase considerably when sulfate availability is lower (as indexed by salinity; Poffenbarger et al., 2011). Based on the higher net radiative impact of CH_4, climatic benefits of CO_2 uptake and the sequestration illustrated by most of the sites in Table 15A.1, p. 642, may be offset partially by CH_4 release in lower-salinity tidal wetlands (Whiting and Chanton 2001).

Here are reported annual CH_4 fluxes from tidal wetlands across North America (see Table 15A.2, p. 644), with values from studies published in 2011 or earlier taken from Poffenbarger et al. (2011). For studies published after 2011, the same methodology was used as Poffenbarger et al. (2011) in analyzing CH_4 flux data and reporting average annual CH_4

Table 15.2. Carbon Accumulation Rate (CAR) and Associated Data for Tidal Estuarine (Salt and Brackish) Marsh[a]

Region	n	Mean CAR ± 2σ[b] (g C per m^2 per year)	Regional Tidal Wetland Burial[c] ± 2σ (Tg C per year)
High Latitudes	25	301 ± 155	0.5 ± 0.2
Atlantic Coast	59	126 ± 87	1.4 ± 1.0
Pacific Coast	18	173 ± 92	0.6 ± 0.3
Gulf of Mexico	23	293 ± 210	6.6 ± 4.7
North America	125	236 ± 124	9.1 ± 4.8

Notes

a) From Ouyang and Lee (2014).

b) 2σ = 2 standard errors.

c) Regional burial calculated for all tidal wetland types regardless of salinity or vegetation type.

d) Key: n, number of sites; g C, grams of carbon; Tg C, teragrams of carbon.

emissions. If CH_4 emissions were measured over all seasons of the year with the annual rate unreported, calculations were made by extracting emission rates from tables and figures and then interpolating between time points. Finally, although this was only the case in a few studies, for short-term studies lasting a few days to months over the growing season, average daily CH_4 emissions were calculated and then converted to annual fluxes using the rate conversion factors determined by Bridgham et al. (2006). The compilation resulted in CH_4 flux measurements at 51 sites in North America.

The compilation, illustrated in Figure 15.3, this page, continues to support the role of salinity as a predictor of CH_4 emissions observed by Poffenbarger et al. (2011). However, there is considerable variability among methods and sites in annual CH_4 emissions in fresh and brackish (i.e., oligohaline and mesohaline) wetlands, indicating the need for further studies to help improve understanding of the drivers and sensitivities of CH_4 fluxes in these common salinity ranges. Tidal wetlands in the salinity range of 0 to 5 practical salinity units (PSU; i.e., fresh-oligohaline) show an average (±2 standard errors) CH_4 emission of 55 ± 48 g CH_4 per m^2 per year, whereas tidal wetlands in the salinity range of

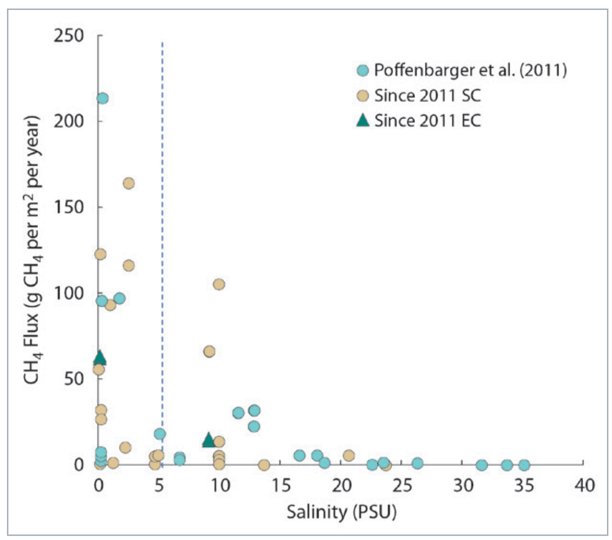

Figure 15.3. Tidal Marsh Methane (CH_4) Emissions Versus Salinity. Approaches to measuring atmospheric CH_4 flux are coded by method as SC (static chamber) and EC (eddy covariance flux tower). CH_4 flux is in grams (g); salinity is in practical salinity units (PSU). The dashed line denotes the demarcation of fresh and oligohaline marshes (0 to 5 PSU) versus mesohaline to saline marshes (5 to 35 PSU).

5 to 38 PSU (i.e., mesohaline to fully saline) emit CH_4 at an average rate of 11 ± 13 g CH_4 per m^2 per year. The spatially integrated tidal wetland CH_4

emission rate, computed by multiplying the fluxes for fresh-oligohaline and mesohaline-saline systems by their respective areas (5,491 and 33,118 km^2; see Table 15.1, p. 604), results in 0.29 ± 0.27 and 0.35 ± 0.43 Tg CH_4 per year, respectively, totaling 0.65 ± 0.48 Tg CH_4 per year (0.49 ± 0.36 Tg C per year) across the entire salinity gradient. Hence, in North America, fresh-oligohaline and mesohaline-saline systems contribute about equally to the total flux, with the former having high per-unit-area flux rates and low area and the latter having low per-unit-area flux rates and high area.

Lateral Fluxes of Carbon from Wetlands to Estuaries

A significant part of tidal wetland and estuarine carbon budgets is the lateral flux from tidal wetlands to estuaries, which is due mainly to tidal flushing. Twelve estimates of TOC (in both dissolved and particulate forms) exchange (per unit area of wetland) in tidal wetlands of the eastern United States were summarized by Herrmann et al. (2015), and the mean value and 2 standard errors derived in that study (185 ± 71 g C per m^2 per year) were used herein. Similarly, four estimates of DIC exchange in eastern U.S. tidal wetlands were summarized in Najjar et al. (2018), with a mean (±2 standard errors) of 236 ± 120 g C per m^2 per year. With only a small number of DIC flux measurements, the error was doubled. Hence, tidal wetland export of total carbon is estimated to be 421 ± 250 g C per m^2 per year. Applying this to all North American tidal wetlands (see Table 15.1, p. 604) yields a total export of 16 ± 10 Tg C per year; applied to CONUS wetlands only, the estimate of lateral export is 11 ± 7 Tg C per year.

Estuarine CO_2 Outgassing

The SOCCR2 assessment used the global synthesis of Chen et al. (2013), which combined field estimates of outgassing per unit area with the MARCATS areas. Most MARCATS segments were found to be sources of CO_2 to the atmosphere, with the integrated flux over North America at +10 Tg C per year (see Table 15.3, this page). Chen et al. (2013) did not provide error estimates, so expert judgment was used to provide a range. The MARCATS segments in North America contain only 25 individual flux estimates, 15 of which are along the Atlantic coast, and some segments have no measurements at all (in which case data from similar systems were used). There is a possibility of a 100% error in the North American flux, so the estimate was placed at 10 ± 10 Tg C per year. Reduced uncertainty may be possible for distinct regions, but this level of error indicates confidence bounds at a continental scale.

A separate estimate was made of CONUS estuarine outgassing based on the SOCCR2 synthesis of CO_2 flux estimates (see Table 15A.3, p. 647) and the areas from the Coastal Assessment Framework (NOAA 1985). Because only one study was

Table 15.3. Estuarine CO_2 Outgassing for North America[a,e]

MARCATS[b] Segment No.	CO_2 Outgassing[c] (g C per m^2 per year)	Number of Systems	CO_2 Outgassing (Tg C per year)
1	129	3	4.4
2	11	3	0.1
3	174	0	1.1
9	96	2	3.1
10	118	15	4.0
11	–9	1	–0.3
12	–5	1	–0.2
13	–13	0	–2.1
Total North America		25	10.0
Approximate CONUS[d] (2, 9, and 10)		20	7.2

Notes

a) Based on the Global Synthesis of Chen et al. (2013).

b) MARCATS, MARgins and CATchments Segmentation.

c) For regions 3 and 13, where no data were available within the segments, the methods of Chen et al. (2013) were used.

d) CONUS, conterminous United States.

e) Key: CO_2, carbon dioxide; g C, grams of carbon; Tg C, teragrams of carbon.

identified for the Pacific Coast, analysis was limited to the Atlantic and GMx coasts, which contain about 90% of the CONUS estuarine area (see Table 15.1, p. 604). For the Atlantic coast, mean fluxes were first estimated in each of three subregions (GOM, MAB, and SAB) before multiplying by their respective areas. This was done because the outgassing per unit area increases toward the south. This analysis results in an outgassing of 10 ± 6 Tg C per year (best estimate ±2 standard errors), which is larger (but not significantly so) than the Chen et al. (2013) analysis for the three segments covering CONUS (i.e., 7 Tg C per year). The SOCCR2 synthesis is an improvement over Chen et al. (2013) by being based on a larger flux dataset and more accurate CONUS estuarine areas.

Estuarine CH_4 Emissions

Only a very limited number of studies are known to be available and scalable for estimating net CH_4 emissions in North American estuaries. In their global review, Borges and Abril (2011) report only three within North America (de Angeles and Scranton 1993; Bartlett et al., 1985; Sansone et al., 1998), ranging from 0.16 to 5.6 mg CH_4 per m^2 per day. Two recent studies with continuous sampling illustrate temporal and spatial variability. Relatively high emissions were observed in the Chesapeake Bay during summer (28.8 mg CH_4 per m^2 per day; Gelesh et al., 2016). In the Columbia River estuary (Pfeiffer-Herbert et al., 2016), summer emissions were estimated at 1.6 mg CH_4 per m^2 per day; 42% of the CH_4 losses were to the atmosphere, 32% were to the ocean, and 25% were to CH_4 oxidation. When scaled to a year, the estuarine CH_4 fluxes from the above studies range from 0.04 to 8 g C per m^2 per year, which is well below typical CO_2 outgassing rates (e.g., the U.S. Atlantic Coast mean estuarine CO_2 outgassing rate is 104 ± 53 g C per m^2 per year, see Table 15A.3, p. 647). Thus, estuarine CH_4 outgassing is likely a small fraction of estuarine carbon emissions. To be comparable with North American tidal wetland CH_4 emissions (~0.5 Tg CH_4 per year), the mean estuarine CH_4 emissions rate would need to be a conceivable rate of ~0.1 g CH_4 m^2 per year. Unfortunately, the lack of estuarine CH_4 emissions data for North America—and any well-constrained relationship with salinity or other physical parameter—precludes the possibility of making a constrained estimate of estuarine CH_4 emissions for North America.

15.4.4 Total Organic Carbon Budget for Estuaries of the Conterminous United States

The empirical model of Herrmann et al. (2015) was applied to quantify the TOC budget for CONUS estuaries (see Table 15.4, this page). This

Table 15.4. Estuarine Areas and Organic Carbon Regional Budgets for the Conterminous United States[a,c]

Estuary	Area (km^2)	Riverine + Tidal Wetland Input (Tg C per year)	Net Ecosystem Production (Tg C per year)	Burial (Tg C per year)	Export to Shelf (Tg C per year)
Gulf of Mexico	30,586	12.6 ± 3.5	–2.2 ± 0.6	–0.3 ± 0.1	–10.1 ± 3.5
Pacific Coast	6,690	1.4 ± 0.2	0.0 ± 0.2	–0.2 ± 0.1	–1.2 ± 0.2
Atlantic Coast	37,764	5.5 ± 1.3	–1.8 ± 1.0	–0.5 ± 0.3	–3.2 ± 1.3
CONUS[b]	75,040	19.5 ± 3.8	–4.0 ± 1.2	–1.0 ± 0.3	–14.5 ± 3.7

Notes

a) Positive values = input of organic carbon to estuaries; negative values = removal of organic carbon from estuaries. Source: model of Herrmann et al. (2015).

b) CONUS, conterminous United States; best estimate and ±2 standard errors.

c) Key: Tg C, teragrams of carbon.

model takes carbon and nitrogen inputs from a data-constrained watershed model and uses empirical relationships to compute burial and NEP. TOC export to shelf waters is computed by the difference. TOC input from rivers and tidal wetlands to CONUS estuaries is estimated to be 19.5 Tg C per year, with an average of 79% coming from rivers and the rest from tidal wetlands (not shown). Most of the input (74%) is exported from the estuary to the shelf, while 21% is remineralized to CO_2 and 5% is buried in estuarine sediments. Like most estuaries worldwide (Borges and Abril 2011), CONUS estuaries are, in the aggregate, net heterotrophic. However, there are regional differences in NEP, with GMx estuaries remineralizing twice as much of the TOC input as Atlantic estuaries and Pacific estuaries metabolically neutral.

15.4.5 Summary Budgets for Tidal Wetlands and Estuaries

The individual flux estimates above were combined into overall carbon budgets for tidal wetlands and estuaries of CONUS and the rest of North America. CONUS (see Figure 15.4a, this page) has better constraints on the fluxes. Central estimates of CONUS tidal wetland carbon losses and gains are very close to balancing even though they were estimated independently; burial, lateral export, and loss of soil carbon stock are all found to be significant terms of carbon removal that balance carbon uptake from the atmosphere. For the estuarine CONUS balance, riverine carbon delivery at the head of tide was taken from Ch. 14: Inland Waters (41.5 ± 2.0 Tg C per year). Including the tidal wetland delivery (11 ± 7 Tg C per year), CONUS estuaries thus were found to receive a total of 53 ± 7 Tg C per year from upland sources. With about 15% (best estimate) of this input outgassed and only a few percent buried, the resulting net total carbon flux from estuaries to shelf waters is 40 ± 9 Tg C.

The North American carbon budget for tidal wetlands and estuaries (see Figure 15.4b, this page) is similar to the CONUS budget except that most of the fluxes are larger. The net uptake of atmospheric CO_2 by the combined system of tidal wetlands and estuaries is

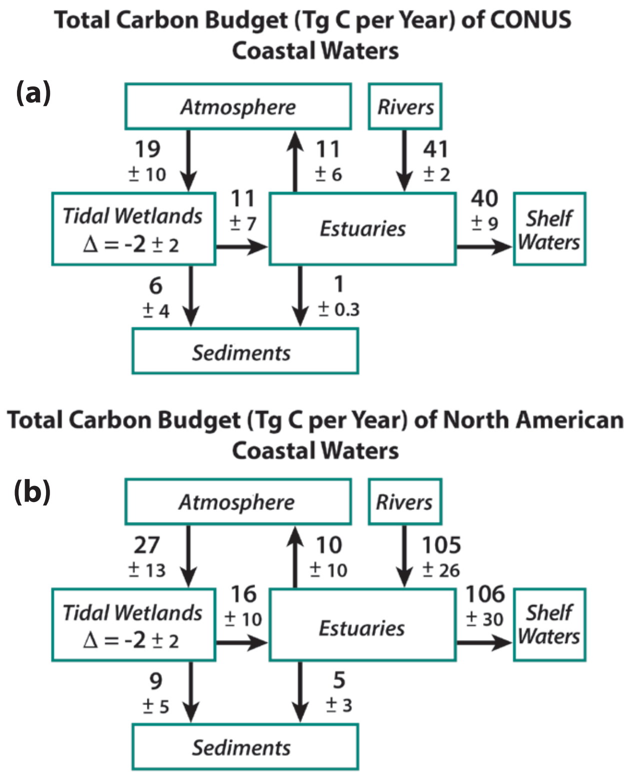

Figure 15.4. Summary Carbon Budgets for Tidal Wetlands and Estuaries. Budgets are given in teragrams of carbon (Tg C) for **(a)** the conterminous United States (CONUS) and **(b)** North America, with errors of ± 2 standard errors.

17 ± 16 Tg C per year. The riverine flux of 105 Tg C per year from Ch. 14: Inland Waters was used and assigned an error of 25%. Lacking direct estimates of carbon burial in North American estuaries, the CONUS estimate was used (see Table 15.4, p. 614) and scaled to all North American estuaries; the error is doubled to reflect this extrapolation. The carbon flux from North American estuaries to the shelf waters, estimated as a residual, is 106 ± 30 Tg C per year.

15.5 Indicators, Trends, and Feedbacks

All indications suggest that most North American coastal and estuarine environments, from Canada to Mexico, are changing rapidly as a result of global- and local-scale changes induced by climate alteration and human activities. The sustainability and quality of estuarine and intertidal wetland habitats, including the magnitude and direction of carbon fluxes, are uncertain, especially due to limited monitoring time series relevant to changing extents and conditions of these habitats. Simulation models have illustrated the long-term sensitivity of coastal carbon fluxes to land-use and management practices while decadal and interannual variations of carbon export are attributable primarily to climate variability and extreme flooding events (Ren et al., 2015; Tian et al., 2015, 2016). Further, tidal wetland sustainability is strongly influenced by human modifications that generally reduce resilience (e.g., groundwater withdrawal, lack of sediment, nutrient loading, and ditching; Kirwan and Megonigal 2013).

Climatic changes affect entire watersheds, so the integration of small changes to terrestrial carbon cycling leads to a significant impact on the quantity, quality, and seasonality of riverine inputs to coastal zones (Bergamaschi et al., 2012; Tian et al., 2016). Within wetlands, accelerating sea level rise and increasing temperature yield a range of responses from enhanced wetland flushing, salinity intrusion, and productivity to enhanced respiration, tidal carbon export, and CH_4 emissions, which have all been postulated. Increased rates of sea level rise may enhance sedimentation and carbon burial rates up to a threshold of marsh resilience, above which erosion processes will dominate (Morris et al., 2016). This effect of accelerated sea level rise on morphology also affects carbon fluxes in shallow estuaries, whereby the loss of barrier islands to erosion will increase tidal mixing.

Estuaries show significant regional drivers of carbon cycling, such as the dominance of land-use change in Atlantic coast (Shih et al., 2010) and GMx (Stets and Striegl 2012) watersheds. In Pacific coast estuaries, ocean drivers (i.e., upwelling patterns) and rainfall variability are dominant controls on carbon fate and CO_2 degassing from Alaska to Mexico. In Arctic regions, along both Pacific and Atlantic coastlines, ice-cover melt and permafrost thaw appear to be critical drivers of wetland extent and estuarine mixing. Tidal wetland carbon dynamics, however, show more local variability than regional variability, with multivariate drivers of extent and carbon fluxes, such as sediment supply (Day et al., 2013), nutrient supply (Swarzenski et al., 2008), tidal restrictions (Kroeger et al., 2017), and subsurface water or hydrocarbon withdrawal (Kolker et al., 2011). These coastal drivers illustrate the complexity of projecting carbon fluxes and their potential to alter fundamental habitat quality. For example, estuarine acidification is observed along all coastlines with potential stress to shell fisheries (Ekstrom et al., 2015), often with changes in riverine input, circulation, and local biological dynamics more significant than direct atmospherically driven ocean acidification (Salisbury et al., 2008).

Thus, expected changes in climate and land use for the remainder of this century likely will have a major impact on carbon delivery to and processing in tidal wetlands and estuaries. While terrestrial carbon loads likely will continue to drive ecosystem heterotrophy, extreme flooding events might shunt material directly to the continental shelf, thus decreasing processing, transformation, and burial in the estuary and tidal wetlands. Overall, estuarine area likely will increase relative to that of tidal wetlands (Fagherazzi et al., 2013; Mariotti and Fagherazzi 2013; Mariotti et al., 2010), and estuarine production will become more based on phytoplankton relative to benthic algae and macrophytes (Hopkinson et al., 2012). While this trajectory may be reversible (see Cloern et al., 2016), by the end of this century tidal wetland and estuary net CO_2 uptake and storage as organic carbon quite likely will be significantly reduced throughout the United States due to passive and active loss of tidally influenced lands.

15.5.1 Observational Approaches

Coastal observations of carbon stocks and fluxes cross many spatial and temporal scales because of their intersection in multiple contexts: past or future, land or ocean, and managed or unmanaged. A variety of observational approaches has been applied to study tidal wetland habitats and carbon fluxes and exchanges with the atmosphere and adjacent estuarine and ocean waters. Currently

lacking is a standardized, consistent methodology on carbon-relevant wetland mapping, wetland carbon flux monitoring, and repeated assessment. Wetland mapping, inventories, and sampling efforts include the National Wetlands Inventory (USFWS NWI 2017), a national effort to map and classify the wetland resources in the United States (data updated at a rate of 2% per year), using aerial photography and high spatial resolution remote-sensing color infrared imagery. Light detection and ranging, or LIDAR, imagery has been applied to develop high-resolution digital elevation models for wetlands and incorporate those maps into coastal resilience (NOAA 2015) and response mapping (USGS 2018). Satellite optical (e.g., Landsat; see Appendix C: Selected Carbon Cycle Research Observations and Measurement Programs, p. 821) and synthetic aperture radar (SAR) imagery has been used for decades in mapping wetland structure and biomass, with tidal hydrologies potentially interpretable through repeat measures. High-resolution satellite ocean color observations can be used to examine wetland impacts on estuarine carbon dynamics and stocks, which, combined with hydrodynamic models, may provide information on lateral fluxes and wetland contributions to estuarine and coastal carbon budgets, especially in the actively restoring Mississippi-Atchafalaya River Delta. However, existing remote-sensing algorithms could be improved, adding the capability for representing and quantifying carbon-related properties in highly turbid estuarine and nearshore waters (Son et al., 2014). Various ground-based approaches have been applied to validate mapped carbon stocks and inventories. Deep soil cores provide quantification of carbon stocks and, when dated, can provide long-term rates of net carbon accumulation or loss (Callaway et al., 2012). Exchanges of CO_2 and CH_4 between wetlands and the atmosphere have been measured historically using static (closed) chamber systems, but, increasingly, continuous eddy covariance approaches are being deployed (Forbrich and Giblin 2015; Knox et al., 2018). Continuous gas flux measurements (i.e., NEE) over a range of temporal scales (hours to days to seasons to years) can be very effective at quantifying photosynthesis and respiration in tidal wetlands. An example of observational NEE data from estuarine ecosystems is illustrated in Figure 15.5a, p. 618. Similarly, in Figure 15.5b, p. 618, observational NEE from a tidal wetland ecosystem is shown. Estuarine NEE is typically quantified using measurements of the gradient in partial pressure across the air-water interface in combination with a model of the gas transfer velocity; more direct approaches are needed to reduce uncertainty (e.g., McGillis et al., 2001; Orton et al., 2010). Deployment of automated water quality sondes and optical sensors within channels of tidal wetlands provides a method for continuous bidirectional measurements of physicochemical and optical parameters that can be used as proxies for hydrological carbon concentrations and flux (Wang et al., 2016). These findings emphasize the importance of time-series measurements to provide *in situ* measurements of variability across timescales.

15.5.2 Modeling Approaches

While there have been numerous applications of three-dimensional estuarine biogeochemical models (Azevedo et al., 2014; Feng et al., 2015; Ganju et al., 2012; Irby et al., 2016; Kenov Ascione et al., 2014), none specifically allow integration with hydrological exchange of tidal wetlands. With unstructured meshes that provide topological flexibility, the Finite Volume Community Ocean Model (FVCOM; Chen et al., 2003) and the Semi-implicit Cross-scale Hydroscience Integrated System Model (SCHISM; Ye et al., 2016, 2018) have been successfully applied to wetland-estuarine environments. Currently, there are no biogeochemical models that include accurate parameterizations for the sources and sinks that drive variability in carbon fluxes, amount, and quality at the wetland-estuary interface (e.g., allochthonous sources, photochemical transformation, and viral lysis). Further, coupled biogeochemical-geomorphic models are necessary for full tidal wetland carbon accounting and projection with accelerated sea level rise, but they have yet to be validated successfully (Kirwan et al., 2010). Efforts to

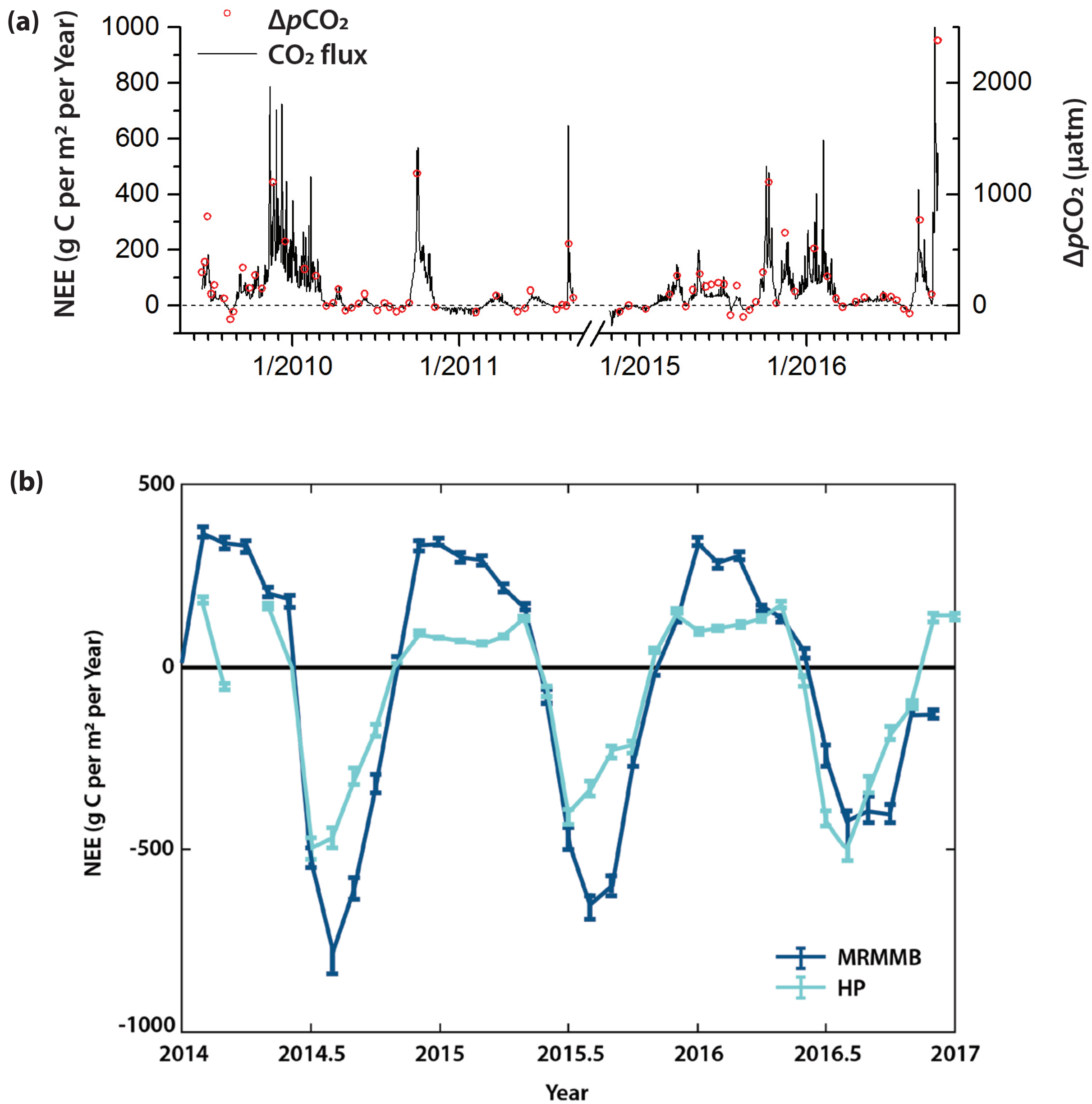

Figure 15.5. Example Observational Net Ecosystem Exchange (NEE) Data from (a) an Estuarine Ecosystem and (b) a Tidal Wetland Ecosystem. (a) NEE of carbon dioxide (CO_2, black line) and the partial pressure difference of CO_2 (ΔpCO_2) between air and water (red circles) in the Neuse River Estuary in North Carolina. NEE is positive when flux is from the water to the atmosphere. The ΔpCO_2 is positive when water pCO_2 is greater than atmospheric pCO_2. Fluxes were estimated using the pCO_2 measured during spatial surveys (Crosswell et al., 2012, 2014; Van Dam et al., 2018) and a gas transfer parameterization based on local wind speed (Jiang et al., 2008). These studies present alternative gas transfer parameterizations and associated errors. **(b)** Data are from restored coastal tidal wetlands in the New Jersey Meadowlands. The dark blue line represents the Marsh Resource Meadowlands Mitigation Bank (MRMMB; Duman and Schäfer, 2018), and the teal line, the Hawk Property (HP) natural wetland. Error bars are standard deviation of the mean of all measurements during this period (monthly). Key: g C, grams of carbon; µatm, microatmospheres.

couple tidal wetland lateral exchanges with estuarine dynamics are ongoing.

Empirical approaches to modeling include synthetic cross-site comparisons and relationships. The National Wetlands Condition Assessment (U.S. EPA 2016) illustrates homeostasis among tidal wetland soil carbon densities spatially and downcore (Nahlik and Fennessy 2016). National Aeronautics and Space Administration (NASA) synthesis efforts, which include the Wetland-Estuary Transports and Carbon Budgets (WETCARB; NASA 2017b) project and the Blue Carbon Monitoring System (Blue CMS; NASA 2017a) project, have integrated literature-derived field data and national datasets (e.g., USFWS and U.S. Department of Agriculture) and identified key differences and similarities among tidal wetland and estuarine processes for CONUS. These approaches provide boundary conditions for new observations and identify critical knowledge gaps.

Key areas to aid further research and development are:

- Mapping approaches that characterize key drivers of tidal carbon accounting (organic carbon burial and CH_4 production), such as multiple salinity classes, relative elevations, and tidal boundaries;
- Unbiased, landscape-level sampling protocol to quantify sediment carbon stock change in tidal wetlands (similar to U.S. Forest Service Forest Inventory Analysis approaches for carbon accounting);
- Remote-sensing capability suitable for highly turbid estuarine waters;
- Networks for continuous measurements of wetland-atmosphere exchanges (CO_2 and CH_4 emissions) and wetland-ocean exchanges (dissolved and particulate carbon fluxes) and better constraint and linkage of these important fluxes;
- New biogeochemical models that account for critical processes at the wetland-estuary interface, both ocean drivers (sea level rise) as well as watershed influences (land use); and
- Estuarine gas flux monitoring, including CO_2 and CH_4, especially in large, undersampled, episodic or rapidly changing environments, such as high latitudes (Arctic).

15.6 Societal Drivers, Impacts, and Carbon Management

As land- and freshwater-use changes have an outsized effect on estuarine carbon dynamics, societal drivers are at the heart of future projections for coastal zone carbon cycling. Dissolved carbon inputs are thought to have increased over the past century to Atlantic and GMx estuaries through riverine delivery, largely as a result of agricultural developments (Raymond et al., 2008; Tian et al., 2016). Similarly, delivery of nutrients from agricultural or urban growth and intensification can stimulate primary production in surface waters and respiration in bottom waters, leading to hypoxia and acidification in subsurface estuarine habitats (Cai et al., 2011; Feely et al., 2010; Irby et al., 2018). These human inputs reflect potential pathways for carbon management within estuaries by state, local, or provincial agencies and stakeholders (Chan et al., 2016; Washington State Blue Ribbon Panel on Ocean Acidification 2012). One step removed from carbon are the rich biological resources that have supported human populations on North American estuaries for millennia (e.g., Jackley et al., 2016), which link carbon management to fisheries and ecosystem management processes more broadly (Cooley et al., 2015). As ocean warming and CO_2 uptake drive changes in estuarine circulation, metabolism, and biogeochemistry, myriad changes to estuarine carbon cycles are expected over both short and long timescales, with impacts ranging from direct effects on individual species of ecosystem or economic importance to indirect effects on human health and livelihoods through stimulation of disease vectors (Bednarsek et al., 2017; McCabe et al., 2016; Waldbusser et al., 2014). Broad thinking about societal drivers of carbon cycle change and its ecosystem impacts, as well

as building effective partnerships with diverse stakeholders, will be critical to effective management of estuarine carbon cycle problems over the coming decades (DeFries and Nagendra 2017).

Coastal wetlands in temperate and tropical latitudes are a "directly or indirectly" managed landscape component, with increasing pressures from human stressors and sea level rise. Given their role in linking land, ocean, and atmospheric carbon fluxes, the increasing rate of global wetland loss and degradation is concerning. Tidal wetland areas in the United States have recently experienced relatively low rates of conversion and loss: ~0.2% per year, according to NOAA Coastal Change and Analysis Program (C-CAP) data from 1996 to 2010, with 92% of all loss occurring in Louisiana (Couvillion et al., 2017; Holmquist et al., 2018b). However, direct and indirect conversions of tidal wetlands to drained or impounded land uses continue actively along coastlines globally. In Mexico, 10% of mangrove area has been lost from 1980 to 2015, resulting in CO_2 emissions ranging from 0.4 to 1 Tg C per year (Troche-Souza et al., 2016); while GMx has more mangrove area, loss is high on the Pacific Coast due primarily to anthropogenic land-use changes.

Coastal "blue carbon" ecosystems—tidal marshes, mangroves, and estuarine sea grasses—are characterized by high areal rates of carbon sequestration, low rates of CH_4 and nitrous oxide (N_2O) emissions, and large soil carbon pools (Howard et al., 2017). Because the influence of coastal ecosystems on carbon cycles greatly exceeds their area (Najjar et al., 2018), activities that affect the conservation, degradation, or restoration of these ecosystems have implications for greenhouse gas (GHG) emissions and national GHG accounting (Kennedy et al., 2014). Loss of tidal hydrology likely shifts tidal wetlands from sinks to sources as large soil carbon reservoirs in tidal wetlands can become large sources of CO_2 emissions when disturbed (Pendleton et al., 2012), and freshwater dominance can dramatically impact CH_4 emissions (Kroeger et al., 2017). Further, nitrate pollution can dramatically impact N_2O emissions (Moseman-Valtierra et al., 2011).

In 2013, the Intergovernmental Panel on Climate Change (IPCC) issued guidance on including management of seagrasses, tidal marshes, and mangroves as an anthropogenic carbon flux in national GHG inventories (Kennedy et al., 2014). Currently a number of countries, including the United States, are in the process of implementing these guidelines (U.S. EPA 2017), an action which would be a major step toward reducing uncertainties in national carbon budgets and understanding the roles played by coastal tidal wetland management in national GHG emissions. This new information includes the relatively strong long-term sink for carbon in tidal and subtidal wetland soils, relatively limited CH_4 emissions in saline wetlands, and relatively large GHG emissions associated with wetland loss. In addition to improved knowledge of tidal wetland carbon balance, inclusion of tidal wetlands in the U.S. national GHG inventory provides an opportunity for enhanced estimation of the ecosystem services these wetlands offer to coastal communities. Ongoing research on feedbacks among hydrology, geomorphology, nutrient availability, plant productivity, and microbial activity is needed to understand and manage the impacts of human activities on the GHG balance of these ecosystems.

15.7 Synthesis, Knowledge Gaps, and Outlook

The CCARS synthesis report (Benway et al., 2016) is the most comprehensive attempt to develop a science plan for carbon cycle research of North American coastal systems. While clarifying key regional differences in processes and projections, this synthesis effort also exposed major knowledge gaps and disconnects between measurement and modeling scales. These knowledge gaps are currently being explored by multiple synthesis efforts, and below is a review of some of the major gaps being investigated.

15.7.1 Lateral Exchanges Between Tidal Wetlands and Estuaries

Estimates of lateral fluxes of carbon between tidal wetlands and estuaries are mostly based on discrete sampling events at monthly to seasonal intervals,

with sampling resolution from hourly to one half of a tidal cycle, leaving the majority of time unsampled and thus requiring large interpolation between sampling events and producing substantial uncertainty in export fluxes (Downing et al., 2009; Ganju et al., 2012). A recent estimate of the DIC lateral flux from a pristine intertidal wetland marsh on Cape Cod, Massachusetts, with minute-scale resolution revealed that previous estimates of marsh DIC export—such as those summarized by Najjar et al. (2018) and used here—may be severalfold too low (Wang et al., 2016). Previous studies generally show a positive carbon export from tidal wetlands to estuaries but may not fully resolve the export magnitude and temporal heterogeneity, which, in turn, are controlled by variability in water flux and constituent concentration across timescales from minutes to tidal cycles to years. Such observational gaps extend beyond DIC to include DOC and particulate organic carbon (POC) as well. In particular, the fate of exported POC from eroding marshes, though virtually unknown, is important for carbon accounting. Future studies should be directed to capture appropriate temporal scales of variability of carbon exports from marshes to accurately constrain lateral exchanges.

15.7.2 Coastal Subhabitat Boundaries

The definition of estuarine subhabitat within the coastal ocean is fluid, primarily associated with bottom depth and mixing processes. This boundary may not be mappable, but the absence of a robust definition inhibits future monitoring efforts and projections. Progress has been made in defining estuaries and quantifying their fundamental characteristics (such as residence time) in CONUS via NOAA's Coastal Assessment Framework (NOAA 2017). Such a framework has been essential for scaling up carbon and nitrogen fluxes from limited data (Herrmann et al., 2015; Najjar et al., 2018) and is greatly needed for all of North America. The global estuarine delineation based on MARCATS (Project Geocarbon 2017) has been very helpful, but the coarse resolution (i.e., 0.5 degrees) is a concern. For coastal wetland boundaries, multiple criteria have been used by different entities: political boundaries, salinity gradients, elevation thresholds, and tidal criteria. This variability has led to great confusion in the literature (e.g., Lu et al., 2017), in agency policies, and in market-based carbon accounting protocols. A strong gap is the lack of a boundary mapped for head of tide. Tidal wetlands, by definition, cross a wide range of salinities (i.e., saline, brackish, and freshwater), with the singular distinction of having a hydroperiod influenced by ocean tides (paraphrased from web link; U.S. EPA 2016). Networks of available data may be useful in monitoring this boundary, as it is a key distinction of carbon dynamics in coastal habitats. These networks include, for example, a NOAA repository of coastal LIDAR; NOAA tide gauge networks; USFWS wetland mapping efforts; and USGS Land Change Monitoring, Assessment, and Prevention (LCMAP; USGS 2017). In the absence of a mapped boundary, spatial accounting of tidal and estuarine extent—current, past, and future—is fraught with uncertainty, with a likely underestimate of at least 50% for freshwater tidal wetlands alone.

15.7.3 Spatial Variability in Burial Rates and in Air-Water Flux

Because of ocean influences and similar processes along coastlines, spatial variability can be much greater within an estuarine and tidal wetland complex than among regions. Tracking the drivers of spatial variability in ecosystem properties—sea level, bathymetry, river flow, elevation, soil properties, and vegetation types—can greatly improve the use of remotely sensed data to validate carbon flux models and their variability between years. Accounting processes generally rely on spatial data, and mapping stocks and fluxes in these spatially dynamic habitats will require improved use of geospatial datasets and, thus, improved attribution of location information with observations. Relative sea level rise is particularly variable in its magnitude and influence. Geomorphic models (e.g., Kirwan and Megonigal 2013; Morris et al., 2016) are improving understanding of the sustainability of wetland carbon storage, showing enhanced carbon sequestration under modest

increases in sea level but rapid carbon emissions after wetland accretion reaches its conditional "tipping point." Empirically, many GMx wetlands undergoing land subsidence appear to have crossed their threshold of sustainability and are being rapidly eroded or drowned (Couvillion et al., 2017).

15.7.4 Other Greenhouse Gases: CH_4 and N_2O

The bulk of data on CH_4 and N_2O fluxes in tidal wetlands is modeled from pore-water measurements in profile or from atmospheric chamber measurements under static conditions. However, these methods generate an incomplete picture of these dynamic environments and fluid boundaries. The growing network of eddy covariance and other continuous data-rich approaches ("movies" instead of "snapshots") is improving the understanding of the episodic nature of these processes and emergent thresholds of concern. Nitrous oxide fluxes likely are heightened under enhanced nitrate runoff (i.e., "nitrate saturation"; Firestone and Davidson 1989), but documentation is poor. Further, CH_4 production is likely low when sulfate is available (Poffenbarger et al., 2011), but it is enhanced by increased carbon fixation, such as through global changes that include rising atmospheric CO_2 concentrations or invasions of more productive species (e.g., *Phragmites australis*; Martin and Moseman-Valtierra 2015; Mueller et al., 2016).

Estuarine CH_4 emissions currently appear to be a small fraction of global emissions (i.e., <1%; Borges and Abril 2011), but they may be poised to increase with enhanced rates of methanogenesis in response to organic matter inputs and hypoxia expansion under future conditions (Gelesh et al., 2016). A seaward decrease in near-surface porewater concentrations of CH_4 is observed often, likely due to both increasing sulfate availability and *in situ* water column oxidation. Water column CH_4 and pCO_2 are positively correlated in well-mixed estuaries, suggesting *in situ* production from organic matter transferred from surface waters to methane-producing bottom waters (Borges and Abril 2011). Like tidal wetlands, many estimates of emission rates are modeled from profiles of surface and porewater concentrations of CH_4, but continuous sampling and eddy covariance data likely will reduce uncertainty in emissions and allow better characterization of the physical and biogeochemical processes associated with atmospheric CH_4 emissions.

15.7.5 Regional Gaps

Much assessment has been focused on estuaries along different regions of the Atlantic Coast (e.g., GOM, MAB, and SAB), but modeled carbon fluxes for large estuaries still remain poorly constrained. For example, few measurements of air-water CO_2 flux are available for upscaling within the Chesapeake Bay, the largest East Coast estuary (e.g., Cai et al., 2017).

The Gulf of Mexico also is well studied, but it has surprisingly few gas flux measurements in its tidal wetlands and estuaries (see, however, Holm et al., 2016). One of the most extensive regional monitoring programs, Louisiana's Coastwide Reference Monitoring System (CRMS 2017), supports GMx soil and vegetation stock change assessments and predictive models through annual records of tidal wetland conditions. These data also help illustrate the wide within-watershed variability in conditions, such as land subsidence (Jankowski et al., 2017), that drive organic carbon accretion, erosion, and mineralization processes. In addition, the Texas Commission on Environmental Quality (TCEQ) has been maintaining quarterly measurements of total alkalinity and pH in all coastal estuaries across the state in the northwestern GMx since 1969 (TCEQ 2017). This dataset may offer insight on multidecadal changes in CO_2 flux that await further investigation.

In contrast, Pacific Coast estuaries lack published carbon cycle measurements with sufficient resolution and duration to afford insight into short- or long-term changes associated with climate or human-caused forcing. Observation and modeling gaps are notably large in the Gulf of Alaska and Central American isthmus regions. For instance, very few studies have addressed CO_2 cycling and air-sea

exchange in lagoons (Ávila-López et al., 2017), a dominant habitat type in the tropical Pacific and the Gulf of California in Mexico. Estimates of air-sea exchange of climate-reactive gases (e.g., CO_2, CH_4, and N_2O) in open waters of Pacific Coast estuaries, along with estimates of primary production and carbon burial, are insufficient for a systematic analysis.

Finally, high-latitude estuaries are experiencing rapid shifts in salinity and seasonality, making relationships between climatic drivers difficult to assess. Some clear data needs for a monitoring framework in Arctic systems include depths of coastal peats along rivers, the sensitivity of productivity to rising temperatures and longer growing seasons, terrestrial carbon fluxes (including DOC and DIC), and the long-term prognosis for coastal erosion rates due to relative sea level rise.

Carbon stock and flux data from Pacific Islands, Puerto Rico, and Hawai'i are not included in this chapter because of their limited datasets (Fagan and MacKenzie 2007; MacKenzie et al., 2012) and the inability to extrapolate their data in space and time. Emerging carbon assessments may be useful for upscaling (Selmants et al., 2017), but the necessary measurements are lacking to estimate carbon fluxes of similar confidence as reported herein for continental coastlines. Hence, there is a clear need for studies of carbon cycling in the coastal environments of Pacific Islands, Puerto Rico, and Hawai'i.

15.7.6 Outlook and Conclusion

Current outlooks and understanding of tidal wetland and estuarine carbon cycling are represented herein, recognizing that synthetic and novel research activities are ongoing. The current state of knowledge represented is sufficient to identify predictable processes and responses, but uncertainty in modeling is higher when applied at continental scales and across datasets of varied confidence. Whereas coastal habitats have distinct responses to myriad global changes, regional and temporal drivers of carbon exchanges and internal processing remain critical knowledge gaps. Monitoring advances, such as high-frequency field data, remotely sensed imagery, and data integration platforms, may shed light on the carbon dynamics at the land-ocean margin and provide the clarity needed to close continental-scale carbon budgets. Improved confidence in projected changes of coastal carbon storage and processing is needed for contributing to more effective policy and management decisions in coastal communities and nationally within North America.

SUPPORTING EVIDENCE

KEY FINDING 1

The top 1 m of tidal wetland soils and estuarine sediments of North America contains 1,886 ± 1,046 teragrams of carbon (Tg C) (*high confidence, very likely*).

Description of evidence base

Several sources were available to verify the extent of intertidal wetland and subtidal habitats in North America for Key Finding 1. First, the U.S Fish and Wildlife Service National Wetlands Inventory (USFWS NWI 2017) is a conservative but definitive source due to inclusion of tidal modifiers to clarify hydrology. Second, a synthesis of Mexican, Canadian, and U.S. saline coastal habitats was provided by the Commission for Environmental Cooperation (CEC 2016). For carbon density in intertidal wetland environments, a synthesis of datasets from tidal wetland habitats reviewed (Chmura et al., 2003; Ouyang and Lee 2014; Holmquist et al., 2018a) found a very narrow distribution measured in kilograms (kg; 27.0 ± 13.0 kg C per m^3) in wetland carbon stocks across North American tidal wetlands, regardless of salinity or vegetation type, as did a national dataset review (28.0 ± 7.8; Nahlik and Fennessy 2016). A global synthesis (Sanderman et al., 2018) provided data to synthesize a new estimate for Mexico's mangroves (31.8 ± 1.3 kg C per m^3). For carbon stocks in seagrass environments, synthetic data from literature reviews reporting bulk density and organic carbon along 1-m profiles were used for coast-specific estimates: 2.0 ± 1.3 for the Atlantic Coast, 3.1 ± 2.4 for the Gulf of Mexico coast, 1.4 ± 1.2 for the Pacific Coast, and 2.0 for boreal and Arctic regions. For carbon density in estuarine open-water sediments, coastal regions played no clear role and geomorphic settings were not available (Smith et al., 2015), so a mean of 1.0 kg per m^3 was chosen, using a literature-based average for total organic carbon (TOC) content (0.4% organic carbon; range 0.17% to 2%; Premuzic et al., 1982; Kennedy et al., 2010) coupled with a literature average of percentage of dry bulk densities (2.6 g C per cm^3; Muller and Suess 1979).

Major uncertainties

Uncertainties vary for each subhabitat, and these data likely represent an underestimate of total stocks, which may be many meters deep. For tidal wetland soils to 1 m in depth, the primary uncertainty is in underestimates of mapped boundaries, with, for example, no accounting of freshwater tidal systems in either Mexico or Canada, and likely undercounting of freshwater tidal wetlands in the United States. For seagrass, the spatial data are conservative estimates of located and documented habitat, although seagrass populations can shift boundaries rapidly and potentially there are far more currently unmapped seagrass beds in North America. For estuarine spatial data, the boundaries are constrained by bathymetry maps, which generally are more uncertain in higher latitudes. In contrast, carbon densities have narrow ranges in tidal wetland and estuarine soils but a skewed representation in seagrass soils, a difference which may be due to limited sampling in northern latitudes.

Assessment of confidence based on evidence and agreement, including short description of nature of evidence and level of agreement

There is theoretical and empirical convergence on tidal marsh carbon densities but a likely bias to underrepresenting tidal freshwater habitats. Further, seagrass carbon densities show a wider range and an apparent latitudinal gradient of decreasing carbon density from tropical to temperate

environments. Geomorphic variability (e.g., shallow waters versus fjords) in estuarine sediments may reduce uncertainty in stock assessments, but map layers are not available for North America.

Estimated likelihood of impact or consequence, including short description of basis of estimate

The likely impact of information is high because it has not been synthesized previously at the continental scale.

Summary sentence or paragraph that integrates the above information

For Key Finding 1, although sediment carbon densities in tidal wetlands are high with a narrow range and carbon densities in subtidal habitats are substantially lower with a wider range, there are still underrepresented samples from high-latitude regions, especially tidal forested wetlands and subtidal seagrasses. Further, the data reported thus far are limited to documented tidal habitats, although there is an appreciation that large areas are likely missing for freshwater tidal marsh and for seagrass extent.

KEY FINDING 2

Soil carbon accumulation rate (i.e., sediment burial) in North American tidal wetlands is currently 9 ± 5 Tg C per year (*high confidence, likely*), and estuarine carbon burial is 5 ± 3 Tg C per year (*low confidence, likely*).

Description of evidence base

Carbon burial, which accounts for all carbon accumulated in coastal sediments over an annual time period, has been documented for Key Finding 2, with geological approaches in multiple studies. Accumulation of carbon stock over a period of time using a marker horizon is relevant to specific periods of time by the method used (e.g., recent years, marker horizons, and radioisotope tracers of different decay rates). The data reported here refer to isotopes of cesium (^{137}Cs) and lead (^{210}Pb) dates alone, thus representing long-term average annual accretion rates for the past 50 years (since 1963). Rates of burial (Ouyang and Lee 2014; n = 125 samples) provide a range for comparison with other reviews that do account for mangrove subhabitats. No significant differences in carbon burial are detected for habitat types by salinity or vegetation type when comparing with Chmura et al. (2003) or with Breithaupt et al. (2014). Estuarine carbon burial is estimated for CONUS using the model of Herrmann et al. (2015) and scaled to all of North America using estimates of estuarine area.

Major uncertainties

Carbon burial rate is a bulk measure of multiple processes, both old and new carbon inputs as well as both autochthonous and allochthonous sources. As such, carbon burial through those processes has varied drivers, with different dominating processes across the landscape. Overestimation is possible when accretion of mineral sediment brings lower carbon densities than equilibrium conditions. Underestimates are possible when accretion is reported at historic rates and not adjusted for current rates of sea level rise. Mapped areas are a likely underestimate because they do not include freshwater tidal marshes in Canada or Alaska. Further, high uncertainties are associated with wide ranges of rates through different dating approaches. Estuarine carbon burial rate uncertainties stem from errors in the model of Herrmann et al. (2015) and, more

importantly, the scaling of CONUS results to all of North America. Particularly problematic is the lack of rigorous mapping of estuarine extent outside of CONUS.

Assessment of confidence based on evidence and agreement, including short description of nature of evidence and level of agreement

Because mapping limitations and 50-year averages of tidal wetland carbon accumulation are inferred rather than being the current rates under accelerated sea level rise, these estimates likely are lower than the actual rates of burial. Thus, while these data represent measured rates, this analysis relies on a fairly small range of locations and a small subset of available published data. Estuarine burial rates are not confident because Canada and Mexico have limited data applicable to the modeling strategy of Herrmann et al. (2015).

Estimated likelihood of impact or consequence, including short description of basis of estimate

The likely impact of the information on tidal wetland and estuarine burial is high, as it has not yet been synthesized at the continental scale.

Summary sentence or paragraph that integrates the above information

For Key Finding 2, burial of carbon sourced from within wetlands and from terrestrial sources is similar among regions and wetland types, driven primarily by accretion rates, which are tied to geomorphic feedbacks with sea level rise. Burial of carbon in estuaries is linked most closely to residence time and total nitrogen input.

KEY FINDING 3

The lateral flux of carbon from tidal wetlands to estuaries is 16 ± 10 Tg C per year for North America (*low confidence, likely*).

Description of evidence base

In Key Finding 3, 16 studies were conducted to quantify the lateral flux of organic carbon (12 studies) and inorganic carbon (4 studies) from tidal wetlands to estuaries at individual locations. The organic carbon flux studies are summarized in Herrmann et al. (2015) and the inorganic carbon flux studies are summarized in Najjar et al. (2018). These studies were scaled to all of North America using estimates of tidal wetland area.

Major uncertainties

The major uncertainty in this Key Finding is the limited spatial and temporal extents of the 16 individual flux measurements. Tidal wetlands are highly heterogeneous and vary in their processing of carbon on a wide variety of timescales. Hence, tidal wetlands are likely to have been undersampled in terms of lateral exchanges. However, tidal wetlands consistently export carbon and the range of estimates is less than an order of magnitude.

Assessment of confidence based on evidence and agreement, including short description of nature of evidence and level of agreement

The low confidence is due to the limited number of measurements and time periods. There is appreciation, however, that at a continental scale, there is a strong likelihood that tidal wetlands export carbon to estuaries, although the magnitude of the flux is highly uncertain.

Estimated likelihood of impact or consequence, including short description of basis of estimate

This flux represents 60% (best estimate) of the net uptake of atmospheric carbon by tidal wetlands. Per knowledge gained, this is the first such estimate for North America.

Summary sentence or paragraph that integrates the above information

For Key Finding 3, there is enough information to make a first-order estimate of the flux of carbon from tidal wetlands to estuaries for North America as a whole, and there is high confidence in the order of magnitude of the flux. The high heterogeneity of tidal wetland systems and limited field data prevent a more accurate estimate of the flux.

KEY FINDING 4

In North America, tidal wetlands remove 27 ± 13 Tg C per year from the atmosphere, estuaries outgas 10 ± 10 Tg C per year to the atmosphere, and the net uptake by the combined wetland-estuary system is 17 ± 16 Tg C per year (*low confidence, likely*).

Description of evidence base

The uptake of atmospheric carbon dioxide (CO_2) by tidal wetlands is assessed for Key Finding 4 by net ecosystem exchange (NEE) estimates from eddy covariance measurements. It is similar to an alternative estimate of uptake that assumes uptake as the sum of burial (8 Tg C) and lateral export (16 Tg C). Burial and lateral exports are discussed in the supporting evidence for Key Findings 2 and 3. Estuarine outgassing is based on studies of individual estuary summaries (Chen et al., 2013) and estuarine areas (Laruelle et al., 2013). The flux of the combined system is a simple sum of the fluxes from tidal wetlands and estuaries and compounded error.

Major uncertainties

The major uncertainties in this Key Finding are the limited spatial and temporal extents of tidal wetland atmospheric flux measurements, burial, lateral flux, and estuarine outgassing measurements. Estuarine outgassing uncertainties also stem from the low spatial resolution of the datasets used to estimate areas.

Assessment of confidence based on evidence and agreement, including short description of nature of evidence and level of agreement

There is low confidence on this calculation at the scale of North America. The low confidence is due to the residual between competing fluxes; on the one hand, there is strong likelihood that tidal wetlands take up CO_2 from the atmosphere and estuaries outgas CO_2 to the atmosphere and, on the other hand, that there is large uncertainty in the magnitude of each, assessments which stem from the high spatial and temporal variability of these systems and the limited field data. The fate of carbon released from tidal wetland degradation remains unknown.

Estimated likelihood of impact or consequence, including short description of basis of estimate

These are not major fluxes in the carbon budget of North America, but they are regionally important. Accounting for current knowledge, such estimates are the first for North America.

Summary sentence or paragraph that integrates the above information

For Key Finding 4, there is enough information to make first-order estimates of the exchange of atmospheric CO_2 with tidal wetlands and estuaries for North America as a whole. The high heterogeneity of these systems and limited field data prevent a more accurate estimate of the flux.

KEY FINDING 5

Research and modeling needs are greatest for understanding responses to accelerated sea level rise; mapping tidal wetland and estuarine extent; and quantifying carbon dioxide and methane exchange with the atmosphere, especially in large, undersampled, and rapidly changing regions (*high confidence, likely*).

Description of evidence base

Tidal wetland and estuarine area are first-order drivers of the spatially integrated flux (e.g., in units of Tg C per year) of all carbon fluxes in these ecosystems. The lack of an accurate quantification of tidal wetland and estuarine area, particularly in Canada and Mexico, is thus a major gap in understanding the role of tidal wetlands and estuaries in the carbon cycling of North America. Carbon cycle research is largely motivated by the impact of greenhouse gases on climate and how climate change affects fluxes of these gases to the atmosphere from terrestrial and aquatic systems. However, the database of tidal wetland and estuarine CO_2 and CH_4 exchanges with the atmosphere is severely limited. In particular, direct estimates of these fluxes are rare. Furthermore, some of the most poorly sampled regions are those that are changing the most rapidly (e.g., the Arctic).

Major uncertainties

There are few uncertainties in Key Finding 5 because there is a clear lack of data on extent and atmospheric exchange.

Assessment of confidence based on evidence and agreement, including short description of nature of evidence and level of agreement

Confidence is high in Key Finding 5 because systematic studies (with error estimates) of tidal wetlands and estuaries are extremely limited. Very few direct estimates of exchanges of atmospheric CO_2 and CH_4 with tidal wetlands and estuaries exist. While research needs are present in other aspects of the tidal wetland and estuarine carbon cycling, these needs are unlikely to be more pressing than the needs for quantifying area and gas exchange with the atmosphere.

Estimated likelihood of impact or consequence, including short description of basis of estimate

Key Finding 5 is not an estimate but a recommendation. It could impact future research on tidal wetland and estuarine carbon cycling in North America.

Summary sentence or paragraph that integrates the above information

Key Finding 5 synthesizes the existing research on tidal wetland and estuarine carbon cycling in North America, providing a future direction for research in this area.

REFERENCES

Adame, M. F., J. B. Kauffman, I. Medina, J. N. Gamboa, O. Torres, J. P. Caamal, M. Reza, and J. A. Herrera-Silveira, 2013: Carbon stocks of tropical coastal wetlands within the karstic landscape of the Mexican caribbean. *PLOS One*, **8**(2), e56569, doi: 10.1371/journal.pone.0056569.

Alin, S., R. Brainard, N. Price, J. Newton, A. Cohen, W. Peterson, E. DeCarlo, E. Shadwick, S. Noakes, and N. Bednaršek, 2015: Characterizing the natural system: Toward sustained, integrated coastal ocean acidification observing networks to facilitate resource management and decision support. *Oceanography*, **25**(2), 92-107, doi: 10.5670/oceanog.2015.34.

AMAP, 2011: *Snow, Water, Ice and Permafrost in the Arctic (SWIPA).* Climate change and the cryosphere, Arctic Monitoring and Assessment Programme, 538 pp.

Artigas, F., J. Y. Shin, C. Hobble, A. Marti-Donati, K. V. R. Schäfer, and I. Pechmann, 2015: Long term carbon storage potential and CO_2 sink strength of a restored salt marsh in New Jersey. *Agricultural and Forest Meteorology*, **200**, 313-321, doi: 10.1016/j.agrformet.2014.09.012.

Ávila-López, M. C., J. M. Hernández-Ayón, V. F. Camacho-Ibar, A. F. Bermúdez, A. Mejía-Trejo, I. Pacheco-Ruiz, and J. M. Sandoval-Gil, 2017: Air–water CO_2 fluxes and net ecosystem production changes in a Baja California coastal lagoon during the anomalous North Pacific warm condition. *Estuaries and Coasts*, **40**(3), 792-806, doi: 10.1007/s12237-016-0178-x.

Azevedo, I. C., A. A. Bordalo, and P. Duarte, 2014: Influence of freshwater inflow variability on the Douro Estuary primary productivity: A modelling study. *Ecological Modelling*, **272**, 1-15, doi: 10.1016/j.ecolmodel.2013.09.010.

Barr, J. G., V. Engel, J. D. Fuentes, J. C. Zieman, T. L. O'Halloran, T. J. Smith, and G. H. Anderson, 2010: Controls on mangrove forest-atmosphere carbon dioxide exchanges in western Everglades National Park. *Journal of Geophysical Research: Biogeosciences*, **115**(G2), doi: 10.1029/2009JG001186.

Barr, J. G., V. Engel, T. J. Smith, and J. D. Fuentes, 2012: Hurricane disturbance and recovery of energy balance, CO_2 fluxes and canopy structure in a mangrove forest of the Florida Everglades. *Agricultural and Forest Meteorology*, **153**, 54-66, doi: 10.1016/j.agrformet.2011.07.022.

Bartlett, K. B., D. S. Bartlett, R. C. Harriss, and D. I. Sebacher, 1987: Methane emissions along a salt marsh salinity gradient. *Biogeochemistry*, **4**(3), 183-202, doi: 10.1007/bf02187365.

Bartlett, K. B., R. C. Harriss, and D. I. Sebacher, 1985: Methane flux from coastal salt marshes. *Journal of Geophysical Research: Atmospheres*, **90**(D3), 5710-5720, doi: 10.1029/JD090iD03p05710.

Bauer, J. E., W. J. Cai, P. A. Raymond, T. S. Bianchi, C. S. Hopkinson, and P. A. Regnier, 2013: The changing carbon cycle of the coastal ocean. *Nature*, **504**(7478), 61-70, doi: 10.1038/nature12857.

Baumann, H., R. B. Wallace, T. Tagliaferri, and C. J. Gobler, 2015: Large natural ph, CO_2 and O_2 fluctuations in a temperate tidal salt marsh on diel, seasonal, and interannual time scales. *Estuaries and Coasts*, **38**(1), 220-231, doi: 10.1007/s12237-014-9800-y.

Bednarsek, N., R. A. Feely, N. Tolimieri, A. J. Hermann, S. A. Siedlecki, G. G. Waldbusser, P. McElhany, S. R. Alin, T. Klinger, B. Moore-Maley, and H. O. Portner, 2017: Exposure history determines pteropod vulnerability to ocean acidification along the U.S. west coast. *Scientific Reports*, **7**(1), 4526, doi: 10.1038/s41598-017-03934-z.

Benway, H., S. Alin, E. Boyer, W.-J. Cai, P. Coble, J. Cross, M. Friedrichs, M. Goñi, P. Griffith, M. Herrmann, S. Lohrenz, J. Mathis, G. McKinley, R. Najjar, C. Pilskaln, S. Siedlecki, and R. L. Smith, 2016: *A Science Plan for Carbon Cycle Research in North American Coastal Waters. Report of the Coastal Carbon Synthesis (CCARS) Community Workshop, August 19-21, 2014.* Ocean Carbon and Biogeochemistry Program and North American Carbon Program, 84 pp. [https://www.us-ocb.org/coastal-carbon-synthesis-ccars/]

Bergamaschi, B. A., R. A. Smith, M. J. Sauer, and J. S. Shih, 2012: Terrestrial fluxes of sediments and nutrients to Pacific coastal waters and their effects on coastal carbon storage rates. In: *Baseline and Projected Future Carbon Storage and Greenhouse-Gas Fluxes in Ecosystems of the Western United States.* [Z. Zhu and B. Reed (eds.)]. U.S. Department of the Interior. U.S. Geological Survey Professional Paper 1797, 143-158 pp. [https://pubs.usgs.gov/pp/1797/]

Bergamaschi, B., and L. Windham-Myers, 2018: Published data. AmeriFlux US-Srr Suisun marsh - Rush Ranch. doi: 10.17190/AMF/1418685.

Bhatt, U. S., D. A. Walker, M. K. Raynolds, J. C. Comiso, H. E. Epstein, G. Jia, R. Gens, J. E. Pinzon, C. J. Tucker, C. E. Tweedie, and P. J. Webber, 2010: Circumpolar Arctic tundra vegetation change is linked to sea ice decline. *Earth Interactions*, **14**(8), 1-20, doi: 10.1175/2010ei315.1.

Bianchi, T. S., 2006: *Biogeochemistry of Estuaries.* Oxford University Press, 720 pp.

Bianchi, T. S., and M. A. Allison, 2009: Large-river delta-front estuaries as natural "recorders" of global environmental change. *Proceedings of the National Academy of Sciences USA*, **106**(20), 8085-8092, doi: 10.1073/pnas.0812878106.

Bianchi, T. S., M. A. Allison, J. Zhao, X. Li, R. S. Comeaux, R. A. Feagin, and R. W. Kulawardhana, 2013: Historical reconstruction of mangrove expansion in the Gulf of Mexico: Linking climate change with carbon sequestration in coastal wetlands. *Estuarine, Coastal and Shelf Science*, **119**, 7-16, doi: 10.1016/j.ecss.2012.12.007.

Borges, A. V., 2005: Do we have enough pieces of the jigsaw to integrate CO_2 fluxes in the coastal ocean? *Estuaries*, **28**(1), 3-27, doi: 10.1007/bf02732750.

Borges, A. V., and G. Abril, 2011: Carbon dioxide and methane dynamics in estuaries. In: *Treatise on Estuarine and Coastal Science*. [E. Wolanski and D. McLusky (eds.)]. Academic Press, 119-161 pp.

Borges, A. V., and N. Gypens, 2010: Carbonate chemistry in the coastal zone responds more strongly to eutrophication than ocean acidification. *Limnology and Oceanography*, **55**(1), 346-353, doi: 10.4319/lo.2010.55.1.0346.

Borges, A. V, B. Delille, and M. Frankignoulle, 2005: Budgeting sinks and sources of CO_2 in the coastal ocean: Diversity of ecosystems counts. *Geophysical Research Letters*, **32**(14), doi: 10.1029/2005gl023053.

Boyer, E. W., R. W. Howarth, J. N. Galloway, F. J. Dentener, P. A. Green, and C. J. Vörösmarty, 2006: Riverine nitrogen export from the continents to the coasts. *Global Biogeochemical Cycles*, **20**(1), doi: 10.1029/2005gb002537.

Breithaupt, J. L., J. M. Smoak, T. J. Smith, and C. J. Sanders, 2014: Temporal variability of carbon and nutrient burial, sediment accretion, and mass accumulation over the past century in a carbonate platform mangrove forest of the Florida Everglades. *Journal of Geophysical Research: Biogeosciences*, **119**(10), 2032-2048, doi: 10.1002/2014jg002715.

Bricker, S., B. Longstaff, W. Dennison, A. Jones, K. Boicourt, C. Wicks, and J. Woerner, 2007: *Effects of Nutrient Enrichment in the Nation's Estuaries: A Decade of Change. National Estuarine Eutrophication Assessment Update.* NOAA's National Centers for Coastal Ocean Science, 328 pp. [https://yosemite.epa.gov/oa/EAB_Web_Docket.nsf/(Filings)/3BE82A42C7ED8C3585257B120059CB8A/$File/Opposition%20to%20Petition%20for%20Review%20--%20Ex.%2010%20Part1...23.53.pdf]

Bridgham, S. D., J. P. Megonigal, J. K. Keller, N. B. Bliss, and C. Trettin, 2006: The carbon balance of North American wetlands. Wetlands, 26(4), 889-916, doi: 10.1672/0277-5212(2006)26[889:tcbona]2.0.co;2.

Brown, S. C., 2006: *Arctic Wings: Birds of the Arctic National Wildlife Refuge.* Mountaineers Books. Seattle, WA.

Caffrey, J. M., 2004: Factors controlling net ecosystem metabolism in U.S. estuaries. *Estuaries*, **27**(1), 90-101, doi: 10.1007/bf02803563.

Cahoon, D. R., 2006: A review of major storm impacts on coastal wetland elevations. *Estuaries and Coasts*, **29**(6), 889-898, doi: 10.1007/bf02798648.

Cai, W. J., 2011: Estuarine and coastal ocean carbon paradox: CO_2 sinks or sites of terrestrial carbon incineration? *Annual Review of Marine Science*, **3**, 123-145, doi: 10.1146/annurev-marine-120709-142723.

Cai, W. J., and Y. Wang, 1998: The chemistry, fluxes, and sources of carbon dioxide in the estuarine waters of the Satilla and Altamaha Rivers, Georgia. *Limnology and Oceanography*, **43**(4), 657-668, doi: 10.4319/lo.1998.43.4.0657.

Cai, W. J., W. J. Huang, G. W. Luther, 3rd, D. Pierrot, M. Li, J. Testa, M. Xue, A. Joesoef, R. Mann, J. Brodeur, Y. Y. Xu, B. Chen, N. Hussain, G. G. Waldbusser, J. Cornwell, and W. M. Kemp, 2017: Redox reactions and weak buffering capacity lead to acidification in the Chesapeake Bay. *Nature Communications*, **8**(1), 369, doi: 10.1038/s41467-017-00417-7.

Cai, W.-J., X. Hu, W.-J. Huang, M. C. Murrell, J. C. Lehrter, S. E. Lohrenz, W.-C. Chou, W. Zhai, J. T. Hollibaugh, Y. Wang, P. Zhao, X. Guo, K. Gundersen, M. Dai, and G.-C. Gong, 2011: Acidification of subsurface coastal waters enhanced by eutrophication. *Nature Geoscience*, **4**(11), 766-770, doi: 10.1038/ngeo1297.

Callaway, J. C., E. L. Borgnis, R. E. Turner, and C. S. Milan, 2012: Carbon sequestration and sediment accretion in San Francisco Bay tidal wetlands. *Estuaries and Coasts*, **35**(5), 1163-1181, doi: 10.1007/s12237-012-9508-9.

Camacho-Ibar, V. F., J. D. Carriquiry, and S. V. Smith, 2003: Non-conservative P and N fluxes and net ecosystem production in San Quintin Bay, México. *Estuaries*, **26**(5), 1220-1237, doi: 10.1007/bf02803626.

Canuel, E. A., S. S. Cammer, H. A. McIntosh, and C. R. Pondell, 2012: Climate change impacts on the organic carbon cycle at the land-ocean interface. *Annual Review of Earth and Planetary Sciences*, **40**(1), 685-711, doi: 10.1146/annurev-earth-042711-105511.

Cavanaugh, K. C., J. R. Kellner, A. J. Forde, D. S. Gruner, J. D. Parker, W. Rodriguez, and I. C. Feller, 2014: Poleward expansion of mangroves is a threshold response to decreased frequency of extreme cold events. *Proceedings of the National Academy of Sciences USA*, **111**(2), 723-727, doi: 10.1073/pnas.1315800111.

CCSP, 2007: *First State of the Carbon Cycle Report (SOCCR): The North American Carbon Budget and Implications for the Global Carbon Cycle. A Report by the U.S. Climate Change Science Program and the Subcommittee on Global Change Research.* [A. W. King, L. Dilling, G. P. Zimmerman, D. M. Fairman, R. A. Houghton, G. Marland, A. Z. Rose, and T. J. Wilbanks (eds.)]. National Oceanic and Atmospheric Administration, National Climatic Data Center, Asheville, NC, USA, 242 pp.

CEC, 2016: *North American Blue Carbon, 2015 Map Files*. Commission for Environmental Cooperation. [http://www.cec.org/tools-and-resources/map-files/north-american-blue-carbon-2017]

CEC, 2017: *Seagrass Sediment Sampling Protocol and Field Study Montreal, Canada*. Commission for Environmental Cooperation, 48 pp.

Chan, F., A. B. Boehm, J. A. Barth, E. A. Chornesky, A. G. Dickson, R. A. Feely, B. Hales, T. M. Hill, G. Hofmann, D. Ianson, T. Klinger, J. Largier, J. Newton, T. F. Pedersen, G. N. Somero, M. Sutula, W. W. Wakefield, G. G. Waldbusser, S. B. Weisberg, and E. A. Whiteman, 2016: *The West Coast Ocean Acidification and Hypoxia Science Panel: Major Findings, Recommendations, and Actions.* California Ocean Science Trust. [http://westcoastoah.org/wp-content/uploads/2016/04/OAH-Panel-Key-Findings-Recommendations-and-Actions-4.4.16-FINAL.pdf]

Chan, F., J. A. Barth, C. A. Blanchette, R. H. Byrne, F. Chavez, O. Cheriton, R. A. Feely, G. Friederich, B. Gaylord, T. Gouhier, S. Hacker, T. Hill, G. Hofmann, M. A. McManus, B. A. Menge, K. J. Nielsen, A. Russell, E. Sanford, J. Sevadjian, and L. Washburn, 2017: Persistent spatial structuring of coastal ocean acidification in the California current system. *Scientific Reports*, **7**(1), 2526, doi: 10.1038/s41598-017-02777-y.

Chen, C. T. A., T. H. Huang, Y. C. Chen, Y. Bai, X. He, and Y. Kang, 2013: Air–sea exchanges of CO_2 in the world's coastal seas. *Biogeosciences*, **10**(10), 6509-6544, doi: 10.5194/bg-10-6509-2013.

Chen, C., H. Liu, and R. C. Beardsley, 2003: An unstructured grid, finite-volume, three-dimensional, primitive equations ocean model: Application to coastal ocean and estuaries. *Journal of Atmospheric and Oceanic Technology*, **20**(1), 159-186, doi: 10.1175/1520-0426(2003)020<0159:augfvt>2.0.co;2.

Chmura, G. L., 2013: What do we need to assess the sustainability of the tidal salt marsh carbon sink? *Ocean and Coastal Management*, **83**, 25-31, doi: 10.1016/j.ocecoaman.2011.09.006.

Chmura, G. L., L. Kellman, L. van Ardenne, and G. R. Guntenspergen, 2016: Greenhouse gas fluxes from salt marshes exposed to chronic nutrient enrichment. *PLOS One*, **11**(2), e0149937, doi: 10.1371/journal.pone.0149937.

Chmura, G. L., S. C. Anisfeld, D. R. Cahoon, and J. C. Lynch, 2003: Global carbon sequestration in tidal, saline wetland soils. *Global Biogeochemical Cycles*, **17**(4), doi: 10.1029/2002gb001917.

Cloern, J. E., S. Q. Foster, and A. E. Kleckner, 2014: Phytoplankton primary production in the world's estuarine-coastal ecosystems. *Biogeosciences*, **11**(9), 2477-2501, doi: 10.5194/bg-11-2477-2014.

Cloern, J., A. Robinson, L. Grenier, R. Grossinger, K. Boyer, J. Burau, E. Canuel, J. DeGeorge, J. Drexler, C. Enright, E. Howe, R. Kneib, A. Mueller-Solger, R. Naiman, J. Pinckney, S. Safran, D. Schoellhamer, and C. Simenstad, 2016: Primary production in the Delta: Then and now. *San Francisco Estuary and Watershed Science*, **14**(3), doi: 10.15447/sfews.2016v14iss3art1.

Colman, S. M., P. C. Baucom, J. F. Bratton, T. M. Cronin, J. P. McGeehin, D. Willard, A. R. Zimmerman, and P. R. Vogt, 2002: Radiocarbon dating, chronologic framework, and changes in accumulation rates of Holocene estuarine sediments from Chesapeake Bay. *Quaternary Research*, **57**(1), 58-70, doi: 10.1006/qres.2001.2285.

Contreras-Espinosa, F., and B. G. Warner, 2004: Ecosystem characteristics and management considerations for coastal wetlands in Mexico. *Hydrobiologia*, **511**(1), 233-245, doi: 10.1023/b:hydr.0000014097.74263.54.

Cooley, S., E. Jewett, J. Reichert, L. Robbins, G. Shrestha, D. Wieczorek, and S. Weisberg, 2015: Getting ocean acidification on decision makers' to-do lists: Dissecting the process through case studies. *Oceanography*, **25**(2), 198-211, doi: 10.5670/oceanog.2015.42.

Couvillion, B. R., H. Beck, D. Schoolmaster, and M. Fischer, 2017: Land area change in coastal Louisiana (1932 to 2016). *Scientific Investigations Map 3381*, doi: 10.3133/sim3381. [http://pubs.er.usgs.gov/publication/sim3381]

CRMS, 2017: *Louisiana Coastwide Reference Monitoring System*. [https://www.lacoast.gov/crms2/home.aspx]

Crosswell, J. R., I. C Anderson, J. W. Stanhope, B. Van Dam, M. J. Brush, S. Ensign, M. F. Piehler, B. McKee, M. Bost, and H. W. Paerl, 2017: Carbon budget of a shallow, lagoonal estuary: Transformations and source-sink dynamics along the river-estuary-ocean continuum. *Limnology and Oceanography,* **62**(5), S29-S45, doi: 10.1002/lno.10631.

Crosswell, J. R., M. S. Wetz, B. Hales, and H. W. Paerl, 2012: Air-water CO_2 fluxes in the microtidal Neuse River Estuary, North Carolina. *Journal of Geophysical Research: Oceans*, **117**, C08017, doi: 10.1029/2012jc007925.

Crosswell, J. R., M. S. Wetz, B. Hales, and H. W. Paerl, 2014: Extensive CO_2 emissions from shallow coastal waters during passage of Hurricane Irene (August 2011) over the Mid-Atlantic coast of the U.S.A. *Limnology and Oceanography*, **59**(5), 1651-1665, doi: 10.4319/lo.2014.59.5.1651.

Dahl, T. E. 2011: *Status and Trends of Wetlands in the Conterminous United States 2004 to 2009*. U.S. Department of the Interior; Fish and Wildlife Service, Washington, D.C. 108 pp.

Dalrymple, R. W., B. A. Zaitlin, and R. Boyd, 1992: Estuarine facies models; conceptual basis and stratigraphic implications. *Journal of Sedimentary Research*, **62**(6), 1130-1146, doi: 10.1306/d4267a69-2b26-11d7-8648000102c1865d.

Davidson, C. W., 2015: *Spatial and Temporal Variability of Coastal Carbonate Chemistry in the Southern California Region*. M.S. Thesis, Earth Sciences, University of California San Diego, 37 pp.

Davis, K. A., N. S. Banas, S. N. Giddings, S. A. Siedlecki, P. MacCready, E. J. Lessard, R. M. Kudela, and B. M. Hickey, 2014: Estuary-enhanced upwelling of marine nutrients fuels coastal productivity in the U.S. Pacific Northwest. *Journal of Geophysical Research: Oceans*, **119**(12), 8778-8799, doi: 10.1002/2014jc010248.

Day, J., W. Kemp, A. Yanez-Arancibia, and B. C. Crump, 2013: *Estuarine Ecology, 2nd edition.* Wiley-Blackwell 568 pp.

de Angelis, M. A., and M. I. Scranton, 1993: Fate of methane in the Hudson River and Estuary. *Global Biogeochemical Cycles*, **7**(3), 509-523, doi: 10.1029/93gb01636.

DeFries, R., and H. Nagendra, 2017: Ecosystem management as a wicked problem. *Science*, **356**(6335), 265-270, doi: 10.1126/science.aal1950.

DeLaune, R. D., and J. R. White, 2011: Will coastal wetlands continue to sequester carbon in response to an increase in global sea level?: A case study of the rapidly subsiding Mississippi River Deltaic Plain. *Climatic Change*, **110**(1-2), 297-314, doi: 10.1007/s10584-011-0089-6.

DeLaune, R. D., C. J. Smith, and W. H. Patrick, 1983: Methane release from Gulf Coast wetlands. *Tellus B*, **35B**(1), 8-15, doi: 10.1111/j.1600-0889.1983.tb00002.x.

Dessu, S. B., R. M. Price, T. G. Troxler, and J. S. Kominoski, 2018: Effects of sea-level rise and freshwater management on long-term water levels and water quality in the Florida Coastal Everglades. *Journal of Environmental Management*, **211**, 164-176, doi: 10.1016/j.jenvman.2018.01.025.

Di Lorenzo, E., and N. Mantua, 2016: Multi-year persistence of the 2014/15 North Pacific Marine Heatwave. *Nature Climate Change*, **6**(11), 1042-1047, doi: 10.1038/nclimate3082.

Doughty, C. L., J. A. Langley, W. S. Walker, I. C. Feller, R. Schaub, and S. K. Chapman, 2015: Mangrove range expansion rapidly increases coastal wetland carbon storage. *Estuaries and Coasts*, **39**(2), 385-396, doi: 10.1007/s12237-015-9993-8.

Downing, B. D., E. Boss, B. A. Bergamaschi, J. A. Fleck, M. A. Lionberger, N. K. Ganju, D. H. Schoellhamer, and R. Fujii, 2009: Quantifying fluxes and characterizing compositional changes of dissolved organic matter in aquatic systems in situ using combined acoustic and optical measurements. *Limnology and Oceanography: Methods*, **7**(1), 119-131, doi: 10.4319/lom.2009.7.119.

Drexler, J. Z., C. S. de Fontaine, and T. A. Brown, 2009: Peat accretion histories during the past 6,000 years in marshes of the Sacramento–San Joaquin Delta, CA, USA. *Estuaries and Coasts*, **32**(5), 871-892, doi: 10.1007/s12237-009-9202-8.

Duarte, C. M., I. E. Hendriks, T. S. Moore, Y. S. Olsen, A. Steckbauer, L. Ramajo, J. Carstensen, J. A. Trotter, and M. McCulloch, 2013: Is ocean acidification an open-ocean syndrome? Understanding anthropogenic impacts on seawater pH. *Estuaries and Coasts*, **36**(2), 221-236, doi: 10.1007/s12237-013-9594-3.

Duarte, C. M., J. J. Middelburg, and N. Caraco, 2005: Major role of marine vegetation on the oceanic carbon cycle. *Biogeosciences*, **2**(1), 1-8, doi: 10.5194/bg-2-1-2005.

Duman, T., and K. V. R. Schäfer, 2018: Partitioning net ecosystem carbon exchange of native and invasive plant communities by vegetation cover in an urban tidal wetland in the New Jersey Meadowlands (USA). *Ecological Engineering*, **114**, 16-24, doi: 10.1016/j.ecoleng.2017.08.031.

Edwards, K. R., and C. E. Proffitt, 2003: Comparison of wetland structural characteristics between created and natural salt marshes in southwest Louisiana, USA. *Wetlands*, **23**(2), 344-356, doi: 10.1672/10-20.

Ekstrom, J. A., L. Suatoni, S. R. Cooley, L. H. Pendleton, G. G. Waldbusser, J. E. Cinner, J. Ritter, C. Langdon, R. van Hooidonk, D. Gledhill, K. Wellman, M. W. Beck, L. M. Brander, D. Rittschof, C. Doherty, P. E. T. Edwards, and R. Portela, 2015: Vulnerability and adaptation of US shellfisheries to ocean acidification. *Nature Climate Change*, **5**(3), 207-214, doi: 10.1038/nclimate2508.

Ember, L. M., D. F. Williams, and J. T. Morris, 1987: Processes that influence carbon isotope variations in salt-marsh sediments. *Marine Ecology Progress Series*, **36**(1), 33-42, doi: DOI 10.3354/meps036033.

Evans, W., B. Hales, P. G. Strutton, and D. Ianson, 2012: Sea-air CO_2 fluxes in the Western Canadian coastal ocean. *Progress in Oceanography*, **101**(1), 78-91, doi: 10.1016/j.pocean.2012.01.003.

Ezcurra, P., E. Ezcurra, P. P. Garcillan, M. T. Costa, and O. Aburto-Oropeza, 2016: Coastal landforms and accumulation of mangrove peat increase carbon sequestration and storage. *Proceedings of the National Academy of Sciences USA*, **113**(16), 4404-4409, doi: 10.1073/pnas.1519774113.

Fabry, V., J. McClintock, J. Mathis, and J. Grebmeier, 2009: Ocean acidification at high latitudes: The bellwether. *Oceanography*, **22**(4), 160-171, doi: 10.5670/oceanog.2009.105.

Fagan, K. E., and F. T. Mackenzie, 2007: Air–sea CO_2 exchange in a subtropical estuarine-coral reef system, Kaneohe Bay, Oahu, Hawaii. *Marine Chemistry*, **106**(1-2), 174-191, doi: 10.1016/j.marchem.2007.01.016.

Fagherazzi, S., G. Mariotti, P. Wiberg, and K. McGlathery, 2013: Marsh collapse does not require sea level rise. *Oceanography*, **26**(3), 70-77, doi: 10.5670/oceanog.2013.47.

Feely, R. A., S. R. Alin, J. Newton, C. L. Sabine, M. Warner, A. Devol, C. Krembs, and C. Maloy, 2010: The combined effects of ocean acidification, mixing, and respiration on pH and carbonate saturation in an urbanized estuary. *Estuarine, Coastal and Shelf Science*, **88**(4), 442-449, doi: 10.1016/j.ecss.2010.05.004.

Feely, R. A., T. Klinger, J. A. Newton, and M. Chadsey, 2012: *Scientific Summary of Ocean Acidification in Washington State Marine Waters*. National Oceanic and Atmospheric Administration Oceanic and Atmospheric Research Division Special Report.

Feng, Y., M. A. M., Friedrichs, J., Wilkin, H., Tian, Q., Yang, E. E., Hofmann, J. D., Wiggert, R. R., Hood, 2015. Chesapeake Bay nitrogen fluxes derived from a land-estuarine-ocean biogeochemical modeling system: Model description, evaluation and nitrogen budgets. *Journal of Geophysical Research: Biogeosciences*, **120**, 1666-1695, doi:10.1002/2015JG002931.

Firestone, M., and E. Davidson, 1989: Microbiological basis of NO and N_2O production and consumption in soil. In: *Exchange of Trace Gases between terrestrial Ecosystems and the Atmosphere* **47**, [M. O. Andreac and D. S. Schimel (eds.)]. John Wiley and Sons Ltd., 7-21 pp.

Forbrich, I., and A. E. Giblin, 2015: Marsh-atmosphere CO_2 exchange in a New England salt marsh. *Journal of Geophysical Research: Biogeosciences*, **120**(9), 1825-1838, doi: 10.1002/2015jg003044.

Fourqurean, J. W., C. M. Duarte, H. Kennedy, N. Marbà, M. Holmer, M. A. Mateo, E. T. Apostolaki, G. A. Kendrick, D. Krause-Jensen, K. J. McGlathery, and O. Serrano, 2012: Seagrass ecosystems as a globally significant carbon stock. *Nature Geoscience*, **5**(7), 505-509, doi: 10.1038/ngeo1477.

Gabler, C. A., M. J. Osland, J. B. Grace, C. L. Stagg, R. H. Day, S. B. Hartley, N. M. Enwright, A. S. From, M. L. McCoy, and J. L. McLeod, 2017: Macroclimatic change expected to transform coastal wetland ecosystems this century. *Nature Climate Change*, **7**(2), 142-147, doi: 10.1038/nclimate3203.

Gallagher, J. L., R. J. Reimold, R. A. Linthurst, and W. J. Pfeiffer, 1980: Aerial production, mortality, and mineral accumulation-export dynamics in *Spartina alterniflora* and *Juncus roemerianus* plant stands in a Georgia salt marsh. *Ecology*, **61**(2), 303-312, doi: 10.2307/1935189.

Galloway, J. N., A. R. Townsend, J. W. Erisman, M. Bekunda, Z. Cai, J. R. Freney, L. A. Martinelli, S. P. Seitzinger, and M. A. Sutton, 2008: Transformation of the nitrogen cycle: Recent trends, questions, and potential solutions. *Science*, **320**(5878), 889-892, doi: 10.1126/science.1136674.

Ganju, N. K., M. Hayn, S.-N. Chen, R. W. Howarth, P. J. Dickhudt, A. L. Aretxabaleta, and R. Marino, 2012: Tidal and groundwater fluxes to a shallow, microtidal estuary: Constraining inputs through field observations and hydrodynamic modeling. *Estuaries and Coasts*, **35**(5), 1285-1298, doi: 10.1007/s12237-012-9515-x.

Gelesh, L., K. Marshall, W. Boicourt, and L. Lapham, 2016: Methane concentrations increase in bottom waters during summertime anoxia in the highly eutrophic estuary, Chesapeake Bay, U.S.A. *Limnology and Oceanography*, **61**(S1), S253-S266, doi: 10.1002/lno.10272.

Giri, C. P., and J. Long, 2014: Mangrove reemergence in the northernmost range limit of Eastern Florida. *Proceedings of the National Academy of Sciences USA*, **111**(15), E1447-1448, doi: 10.1073/pnas.1400687111.

Giri, C., E. Ochieng, L. L. Tieszen, Z. Zhu, A. Singh, T. Loveland, J. Masek, and N. Duke, 2011: Status and distribution of mangrove forests of the world using Earth observation satellite data. *Global Ecology and Biogeography*, **20**(1), 154-159, doi: 10.1111/j.1466-8238.2010.00584.x.

Hales, B., A. Suhrbier, G. G. Waldbusser, R. A. Feely, and J. A. Newton, 2016: The carbonate chemistry of the "fattening line," Willapa Bay, 2011–2014. *Estuaries and Coasts*, **40**(1), 173-186, doi: 10.1007/s12237-016-0136-7.

Hamilton, S. E., and D. Casey, 2016: Creation of a high spatio-temporal resolution global database of Continuous Mangrove Forest Cover for the 21st century (CGMFC-21). *Global Ecology and Biogeography*, **25**(6), 729-738, doi: 10.1111/geb.12449.

Hernández-Ayón, J. M., V. F. Camacho-Ibar, A. Mejía-Trejo, and A. Cabello-Pasini, 2007: Variabilidad del CO_2 total durante eventos de surgencia en bahía de san quintín, Baja California Mexico. In: *Carbono en Ecosistemas Acuáticos de México*. Secretaría de Medio Ambiente y Recursos Naturales Instituto Nacional de Ecología Centro de Investigaciones Científicas y de Educación de Ensenada, 187-200 pp.

Herrmann, M., R. G. Najjar, W. M. Kemp, R. B. Alexander, E. W. Boyer, W.-J. Cai, P. C. Griffith, K. D. Kroeger, S. L. McCallister, and R. A. Smith, 2015: Net ecosystem production and organic carbon balance of U.S. east coast estuaries: A synthesis approach. *Global Biogeochemical Cycles*, **29**(1), 96-111, doi: 10.1002/2013gb004736.

Hinson, A. L., R. A. Feagin, M. Eriksson, R. G. Najjar, M. Herrmann, T. S. Bianchi, M. Kemp, J. A. Hutchings, S. Crooks, and T. Boutton, 2017: The spatial distribution of soil organic carbon in tidal wetland soils of the continental United States. *Global Change Biology*, 1-13, doi: 10.1111/gcb.13811.

Holm, G. O., B. C. Perez, D. E. McWhorter, K. W. Krauss, D. J. Johnson, R. C. Raynie, and C. J. Killebrew, 2016: Ecosystem level methane fluxes from tidal freshwater and brackish marshes of the Mississippi River Delta: Implications for coastal wetland carbon projects. *Wetlands*, **36**(3), 401-413, doi: 10.1007/s13157-016-0746-7.

Holmquist, J. R., L. Windham-Myers, N. Bliss, S. Crooks, J. T. Morris, J. P. Megonigal, T. Troxler, D. Weller, J. Callaway, J. Drexler, M. C. Ferner, M. E. Gonneea, K. D. Kroeger, L. Schile-Beers, I. Woo, K. Buffington, J. Breithaupt, B. M. Boyd, L. N. Brown, N. Dix, L. Hice, B. P. Horton, G. M. MacDonald, R. P. Moyer, W. Reay, T. Shaw, E. Smith, J. M. Smoak, C. Sommerfield, K. Thorne, D. Velinsky, E. Watson, K. W. Grimes, and M. Woodrey, 2018a: Accuracy and precision of tidal wetland soil carbon mapping in the conterminous United States. *Scientific Reports*, **8**(1), 9478, doi: 10.1038/s41598-018-26948-7.

Holmquist, J., L. Windham-Myers, B. Bernal, K. B. Byrd, S. Crooks, M. E. Gonneea, N. Herold, S. H. Knox, K. D. Kroeger, J. McCombs, J. P. Megonigal, L. Meng, J. T. Morris, A. E. Sutton-Grier, T. G. Troxler, and D. E. Weller, 2018b: Uncertainty in United States coastal wetland greenhouse gas inventorying. *Environmental Research Letters*, 105350, doi: 10.1088/1748-9326/aae157.

Hopkinson, C. S., 1985: Shallow-water benthic and pelagic metabolism. *Marine Biology*, **87**(1), 19-32, doi: 10.1007/bf00397002.

Hopkinson, C. S., 1988: Patterns of organic carbon exchange between coastal ecosystems. In: *Coastal-Offshore Ecosystem Interactions*. Proceedings of a symposium sponsored by SCOR, UNESCO, San Francisco Society, California Sea Grant program, and the U.S. Department of Interior, Mineral Management Service held at San Francisco State University, Tiburon, California, April 7–22, 1986. [B. O. Jansson (ed.)]. Springer Berlin Heidelberg, 122-154 pp.

Hopkinson, C. S., and J. J. Vallino, 1995: The relationships among man's activities in watersheds and estuaries: A model of runoff effects on patterns of estuarine community metabolism. *Estuaries*, **18**(4), 598, doi: 10.2307/1352380.

Hopkinson, C. S., W.-J. Cai, and X. Hu, 2012: Carbon sequestration in wetland dominated coastal systems—a global sink of rapidly diminishing magnitude. *Current Opinion in Environmental Sustainability*, **4**(2), 186-194, doi: 10.1016/j.cosust.2012.03.005.

Hossler, K., and J. E. Bauer, 2013: Amounts, isotopic character, and ages of organic and inorganic carbon exported from rivers to ocean margins: 1. Estimates of terrestrial losses and inputs to the Middle Atlantic Bight. *Global Biogeochemical Cycles*, **27**(2), 331-346, doi: 10.1002/gbc.20033.

Howard, J., A. Sutton-Grier, D. Herr, J. Kleypas, E. Landis, E. McLeod, E. Pidgeon, and S. Simpson, 2017: Clarifying the role of coastal and marine systems in climate mitigation. *Frontiers in Ecology and the Environment*, **15**(1), 42-50, doi: 10.1002/fee.1451.

Howarth, R. W., D. Anderson, J. Cloern, C. Elfring, C. Hopkinson, B. Lapointe, T. Malone, N. Marcus, K. McGlathery, A. Sharpley, and D. Walker, 2000: Nutrient pollution of coastal rivers, bays and seas. *Issues in Ecology*, **7**, 1-15.

Huang, W. J., W. J. Cai, Y. Wang, S. E. Lohrenz, and M. C. Murrell, 2015: The carbon dioxide system on the Mississippi River-dominated continental shelf in the Northern Gulf of Mexico: 1. Distribution and air-sea CO_2 flux. *Journal of Geophysical Research: Oceans*, **120**(3), 1429-1445, doi: 10.1002/2014JC010498.

Hunt, C. W., J. E. Salisbury, and D. Vandemark, 2014: CO_2 input dynamics and air–sea exchange in a large New England estuary. *Estuaries and Coasts*, **37**(5), 1078-1091, doi: 10.1007/s12237-013-9749-2.

Hunt, C. W., J. E. Salisbury, and D. Vandemark, 2011: Contribution of non-carbonate anions to total alkalinity and overestimation of pCO$_2$ in New England and New Brunswick rivers. *Biogeosciences*, **8**(10), 3069-3076, doi: 10.5194/bg-8-3069-2011.

Irby, I. D., M. A. M. Friedrichs, C. T. Friedrichs, A. J. Bever, R. R. Hood, L. W. J. Lanerolle, M. Li, L. Linker, M. E. Scully, K. Sellner, J. Shen, J. Testa, H. Wang, P. Wang, and M. Xia, 2016: Challenges associated with modeling low-oxygen waters in Chesapeake Bay: A multiple model comparison. *Biogeosciences*, **13**(7), 2011-2028, doi: 10.5194/bg-13-2011-2016.

Irby, I. D., M. A. M. Friedrichs, F. Da, and K. E. Hinson, 2018: The competing impacts of climate change and nutrient reductions on dissolved oxygen in Chesapeake Bay. *Biogeosciences*, **15**(9), 2649-2668, doi: 10.5194/bg-15-2649-2018.

Jackley, J., L. Gardner, A. F. Djunaedi, and A. K. Salomon, 2016: Ancient clam gardens, traditional management portfolios, and the resilience of coupled human-ocean systems. *Ecology and Society*, **21**(4), doi: 10.5751/es-08747-210420.

Jankowski, K. L., T. E. Tornqvist, and A. M. Fernandes, 2017: Vulnerability of Louisiana's coastal wetlands to present-day rates of relative sea-level rise. *Nature Communications*, **8**, 14792, doi: 10.1038/ncomms14792.

Jiang, L. Q., W. J. Cai, Y. Wang, and J. E. Bauer, 2013: Influence of terrestrial inputs on continental shelf carbon dioxide. *Biogeosciences*, **10**(2), 839-849, doi: 10.5194/bg-10-839-2013.

Jiang, L.-Q., W.-J. Cai, and Y. Wang, 2008: A comparative study of carbon dioxide degassing in river- and marine-dominated estuaries. *Limnology and Oceanography*, **53**(6), 2603-2615, doi: 10.4319/lo.2008.53.6.2603.

Joesoef, A., W. J. Huang, Y. Gao, and W. J. Cai, 2015: Air–water fluxes and sources of carbon dioxide in the Delaware Estuary: Spatial and seasonal variability. *Biogeosciences*, **12**(20), 6085-6101, doi: 10.5194/bg-12-6085-2015.

Johannessen, S. C., R. W. Macdonald, and D. W. Paton, 2003: A sediment and organic carbon budget for the greater Strait of Georgia. *Estuarine, Coastal and Shelf Science*, **56**(3-4), 845-860, doi: 10.1016/s0272-7714(02)00303-7.

Kathilankal, J. C., T. J. Mozdzer, J. D. Fuentes, P. D'Odorico, K. J. McGlathery, and J. C. Zieman, 2008: Tidal influences on carbon assimilation by a salt marsh. *Environmental Research Letters*, **3**(4), 044010, doi: 10.1088/1748-9326/3/4/044010.

Kelley, C. A., C. S. Martens, and W. Ussler, 1995: Methane dynamics across a tidally flooded riverbank margin. *Limnology and Oceanography*, **40**(6), 1112-1129, doi: 10.4319/lo.1995.40.6.1112.

Kemp, W. M., E. M. Smith, M. Marvin-DiPasquale, and W. R. Boynton, 1997: Organic carbon balance and net ecosystem metabolism in Chesapeake Bay. *Marine Ecology Progress Series*, **150**, 229-248, doi: 10.3354/meps150229.

Kennedy, H., D. M. Alongi, A. Karim, G. Chen, G. L. Chmura, S. Crooks, J. G. Kairo, B. Liao, and G. Lin, 2014: Coastal Wetlands. In: *2013 Supplement to the 2006 Intergovernmental Panel on Climate Change Guidelines for National Greenhouse Gas Inventories: Wetlands*. [T. Hiraishi, T. Krug, K. Tanabe, N. Srivastava, J. Baasansuren, M. Fukuda, et al. (eds.)]. Switzerland, pp 4.1-4.55.

Kennedy, H., J. Beggins, C. M. Duarte, J. W. Fourqurean, M. Holmer, N. Marbà, and J. J. Middelburg, 2010: Seagrass sediments as a global carbon sink: Isotopic constraints. *Global Biogeochemical Cycles*, **24**(4), doi: 10.1029/2010gb003848.

Kenov Ascione, I., F. Campuzano, G. Franz, R. Fernandes, C. Viegas, J. Sobrinho, H. de Pablo, A. Amaral, L. Pinto, M. Mateus, and R. Neves, 2014: Advances in modeling of water quality in estuaries. In: *Remote Sensing and Modeling: Advances in Coastal and Marine Resources*. [C. W. Finkl and C. Makowski (eds.)]. Coastal Research Library 9. Springer, 237-276 pp.

Kirwan, M. L., A. B. Murray, J. P. Donnelly, and D. R. Corbett, 2011: Rapid wetland expansion during European settlement and its implication for marsh survival under modern sediment delivery rates. *Geology*, **39**(5), 507-510, doi: 10.1130/g31789.1.

Kirwan, M. L., and J. P. Megonigal, 2013: Tidal wetland stability in the face of human impacts and sea-level rise. *Nature*, **504**(7478), 53-60, doi: 10.1038/nature12856.

Kirwan, M. L., and L. K. Blum, 2011: Enhanced decomposition offsets enhanced productivity and soil carbon accumulation in coastal wetlands responding to climate change. *Biogeosciences*, **8**(4), 987-993.

Kirwan, M. L., G. R. Guntenspergen, A. D'Alpaos, J. T. Morris, S. M. Mudd, and S. Temmerman, 2010: Limits on the adaptability of coastal marshes to rising sea level. *Geophysical Research Letters*, **37**(23), doi: 10.1029/2010gl045489.

Kirwan, M. L., G. R. Guntenspergen, and J. T. Morris, 2009: Latitudinal trends in *Spartina alterniflora* productivity and the response of coastal marshes to global change. *Global Change Biology*, **15**(8), 1982-1989, doi: 10.1111/j.1365-2486.2008.01834.x.

Knox, S. H., L. Windham-Myers, F. Anderson, C. Sturtevant, and B. Bergamaschi, 2018: Direct and indirect effects of tides on ecosystem-scale CO_2 exchange in a brackish tidal marsh in Northern California. *Journal of Geophysical Research: Biogeosciences*, **123**(3), 787-806, doi: 10.1002/2017JG004048.

Kolker, A. S., M. A. Allison, and S. Hameed, 2011: An evaluation of subsidence rates and sea-level variability in the Northern Gulf of Mexico. *Geophysical Research Letters*, **38**(21), doi: 10.1029/2011gl049458.

Kone, Y. J. M., and A. V. Borges, 2008: Dissolved inorganic carbon dynamics in the waters surrounding forested mangroves of the Ca Mau Province (Vietnam). *Estuarine, Coastal and Shelf Science*, **77**(3), 409-421, doi: 10.1016/j.ecss.2007.10.001.

Krauss, K. W., A. S. From, T. W. Doyle, T. J. Doyle, and M. J. Barry, 2011: Sea-level rise and landscape change influence mangrove encroachment onto marsh in the Ten Thousand Islands Region of Florida, USA. *Journal of Coastal Conservation*, **15**(4), 629-638, doi: 10.1007/s11852-011-0153-4.

Krauss, K. W., and J. L. Whitbeck, 2011: Soil greenhouse gas fluxes during wetland forest retreat along the Lower Savannah River, Georgia (USA). *Wetlands*, **32**(1), 73-81, doi: 10.1007/s13157-011-0246-8.

Krauss, K. W., G. O. Holm, B. C. Perez, D. E. McWhorter, N. Cormier, R. F. Moss, D. J. Johnson, S. C. Neubauer, and R. C. Raynie, 2016: Component greenhouse gas fluxes and radiative balance from two deltaic marshes in Louisiana: Pairing chamber techniques and eddy covariance. *Journal of Geophysical Research: Biogeosciences*, **121**(6), 1503-1521, doi: 10.1002/2015JG003224.

Kroeger, K. D., and M. A. Charette, 2008: Nitrogen biogeochemistry of submarine groundwater discharge. *Limnology and Oceanography*, **53**(3), 1025-1039, doi: 10.4319/lo.2008.53.3.1025.

Kroeger, K. D., S. Crooks, S. Moseman-Valtierra, and J. Tang, 2017: Restoring tides to reduce methane emissions in impounded wetlands: A new and potent blue carbon climate change intervention. *Scientific Reports*, **7**(1), 11914, doi: 10.1038/s41598-017-12138-4.

Lagomasino, D., R. M. Price, D. Whitman, P. K. E. Campbell, and A. Melesse, 2014: Estimating major ion and nutrient concentrations in mangrove estuaries in Everglades National Park using leaf and satellite reflectance. *Remote Sensing of Environment*, **154**, 202-218, doi: 10.1016/j.rse.2014.08.022.

Lane, R. R., S. K. Mack, J. W. Day, R. D. DeLaune, M. J. Madison, and P. R. Precht, 2016: Fate of soil organic carbon during wetland loss. *Wetlands*, **36**(6), 1167-1181, doi: 10.1007/s13157-016-0834-8.

Lara-Lara, J. R., B. E. Frey, and F. L. Small, 1990: Primary production in the Columbia River Estuary I. Spatial temporal variability of properties. *Pacific Science*, **44**(1), 17-37.

Laruelle, G. G., H. H. Dürr, R. Lauerwald, J. Hartmann, C. P. Slomp, N. Goossens, and P. A. G. Regnier, 2013: Global multi-scale segmentation of continental and coastal waters from the watersheds to the continental margins. *Hydrology and Earth System Sciences*, **17**(5), 2029-2051, doi: 10.5194/hess-17-2029-2013.

Laruelle, G. G., R. Lauerwald, B. Pfeil, and P. Regnier, 2014: Regionalized global budget of the CO_2 exchange at the air-water interface in continental shelf seas. *Global Biogeochemical Cycles*, **28**(11), 1199-1214, doi: 10.1002/2014gb004832.

Lu, W., J. Xiao, F. Liu, Y. Zhang, C. Liu, and G. Lin, 2017: Contrasting ecosystem CO_2 fluxes of inland and coastal wetlands: A meta-analysis of eddy covariance data. *Global Change Biology*, **23**(3), 1180-1198, doi: 10.1111/gcb.13424.

Mackenzie, F. T., E. H. De Carlo, and A. Lerman, 2012: Coupled C, N, P, and O biogeochemical cycling at the land-ocean interface. In: *Biogeochemistry,* Vol. 5. Elsevier Inc., 26 pp.

Magenheimer, J. F., T. R. Moore, G. L. Chmura, and R. J. Daoust, 1996: Methane and carbon dioxide flux from a macrotidal salt marsh, Bay of Fundy, New Brunswick. *Estuaries*, **19**(1), 139, doi: 10.2307/1352658.

Marchio, D., M. Savarese, B. Bovard, and W. Mitsch, 2016: Carbon sequestration and sedimentation in mangrove swamps influenced by hydrogeomorphic conditions and urbanization in southwest Florida. *Forests*, **7**(6), 116, doi: 10.3390/f7060116.

Mariotti, G., and S. Fagherazzi, 2013: Critical width of tidal flats triggers marsh collapse in the absence of sea-level rise. *Proceedings of the National Academy of Sciences USA*, **110**(14), 5353-5356, doi: 10.1073/pnas.1219600110.

Mariotti, G., S. Fagherazzi, P. L. Wiberg, K. J. McGlathery, L. Carniello, and A. Defina, 2010: Influence of storm surges and sea level on shallow tidal basin erosive processes. *Journal of Geophysical Research*, **115**(C11), doi: 10.1029/2009jc005892.

Marsh, A. L., K. A. Becraft, and G. A. Somorjai, 2005: Methane dissociative adsorption on the Pt(111) surface over the 300–500 K temperature and 1–10 Torr pressure ranges. *The Journal of Physical Chemistry B*, **109**(28), 13619-13622, doi: 10.1021/jp051718+.

Marsh, A. S., J. A. Arnone, B. T. Bormann, and J. C. Gordon, 2000: The role of equisetum in nutrient cycling in an Alaskan shrub wetland. *Journal of Ecology*, **88**(6), 999-1011, doi: 10.1046/j.1365-2745.2000.00520.x.

Martin, R. M., and S. Moseman-Valtierra, 2015: Greenhouse gas fluxes vary between *Phragmites australis* and native vegetation zones in coastal wetlands along a salinity gradient. *Wetlands*, **35**(6), 1021-1031, doi: 10.1007/s13157-015-0690-y.

Mayorga, E., S. P. Seitzinger, J. A. Harrison, E. Dumont, A. H. W. Beusen, A. F. Bouwman, B. M. Fekete, C. Kroeze, and G. Van Drecht, 2010: Global nutrient export from WaterSheds 2 (NEWS 2): Model development and implementation. *Environmental Modelling and Software*, **25**(7), 837-853, doi: 10.1016/j.envsoft.2010.01.007.

McCabe, R. M., B. M. Hickey, R. M. Kudela, K. A. Lefebvre, N. G. Adams, B. D. Bill, F. M. Gulland, R. E. Thomson, W. P. Cochlan, and V. L. Trainer, 2016: An unprecedented coastwide toxic algal bloom linked to anomalous ocean conditions. *Geophysical Research Letters*, **43**(19), 10366-10376, doi: 10.1002/2016GL070023.

McClelland, J. W., R. M. Holmes, K. H. Dunton, and R. W. Macdonald, 2012: The Arctic Ocean estuary. *Estuaries and Coasts*, **35**(2), 353-368, doi: 10.1007/s12237-010-9357-3.

McGillis, W. R., J. B. Edson, J. E. Hare, and C. W. Fairall, 2001: Direct covariance air-sea CO_2 fluxes. *Journal of Geophysical Research: Oceans*, **106**(C8), 16729-16745, doi: 10.1029/2000jc000506.

McKee, K. L., D. R. Cahoon, and I. C. Feller, 2007: Caribbean mangroves adjust to rising sea level through biotic controls on change in soil elevation. *Global Ecology and Biogeography*, **16**(5), 545-556, doi: 10.1111/j.1466-8238.2007.00317.x.

McLeod, E., G. L. Chmura, S. Bouillon, R. Salm, M. Björk, C. M. Duarte, C. E. Lovelock, W. H. Schlesinger, and B. R. Silliman, 2011: A blueprint for blue carbon: Toward an improved understanding of the role of vegetated coastal habitats in sequestering CO_2. *Frontiers in Ecology and the Environment*, **9**(10), 552-560, doi: 10.1890/110004.

Meeder, J. F., and R. W. Parkinson, 2017: SE Saline Everglades transgressive sedimentation in response to historic acceleration in sea-level rise: A viable marker for the base of the Anthropocene? *Journal of Coastal Research*, **342**, 490-497, doi: 10.2112/jcoastres-d-17-00031.1.

Megonigal, J. P., and W. H. Schlesinger, 2002: Methane-limited methanotrophy in tidal freshwater swamps. *Global Biogeochemical Cycles*, **16**(4), 35-1 to 35-10, doi: 10.1029/2001GB001594.

Meybeck, M., 2003: Global analysis of river systems: From Earth system controls to anthropocene syndromes. *Philosophical Transactions of the Royal Society B. Biological Sciences*, **358**(1440), 1935-1955, doi: 10.1098/rstb.2003.1379.

Montagna, P. A., J. Brenner, J. Gibeaut, and S. Morehead, 2009: Coastal impacts. In: *The Impact of Global Warming on Texas*. [J. Schmandt, J. Clarkson, and G. R. North (eds.)]. University of Texas Press, Austin, TX, 318 pp.

Moore, W. S., 1996: Large groundwater inputs to coastal waters revealed by ^{226}Ra enrichments. *Nature*, **380**(6575), 612-614, doi: 10.1038/380612a0.

Moosdorf, N., J. Hartmann, R. Lauerwald, B. Hagedorn, and S. Kempe, 2011: Atmospheric CO_2 consumption by chemical weathering in North America. *Geochimica et Cosmochimica Acta*, **75**(24), 7829-7854, doi: 10.1016/j.gca.2011.10.007.

Morris, J. T., D. C. Barber, J. C. Callaway, R. Chambers, S. C. Hagen, C. S. Hopkinson, B. J. Johnson, P. Megonigal, S. C. Neubauer, T. Troxler, and C. Wigand, 2016: Contributions of organic and inorganic matter to sediment volume and accretion in tidal wetlands at steady state. *Earths Future*, **4**(4), 110-121, doi: 10.1002/2015EF000334.

Moseman-Valtierra, S., O. I. Abdul-Aziz, J. Tang, K. S. Ishtiaq, K. Morkeski, J. Mora, R. K. Quinn, R. M. Martin, K. Egan, E. Q. Brannon, J. Carey, and K. D. Kroeger, 2016: Carbon dioxide fluxes reflect plant zonation and belowground biomass in a coastal marsh. *Ecosphere*, **7**(11), e01560, doi: 10.1002/ecs2.1560.

Moseman-Valtierra, S., R. Gonzalez, K. D. Kroeger, J. Tang, W. C. Chao, J. Crusius, J. Bratton, A. Green, and J. Shelton, 2011: Short-term nitrogen additions can shift a coastal wetland from a sink to a source of N_2O. *Atmospheric Environment*, **45**(26), 4390-4397, doi: 10.1016/j.atmosenv.2011.05.046.

Mueller, P., R. N. Hager, J. E. Meschter, T. J. Mozdzer, J. A. Langley, K. Jensen, and J. P. Megonigal, 2016: Complex invader-ecosystem interactions and seasonality mediate the impact of non-native phragmites on CH_4 emissions. *Biological Invasions*, **18**(9), 2635-2647, doi: 10.1007/s10530-016-1093-6.

Müller, P. J., and E. Suess, 1979: Productivity, sedimentation rate, and sedimentary organic matter in the oceans—I. Organic carbon preservation. *Deep Sea Research Part A. Oceanographic Research Papers*, **26**(12), 1347-1362, doi: 10.1016/0198-0149(79)90003-7.

Munoz-Anderson, M. A., J. R. Lara-Lara, S. Alvarez-Borrego, C. Bazan-Guzman, and M. de la Cruz-Orozco, 2015: Water-air carbon fluxes in the coastal upwelling zone off Northern Baja California. *Ciencias Marinas*, **41**(2), 157-168, doi: 10.7773/cm.v41i2.2484.

Nahlik, A. M., and M. S. Fennessy, 2016: Carbon storage in US wetlands. *Nature Communications*, **7**, 13835, doi: 10.1038/ncomms13835.

Najjar, R. G., M. Herrmann, R. Alexander, E. W. Boyer, D. J. Burdige, D. Butman, W. J. Cai, E. A. Canuel, R. F. Chen, M. A. M. Friedrichs, R. A. Feagin, P. C. Griffith, A. L. Hinson, J. R. Holmquist, X. Hu, W. M. Kemp, K. D. Kroeger, A. Mannino, S. L. McCallister, W. R. McGillis, M. R. Mulholland, C. H. Pilskaln, J. Salisbury, S. R. Signorini, P. St-Laurent, H. Tian, M. Tzortziou, P. Vlahos, Z. A. Wang, and R. C. Zimmerman, 2018: Carbon budget of tidal wetlands, estuaries, and shelf waters of Eastern North America. *Global Biogeochemical Cycles*, **32**(3), 389-416, doi: 10.1002/2017gb005790.

NASA, 2017a: National Aeronautics and Space Administration, Blue Carbon Monitoring System. [https://water.usgs.gov/nrp/blue-carbon/nasa-blue-cms/]

NASA, 2017b: National Aeronautics and Space Administration, Wetland-Estuary Transports and Carbon Budgets (WETCARB) project. [https://cce.nasa.gov/cgi-bin/cce/cce_profile.pl?project_group_id=3165]

Nellemann, C., E. Corcoran, C. Duarte, L. Vales, C. Fonseca, and G. Grimsditch, 2009: *Blue Carbon - The Role of Healthy Oceans in Binding Carbon.* GRID-Arendal: United Nations Environment Programme. [https://www.grida.no/publications/145]

Neubauer, S. C., R. B. Franklin, and D. J. Berrier, 2013: Saltwater intrusion into tidal freshwater marshes alters the biogeochemical processing of organic carbon. *Biogeosciences*, **10**(12), 8171-8183, doi: 10.5194/bg-10-8171-2013.

Neubauer, S. C., W. D. Miller, and I. C. Anderson, 2000: Carbon cycling in a tidal freshwater marsh ecosystem: A carbon gas flux study. *Marine Ecology Progress Series*, **199**, 13-30.

NOAA, 1985: *National Estuarine Inventory Data Atlas. Volume 1: Physical and Hydrologic Characteristics.* National Ocean Service, National Oceanic and Atmospheric Administration. [https://www.greateratlantic.fisheries.noaa.gov/habitat/publications/national_estuarine_inventory_-_ne_region1.pdf]

NOAA, 2015: *Land Cover Atlas*. Coastal Change Analysis Program (C-CAP) Regional Land Cover. National Oceanic and Atmospheric Administration, Office for Coastal Management. Charleston, SC, NOAA Office for Coastal Management. [https://www.coast.noaa.gov/ccapftp]

NOAA, 2017: National Oceanic and Atmospheric Administration Office for Coastal Management, Digital Coast. [https://coast.noaa.gov/digitalcoast/]

Orton, P. M., W. R. McGillis, and C. J. Zappa, 2010: Sea breeze forcing of estuary turbulence and air-water CO_2 exchange. *Geophysical Research Letters*, **37**(13), doi: 10.1029/2010gl043159.

Osland, M. J., A. C. Spivak, J. A. Nestlerode, J. M. Lessmann, A. E. Almario, P. T. Heitmuller, M. J. Russell, K. W. Krauss, F. Alvarez, D. D. Dantin, J. E. Harvey, A. S. From, N. Cormier, and C. L. Stagg, 2012: Ecosystem development after mangrove wetland creation: Plant–soil change across a 20-year chronosequence. *Ecosystems*, **15**(5), 848-866, doi: 10.1007/s10021-012-9551-1.

Ouyang, X., and S. Y. Lee, 2014: Updated estimates of carbon accumulation rates in coastal marsh sediments. *Biogeosciences*, **11**(18), 5057-5071, doi: 10.5194/bg-11-5057-2014.

Packalen, M. S., S. A. Finkelstein, and J. W. McLaughlin, 2014: Carbon storage and potential methane production in the Hudson Bay lowlands since mid-Holocene peat initiation. *Nature Communications*, **5**, 4078, doi: 10.1038/ncomms5078.

Palaima, A., 2012: *Ecology, Conservation, and Restoration of Tidal Marshes: The San Francisco Estuary.* University of California Press, 288 pp.

Paulsen M.-L., A. J. Andersson, L. Aluwihare, T. Cyronak, S. D'Angelo, C. Davidson, H. Elwany, S. Giddings, M. Harvey, H. Page, M. Porrachia, and S. Schroeter, 2017: Temporal changes in seawater carbonate chemistry and carbon export from a Southern California estuary. *Estuaries and Coasts*, **41**(4), 1050-1068, doi: 10.1007/s12237-017-0345-8.

Pendleton, L., D. C. Donato, B. C. Murray, S. Crooks, W. A. Jenkins, S. Sifleet, C. Craft, J. W. Fourqurean, J. B. Kauffman, N. Marba, P. Megonigal, E. Pidgeon, D. Herr, D. Gordon, and A. Baldera, 2012: Estimating global "blue carbon" emissions from conversion and degradation of vegetated coastal ecosystems. *PLOS One*, **7**(9), e43542, doi: 10.1371/journal.pone.0043542.

Perillo, G. M. E., and M. C. Picollo, 1995: Definition and geomorphologic classification of estuaries. In: *Introduction to Estuary Studies*. [M. C. Picollo, G. M. E. Perillo, and Pino-Quivira (eds.)].

Peteet, D., D. Pederson, D. Kurdyla, and T. Guilderson, 2006: Hudson River paleoecology from marshes. In: *Hudson River Fishes and their Environment.* [J. R. Waldman, K. E. Limburg, and D. Strayer (eds.)]. American Fisheries Society Monograph 113-128 pp.

Pfeiffer-Herbert, A. S., F. G. Prahl, B. Hales, J. A. Lerczak, S. D. Pierce, and M. D. Levine, 2016: High resolution sampling of methane transport in the Columbia River near-field plume: Implications for sources and sinks in a river-dominated estuary. *Limnology and Oceanography*, **61**(S1), S204-S220, doi: 10.1002/lno.10221.

Pickart, R. S., L. M. Schulze, G. W. K. Moore, M. A. Charette, K. R. Arrigo, G. van Dijken, and S. L. Danielson, 2013: Long-term trends of upwelling and impacts on primary productivity in the Alaskan Beaufort Sea. *Deep Sea Research Part I: Oceanographic Research Papers*, **79**, 106-121, doi: 10.1016/j.dsr.2013.05.003.

Plafker, G., 1965: Tectonic deformation associated with the 1964 Alaska earthquake: The earthquake of 27 March 1964 resulted in observable crustal deformation of unprecedented areal extent. *Science*, **148**(3678), 1675-1687, doi: 10.1126/science.148.3678.1675.

Poffenbarger, H. J., B. A. Needelman, and J. P. Megonigal, 2011: Salinity influence on methane emissions from tidal marshes. *Wetlands*, **31**(5), 831-842, doi: 10.1007/s13157-011-0197-0.

Premuzic, E. T., C. M. Benkovitz, J. S. Gaffney, and J. J. Walsh, 1982: The nature and distribution of organic matter in the surface sediments of world oceans and seas. *Organic Geochemistry*, **4**(2), 63-77, doi: 10.1016/0146-6380(82)90009-2.

Pritchard, D. W., 1967: What is an estuary: Physical viewpoint. In: *Estuaries.* [G. H. Lauff (ed.)]. American Association for the Advancement of Science, Washington, D.C. Publication No. 83, pp. 3-5.

Project Geocarbon, 2017: Operational global carbon observing system. [http://www.geocarbon.net/images/phocadownload/geocarbon_deliverable3.1.pdf]

Raymond, P. A., and C. S. Hopkinson, 2003: Ecosystem modulation of dissolved carbon age in a temperate marsh-dominated estuary. *Ecosystems*, **6**(7), 694-705, doi: 10.1007/s10021-002-0213-6.

Raymond, P. A., and J. E. Bauer, 2001: Use of ^{14}C and ^{13}C natural abundances for evaluating riverine, estuarine, and coastal DOC and POC sources and cycling: A review and synthesis. *Organic Geochemistry*, **32**(4), 469-485, doi: 10.1016/s0146-6380(00)00190-x.

Raymond, P. A., J. E. Bauer, and J. J. Cole, 2000: Atmospheric CO_2 evasion, dissolved inorganic carbon production, and net heterotrophy in the York River estuary. *Limnology and Oceanography*, **45**(8), 1707-1717, doi: 10.4319/lo.2000.45.8.1707.

Raymond, P. A., N. H. Oh, R. E. Turner, and W. Broussard, 2008: Anthropogenically enhanced fluxes of water and carbon from the Mississippi River. *Nature*, **451**(7177), 449-452, doi: 10.1038/nature06505.

Redfield, A. C., 1967: The ontogeny of a salt marsh estuary. In: *Estuaries.* [G. H. Lauff (ed.)]. American Association for the Advancement of Science, Washington, D.C. Publication No. 83.

Regnier, P., P. Friedlingstein, P. Ciais, F. T. Mackenzie, N. Gruber, I. A. Janssens, G. G. Laruelle, R. Lauerwald, S. Luyssaert, A. J. Andersson, S. Arndt, C. Arnosti, A. V. Borges, A. W. Dale, A. Gallego-Sala, Y. Goddéris, N. Goossens, J. Hartmann, C. Heinze, T. Ilyina, F. Joos, D. E. LaRowe, J. Leifeld, F. J. R. Meysman, G. Munhoven, P. A. Raymond, R. Spahni, P. Suntharalingam, and M. Thullner, 2013: Anthropogenic perturbation of the carbon fluxes from land to ocean. *Nature Geoscience*, **6**(8), 597-607, doi: 10.1038/ngeo1830.

Reid, M. C., R. Tripathee, K. V. R. Schäfer, and P. R. Jaffé, 2013: Tidal marsh methane dynamics: Difference in seasonal lags in emissions driven by storage in vegetated versus unvegetated sediments. *Journal of Geophysical Research: Biogeosciences*, **118**(4), 1802-1813, doi: 10.1002/2013JG002438.

Reimer, J. J., R. Vargas, S. V. Smith, R. Lara-Lara, G. Gaxiola-Castro, J. Martín Hernández-Ayón, A. Castro, M. Escoto-Rodriguez, and J. Martínez-Osuna, 2013: Air-sea CO_2 fluxes in the near-shore and intertidal zones influenced by the California current. *Journal of Geophysical Research: Oceans*, **118**(10), 4795-4810, doi: 10.1002/jgrc.20319.

Reimnitz, E., 1966: *Late Quaternary History and Sedimentation of the Copper River Delta and Vicinity*, Alaska. Ph.D. Thesis, University of California San Diego, CA, 160 pp.

Ren, W., H. Tian, B. Tao, J. Yang, S. Pan, W. J. Cai, S. E. Lohrenz, R. He, and C. S. Hopkinson, 2015: Large increase in dissolved inorganic carbon flux from the Mississippi River to Gulf of Mexico due to climatic and anthropogenic changes over the 21st century. *Journal of Geophysical Research: Biogeosciences*, **120**(4), 724-736, doi: 10.1002/2014JG002761.

Ribas-Ribas, M., J. M. Hernández-Ayón, V. F. Camacho-Ibar, A. Cabello-Pasini, A. Mejia-Trejo, R. Durazo, S. Galindo-Bect, A. J. Souza, J. M. Forja, and A. Siqueiros-Valencia, 2011: Effects of upwelling, tides and biological processes on the inorganic carbon system of a coastal lagoon in Baja, California. *Estuarine, Coastal and Shelf Science*, **95**(4), 367-376, doi: 10.1016/j.ecss.2011.09.017.

Saintilan, N., N. C. Wilson, K. Rogers, A. Rajkaran, and K. W. Krauss, 2014: Mangrove expansion and salt marsh decline at mangrove poleward limits. *Global Change Biology*, **20**(1), 147-157, doi: 10.1111/gcb.12341.

Salisbury, J., M. Green, C. Hunt, and J. Campbell, 2008: Coastal acidification by rivers: A threat to shellfish? *Eos, Transactions American Geophysical Union*, **89**(50), 513-513, doi: 10.1029/2008eo500001.

Sallenger Jr, A. H., K. S. Doran, and P. A. Howd, 2012: Hotspot of accelerated sea-level rise on the Atlantic coast of North America. *Nature Climate Change*, **2**, 884, doi: 10.1038/nclimate1597.

Sanderman, J., T. Hengl, G. Fiske, K. Solvik, M. F. Adame, L. Benson, J. J. Bukoski, P. Carnell, M. Cifuentes-Jara, D. Donato, C. Duncan, E. M. Eid, P. zu Ermgassen, C. J. E. Lewis, P. I. Macreadie, L. Glass, S. Gress, S. L. Jardine, T. G. Jones, E. N. Nsombo, M. M. Rahman, C. J. Sanders, M. Spalding, and E. Landis, 2018: A global map of mangrove forest soil carbon at 30 m spatial resolution. *Environmental Research Letters*, **13**(5), 055002.

Sansone, F. J., T. M. Rust, and S. V. Smith, 1998: Methane distribution and cycling in Tomales Bay, California. *Estuaries*, **21**(1), 66, doi: 10.2307/1352547.

Schäfer, K. V. R., R. Tripathee, F. Artigas, T. H. Morin, and G. Bohrer, 2014: Carbon dioxide fluxes of an urban tidal marsh in the Hudson-Raritan Estuary. *Journal of Geophysical Research: Biogeosciences*, **119**(11), 2065-2081, doi: 10.1002/2014jg002703.

Schepers, L., M. Kirwan, G. Guntenspergen, and S. Temmerman, 2017: Spatio-temporal development of vegetation die-off in a submerging coastal marsh. *Limnology and Oceanography*, **62**(1), 137-150, doi: 10.1002/lno.10381.

Schlesinger, W. H., 2009: On the fate of anthropogenic nitrogen. *Proceedings of the National Academy of Sciences USA*, **106**(1), 203-208, doi: 10.1073/pnas.0810193105.

Schubauer, J. P., and C. S. Hopkinson, 1984: Above- and below-ground emergent macrophyte production and turnover in a coastal marsh ecosystem, Georgia. *Limnology and Oceanography*, **29**(5), 1052-1065, doi: 10.4319/lo.1984.29.5.1052.

Segarra, K. E. A., V. Samarkin, E. King, C. Meile, and S. B. Joye, 2013: Seasonal variations of methane fluxes from an unvegetated tidal freshwater mudflat (Hammersmith Creek, GA). *Biogeochemistry*, **115**(1-3), 349-361, doi: 10.1007/s10533-013-9840-6.

Selmants, P. C., C. P. Giardina, J. D. Jacobi, and Z. Zhu, 2017: *Baseline and Projected Future Carbon Storage and Carbon Fluxes in Ecosystems of Hawai'i.* U.S. Geological Survey Professional Paper 1834, 134 pp, doi: 10.3133/pp1834.

Shih, J. S., R. Alexander, R. A. Smith, E. W. Boyer, G. E. Schwarz, and S. Chung, 2010: *An Initial Sparrow Model of Land Use and In-Stream Controls on Total Organic Carbon in Streams of the Conterminous United States.* U.S. Geological Survey Open File Report 1276. [https://pubs.usgs.gov/of/2010/1276/of2010-1276.pdf]

Smith, R. W., T. S. Bianchi, M. Allison, C. Savage, and V. Galy, 2015: High rates of organic carbon burial in fjord sediments globally. *Nature Geoscience*, **8**(6), 450-453, doi: 10.1038/ngeo2421.

Smith, S. V., and J. T. Hollibaugh, 1997: Annual cycle and interannual variability of ecosystem metabolism in a temperate climate embayment. *Ecological Monographs*, **67**(4), 509-533, doi: 10.1890/0012-9615(1997)067[0509:acaivo]2.0.co;2.

Son, S., M. Wang, and L. W. Harding, 2014: Satellite-measured net primary production in the Chesapeake Bay. *Remote Sensing of Environment*, **144**, 109-119, doi: 10.1016/j.rse.2014.01.018.

Spalding, M., M. Kainuma, and L. Collins, 2010: *World Atlas of Mangroves.* Earthscan, 319 pp. [https://books.google.com/books?id=wzSCkulW9SQC]

Steinberg, P. D., M. T. Brett, J. S. Bechtold, J. E. Richey, L. M. Porensky, and S. N. Smith, 2010: The influence of watershed characteristics on nitrogen export to and marine fate in Hood Canal, Washington, USA. *Biogeochemistry*, **106**(3), 415-433, doi: 10.1007/s10533-010-9521-7.

Stets, E., and R. Striegl, 2012: Carbon export by rivers draining the conterminous United States. *Inland Waters*, **2**(4), 177-184, doi: 10.5268/iw-2.4.510.

Swarzenski, C. M., T. W. Doyle, B. Fry, and T. G. Hargis, 2008: Biogeochemical response of organic-rich freshwater marshes in the Louisiana Delta Plain to chronic river water influx. *Biogeochemistry*, **90**(1), 49-63, doi: 10.1007/s10533-008-9230-7.

TCEQ, 2017: Texas Commission on Environmental Quality. [https://www.tceq.texas.gov/waterquality/]

Thilenius, J. F., 1990: Woody plant succession on earthquake-uplifted coastal wetlands of the Copper River Delta, Alaska. *Forest Ecology and Management*, **33-34**, 439-462, doi: 10.1016/0378-1127(90)90209-t.

Thom, R. M., 1992: Accretion rates of low intertidal salt marshes in the Pacific Northwest. *Wetlands*, **12**(3), 147-156, doi: 10.1007/bf03160603.

Thorhaug, A., H. M. Poulos, J. Lopez-Portillo, T. C. W. Ku, and G. P. Berlyn, 2017: Seagrass blue carbon dynamics in the Gulf of Mexico: Stocks, losses from anthropogenic disturbance, and gains through seagrass restoration. *Science of the Total Environment*, **605-606**, 626-636, doi: 10.1016/j.scitotenv.2017.06.189.

Tian, H., W. Ren, J. Yang, B. Tao, W.-J. Cai, S. E. Lohrenz, C. S. Hopkinson, M. Liu, Q. Yang, C. Lu, B. Zhang, K. Banger, S. Pan, R. He, and Z. Xue, 2015: Climate extremes dominating seasonal and interannual variations in carbon export from the Mississippi River Basin. *Global Biogeochemical Cycles*, **29**(9), 1333-1347, doi: 10.1002/2014gb005068.

Tian, X., B. Sohngen, J. B. Kim, S. Ohrel, and J. Cole, 2016: Global climate change impacts on forests and markets. *Environmental Research Letters*, **11**(3), 035011, doi: 10.1088/1748-9326/11/3/035011.

Troche-Souza, C., M. T. Rodríguez-Zúñiga, S. Velázquez-Salazar, L. Valderrama-Landeros, E. Villeda-Chávez, A. Alcántara-Maya, B. Vázquez-Balderas, M. I. Cruz-López y R. Ressl, 2016: *Manglares de México: Extensión, Distribución y Monitoreo (1970/1980 - 2015).* Comisión Nacional para el Conocimiento y Uso de la Biodiversidad, México. D. F., México.

Troxler, T. G., J. G. Barr, J. D. Fuentes, V. Engel, G. Anderson, C. Sanchez, D. Lagomasino, R. Price, and S. E. Davis, 2015: Component-specific dynamics of riverine mangrove CO_2 efflux in the Florida Coastal Everglades. *Agricultural and Forest Meteorology*, **213**, 273-282, doi: 10.1016/j.agrformet.2014.12.012.

U.S. EPA, 2016: *Inventory of U.S. Greenhouse Gas Emissions and Sinks: 1990-2014.* U.S. Environmental Protection Agency. EPA 430-R-16-002. [https://www.epa.gov/sites/production/files/2016-04/documents/us-ghg-inventory-2016-main-text.pdf]

U.S. EPA, 2017: *Avoiding and Reducing Long-Term Risks of Climate Change: A Technical Report for the Fourth National Climate Assessment.* U.S. Environmental Protection Agency. EPA 430-R-17-00.

USFWS NWI, 2017. *U.S. Fish and Wildlife Service National Wetlands Inventory Product Summary*. U.S. Fish and Wildlife Service. [https://www.fws.gov/wetlands/Data/Wetlands-Product-Summary.html]

USGS, 2018: *U.S. Geological Survey Coastal Change Hazards Portal*. U.S. Geological Survey. [https://marine.usgs.gov/coastalchange-hazardsportal]

USGS, 2017: *U.S. Geological Survey Land Change Monitoring, Assessment, and Projection Initiative*. U.S. Geological Survey. [https://eros.usgs.gov/doi-remote-sensing-activities/2015/land-change-monitoring-assessment-and-projection]

Valderrama Landeros L. H., M. T. Rodríguez-Zúñiga, C. Troche Souza, S. Velázquez Salazar, E. Villeda Chávez, J. A. Alcántara Maya, B. Vázquez Balderas, M. I. Cruz López, and R. Ressl, 2017: Manglares de México: Actualización y exploración de los datos del sistema de monitoreo 1970/1980-2015. Comisión Nacional para el Conocimiento y Uso de la Biodiversidad. Ciudad de México. [http://www.biodiversidad.gob.mx/ecosistemas/manglares2013/pdf/manglares_mexico_2015.pdf]

van Dam, B. R., J. R. Crosswell, I. C. Anderson, and H. W. Paerl, 2018: Watershed-scale drivers of air-water CO_2 exchanges in two lagoonal North Carolina (USA) estuaries. *Journal of Geophysical Research: Biogeosciences*, **123**(1), 271-287, doi: 10.1002/2017JG004243.

van der Heide, T., E. H. van Nes, M. M. van Katwijk, H. Olff, and A. J. Smolders, 2011: Positive feedbacks in seagrass ecosystems: Evidence from large-scale empirical data. *PLOS One*, **6**(1), e16504, doi: 10.1371/journal.pone.0016504.

von Biela, V. R., C. E. Zimmerman, B. R. Cohn, and J. M. Welker, 2012: Terrestrial and marine trophic pathways support young-of-year growth in a nearshore Arctic fish. *Polar Biology*, **36**(1), 137-146, doi: 10.1007/s00300-012-1244-x.

Waldbusser, G. G., B. Hales, C. J. Langdon, B. A. Haley, P. Schrader, E. L. Brunner, M. W. Gray, C. A. Miller, and I. Gimenez, 2014: Saturation-state sensitivity of marine bivalve larvae to ocean acidification. *Nature Climate Change*, **5**(3), 273-280, doi: 10.1038/nclimate2479.

Walling, D. E., and B. W. Webb, 1983: Patterns of sediment yield. In: *Background to Palaeohydrology. A Perspective.* pp. 69-100.

Wang, Z. A., and W.-J. Cai, 2004: Carbon dioxide degassing and inorganic carbon export from a marsh-dominated estuary (the Duplin River): A marsh CO_2 pump. *Limnology and Oceanography*, **49**(2), 341-354, doi: 10.4319/lo.2004.49.2.0341.

Wang, Z. A., K. D. Kroeger, N. K. Ganju, M. E. Gonneea, and S. N. Chu, 2016: Intertidal salt marshes as an important source of inorganic carbon to the coastal ocean. *Limnology and Oceanography*, **61**(5), 1916-1931, doi: 10.1002/lno.10347.

Ward, N. D., T. S. Bianchi, P. M. Medeiros, M. Seidel, J. E. Richey, R. G. Keil, and H. O. Sawakuchi, 2017: Where carbon goes when water flows: Carbon cycling across the aquatic continuum. *Frontiers in Marine Science*, **4**, doi: 10.3389/fmars.2017.00007.

Washington State Blue Ribbon Panel on Ocean Acidification, 2012: *Ocean Acidification: From Knowledge to Action, Washington State's Strategic Response.* Publication no. 12-01-015. [H. Adelsman and L. W. Binder (eds.)]. Washington Department of Ecology, Olympia, Washington. [https://fortress.wa.gov/ecy/publications/documents/1201015.pdf]

Watson, E. B., 2004: Changing elevation, accretion, and tidal marsh plant assemblages in a south San Francisco bay tidal marsh. *Estuaries*, **27**(4), 684-698, doi: 10.1007/bf02907653.

Watson, E. B., C. Wigand, E. W. Davey, H. M. Andrews, J. Bishop, and K. B. Raposa, 2017: Wetland loss patterns and inundation-productivity relationships prognosticate widespread salt marsh loss for southern New England. *Estuaries and Coasts*, **40**(3), 662-681, doi: 10.1007/s12237-016-0069-1.

Weston, N. B., S. C. Neubauer, D. J. Velinsky, and M. A. Vile, 2014: Net ecosystem carbon exchange and the greenhouse gas balance of tidal marshes along an estuarine salinity gradient. *Biogeochemistry*, **120**(1-3), 163-189, doi: 10.1007/s10533-014-9989-7.

Wheatcroft, R. A., M. A. Goñ i, J. A. Hatten, G. B. Pasternack, and J. A. Warrick, 2010: The role of effective discharge in the ocean delivery of particulate organic carbon by small, mountainous river systems. *Limnology and Oceanography*, **55**(1), 161-171, doi: 10.4319/lo.2010.55.1.0161.

Whiting, G. J., and J. P. Chanton, 2001: Greenhouse carbon balance of wetlands: Methane emission versus carbon sequestration. *Tellus B*, **53**(5), 521-528, doi: 10.1034/j.1600-0889.2001.530501.x.

Wilson, B. J., B. Mortazavi, and R. P. Kiene, 2015: Spatial and temporal variability in carbon dioxide and methane exchange at three coastal marshes along a salinity gradient in a northern Gulf of Mexico estuary. *Biogeochemistry*, **123**(3), 329-347, doi: 10.1007/s10533-015-0085-4.

Wollast R., 1991: The coastal carbon cycle: Fluxes, sources and sinks. In: *Ocean Margin Processes in Global Change*. [R. F. C. Mantoura, J.-M. Martin, and R. Wollast (eds.)]. J. Wiley & Sons, Chichester, pp. 365–382.

Yao, H., and X. Hu, 2017: Responses of carbonate system and CO_2 flux to extended drought and intense flooding in a semiarid subtropical estuary. *Limnology and Oceanography*, **62**(S1), S112-S130, doi: 10.1002/lno.10646.

Ye, F., Y. J. Zhang, H. V. Wang, M. A. M. Friedrichs, I. D. Irby, E. Alteljevich, A. Valle-Levinson, Z. Wang, H. Huang, J. Shen, and J. Du, 2018: A 3D unstructured-grid model for Chesapeake Bay: Importance of bathymetry. *Ocean Modelling*, **127**, 16-39, doi: 10.1016/j.ocemod.2018.05.002.

Ye, F., Y. J. Zhang, M. A. M. Friedrichs, H. V. Wang, I. D. Irby, J. Shen, and Z. Wang, 2016: A 3D, cross-scale, baroclinic model with implicit vertical transport for the upper Chesapeake Bay and its tributaries. *Ocean Modelling*, **107**, 82-96, doi: 10.1016/j.ocemod.2016.10.004.

Zhang, J. Z., and C. J. Fischer, 2014: Carbon dynamics of Florida Bay: Spatiotemporal patterns and biological control. *Environmental Science and Technology*, **48**(16), 9161-9169, doi: 10.1021/es500510z.

Zhang, K., B. Thapa, M. Ross, and D. Gann, 2016: Remote sensing of seasonal changes and disturbances in mangrove forest: A case study from South Florida. *Ecosphere*, **7**(6), e01366, doi: 10.1002/ecs2.1366.

Appendix 15A
Supplemental Data Tables

Table 15A.1. Summary of North American Carbon Dioxide Exchange Between Tidal Wetlands and the Atmosphere (Net Ecosystem Exchange[a]) from Continuous Measurements[b]

System Name and Type	Location	EC/SC	Year	NEE (g C per m^2 per year)	Source
Pacific Coast					
Rush Ranch, Suisun Bay, brackish marsh	California	EC	2014–2015 2015–2016 2016–2017	14 –190 –222	Bergamaschi and Windham-Myers (2018)
Atlantic Coast					
Plum Island, salt marsh	Massachusetts	EC	2012 2013 2014	–255.6 –336.0 –279.6	Forbrich and Giblin (2015)
Waquoit Bay, salt marsh	Massachusetts	SC	2015	–160.0	Moseman-Valtierra et al. (2016)
Hudson-Raritan Estuary, restored salt marsh	New Jersey	EC	2009 2011 2012	984[c] –64.8 –309.6	Schäfer et al. (2014)
Hudson-Raritan Estuary, restored salt marsh	New Jersey	EC	2011–2012	–213.6	Artigas et al. (2015)
Delaware Bay, tidal fresh marsh	New Jersey	SC	2007 2008	–256.8 61.2	Weston et al. (2014)
Delaware Bay, oligohaline marsh	New Jersey	SC	2007 2008	93.6 –45.6	Weston et al. (2014)
Delaware Bay, mesohaline marsh	New Jersey	SC	2007 2008	–115.2 –171.6	Weston et al. (2014)
Fowling Point, salt marsh	Virginia	SC	2007	–129.6	Kathilankal et al. (2008)

Continued on next page

(Continued)

Table 15A.1. Summary of North American Carbon Dioxide Exchange Between Tidal Wetlands and the Atmosphere (Net Ecosystem Exchange[a]) from Continuous Measurements[b]

System Name and Type	Location	EC/SC	Year	NEE (g C per m^2 per year)	Source
Springfield Creek, tidal fresh marsh	South Carolina	SC	2009	–295.2	Neubauer et al. (2013)
Gulf of Mexico					
Pointe-aux-Chenes, brackish marsh	Louisiana	EC	2011	–337.2	Holm et al. (2016)
Salvador, tidal fresh marsh	Louisiana	EC	2011	170.4	Holm et al. (2016)
Florida Bay, mangrove	Florida	EC	2004 2005 2007 2008 2009	–1172.4 –1176 –823.2 –806.4 –926.4	Barr et al. (2010); Barr et al. (2012)
Mobile Bay, tidal fresh marsh	Alabama	SC	2011	893.4	Wilson et al. (2015)
Mobile Bay, brackish marsh	Alabama	SC	2011	517.8	Wilson et al. (2015)
Mobile Bay, salt marsh	Alabama	SC	2011	410.2	Wilson et al. (2015)

Notes

a) NEE, Net ecosystem exchange; g C, grams of carbon.

b) Continuous measurements: eddy covariance (EC) or static chamber (SC). Positive values = atmospheric carbon dioxide (CO_2) source. Negative values = atmospheric CO_2 sink. Annual estimate (mean) provided.

c) Mudflat habitat (very little data available in literature).

Table 15A.2. Tidal Wetland Methane Flux by Discrete Static Chamber Data or Continuous Eddy Covariance[a] Data

Site Name	Location	Year	EC/SC	Salinity (PSU[b])	CH_4 Flux (g C per m^2 per year)[c]	Reference
Atlantic Coast						
Upland edge High marsh Middle marsh Low marsh	New Brunswick	1993	SC	**23.5** **31.6** **33.7** **35.1**	1.0 0.2 0.2 0.2	Magenheimer et al. (1996)
Dipper Harbour Kouchibouguac	New Brunswick	2011–2012	SC	**23.7** **13.7**	0.1 0.0	Chmura et al. (2016)
Creek Bank High marsh Short *Spartina*	Virginia	1981–1983	SC	18.7 22.6 26.3	0.9 0.3 1.0	Bartlett et al. (1985)
Site 1 Site 2 Site 3	Virginia	1983–1984 1983–1984 1983–1984	SC SC SC	**5.1** **12.8** **16.6**	13.7 16.8 4.2	Bartlett et al. (1987)
Sweet Hall	Virginia	1996–1997	SC	0.25	72.0	Neubauer et al. (2000)
C_3 Ambient CO_2 C_4 Ambient CO_2	Maryland Maryland	1998–1999 1998–1999	SC SC	6.8 6.8	3.5 2.5	Marsh et al. (2005)
Tidal freshwater marsh Oligohaline marsh Mesohaline marsh	Delaware	2007 2008 2007 2008 2007 2008	SC	0.25 0.25 2.5 2.5 10 10	20.0 24.0 123.0 87.0 –5.0 –2.0	Weston et al. (2014)
Wildlife Barbados	Maryland Maryland	2008 2008	SC SC	11.6 12.9	23.0 24.0	Poffenbarger et al. (2011)

Continued on next page

(Continued)

Table 15A.2. Tidal Wetland Methane Flux by Discrete Static Chamber Data or Continuous Eddy Covariance[a] Data

Site Name	Location	Year	EC/SC	Salinity (PSU[b])	CH_4 Flux (g C per m^2 per year)[c]	Reference
Vegetated low marsh Mud flat	New Jersey	2012 2012	SC SC	**5** **5**	4.3 3.8	Reid et al., (2013)
Fox Creek Marsh Kirkpatrick Marsh	Maryland	2013–2014	SC	**10** **10** **10** **10** **10** **10**	79.1 3.9 0.8 10.1 3.4 2.3	Mueller et al. (2016)
GI Near Bank GI Far Bank UF Near Bank UF Far Bank	North Carolina	1990–1991	SC	0.25 0.25 0.25 0.25	6.2 4.3 3.8 2.6	Kelley et al. (1995)
Lower site Upper site	North Carolina	1994–1995	SC	0.25 0.25	1.0 1.4	Megonigal and Schlesinger (2002)
Upper Middle Lower	Georgia Georgia Georgia	2006–2007 2006–2007 2006–2007	SC SC SC	**0.2** **1.3** **4.7**	0.8 1.0 1.0	Krauss and Whitbeck (2011)
Georgia Coastal Ecosystems LTER[d]	Georgia	2008–2009	SC	1	69.8	Segarra et al. (2013)
Brookgreen Gardens	South Carolina	2009	SC	**0.05**	42.0	Neubauer et al. (2013)
Gulf of Mexico						
Fresh Brackish Salt Marsh	Louisiana	1980–1981	SC	0.4 1.8 18.1	160.0 73.0 4.3	DeLaune et al. (1983)

Continued on next page

(Continued)

Table 15A.2. Tidal Wetland Methane Flux by Discrete Static Chamber Data or Continuous Eddy Covariance[a] Data

Site Name	Location	Year	EC/SC	Salinity (PSU[b])	CH_4 Flux (g C per m^2 per year)[c]	Reference
Brackish marsh	Louisiana	2012	EC	9.15	10.4	Holm et al. (2016)
Freshwater marsh	Louisiana	2012	EC	0.23	47.3	Holm et al. (2016)
Freshwater marsh	Louisiana	2013	EC	0.23	46.2	Holm et al. (2016)
Brackish marsh	Louisiana	2012–2013	EC	9.15	11.1	Krauss et al. (2016)
Brackish marsh	Louisiana	2012–2013	SC	9.15	49.6	Krauss et al. (2016)
Freshwater marsh	Louisiana	2012–2013	EC	0.23	47.1	Krauss et al. (2016)
Freshwater marsh	Louisiana	2012–2013	SC	0.23	91.9	Krauss et al. (2016)
Week's Bay	Alabama	2012–2013	SC	**2.3**	7.9	Wilson et al. (2015)
Dog River	Alabama	2012–2013	SC	**4.7**	3.9	Wilson et al. (2015)
Dauphin Island	Alabama	2012–2013	SC	**20.7**	4.3	Wilson et al. (2015)

Notes

a) CH_4, methane; CO_2, carbon dioxide; SC, static chamber; EC, eddy covariance; g C, grams of carbon.

b) Salinity values in bold indicate porewater salinity; otherwise, channel salinity is reported (where PSU = practical salinity units). When salinity was not reported for tidal freshwater wetlands, a value of 0.25 was assigned, which represents the midpoint of their salinity range (0 to 0.5) by definition.

c) Positive values = atmospheric CH_4 source. Negative values = atmospheric CH_4 sink. Annual estimate provided.

d) LTER, Long-term ecological research.

Table 15A.3. Estuarine Carbon Dioxide Outgassing (Emissions) for the U.S. Pacific Coast, Atlantic Coast,[a] and Gulf of Mexico Regions[b,c]

System Name	Location	Subregion	Source	CO_2 Flux (g C per m^2 per year)[c]	CO_2 Flux Integral (Tg C per year)
Pacific Coast: Northwest					
Columbia River	Oregon, WA	Northwest	Evans et al. (2012)	12	NA[d]
Atlantic Coast: Gulf of Maine (GOM) Subregion[a]					
Bellamy Estuary	Massachusetts, USA	GOM	Hunt et al. (2011)	55	
Cocheco Estuary	Massachusetts, USA	GOM	Hunt et al. (2011)	44	
Great Bay	Massachusetts, USA	GOM	Hunt et al. (2011)	43	
Kennebec Estuary	Massachusetts, USA	GOM	Hunt et al. (2014)	30	
Little Bay	Massachusetts, USA	GOM	Hunt et al. (2011)	48	
Oyster Estuary	Massachusetts, USA	GOM	Hunt et al. (2011)	48	
Parker River	Massachusetts, USA	GOM	Raymond and Hopkinson (2003)	13	
			Mean	**40**	**0.22**
			Standard error	**5**	**0.03**
Atlantic Coast: Mid-Atlantic Bight (MAB) Subregion[a]					
Delaware River	Delaware/ New Jersey, USA	MAB	Joesoef et al. (2015)	29	
York River	Virginia, USA	MAB	Raymond et al. (2000)	67	
			Mean	**48**	**1.0**
			Standard error	**19**	**0.4**
Atlantic Coast: South Atlantic Bight (SAB) Subregion[a]					
Altamaha Sound	Georgia, USA	SAB	Jiang et al. (2008)	322	
Doboy Sound	Georgia, USA	SAB	Jiang et al. (2008)	143	
Duplin River	Georgia, USA	SAB	Wang and Cai (2004)	256	
Neuse River	N. Carolina, USA	SAB	Crosswell et al. (2012); Crosswell et al. (2014)	–68	
Pamlico Sound	N. Carolina, USA	SAB	Crosswell et al. (2014)	–180	
Sapelo Sound	Georgia, USA	SAB	Jiang et al. (2008)	126	

Continued on next page

(Continued)

Table 15A.3. Estuarine Carbon Dioxide Outgassing (Emissions) for the U.S. Pacific Coast, Atlantic Coast,[a] and Gulf of Mexico Regions[b,c]

System Name	Location	Subregion	Source	CO_2 Flux (g C per m^2 per year)[c]	CO_2 Flux Integral (Tg C per year)
Satilla River	Georgia, USA	SAB	Cai and Wang (1998)	510	
			Mean	**158**	**1.9**
			Standard error	**88**	**1.1**
Atlantic Coast Totals					
			Mean	**82**	**3.1**
			Standard error	**30**	**1.1**
Gulf of Mexico (GMx)					
Atchafalaya River	Louisiana, USA	GMx	Huang et al. (2015)	504	
Florida Bay	Florida, USA	GMx	Zhang and Fischer (2014)	47	
Mission-Aransas Estuary	Texas, USA	GMx	Yao and Hu (2017)	149	
Mississippi River	Louisiana, USA	GMx	Huang et al. (2015)	444	
Shark River	Florida, USA	GMx	Kone and Borges (2008)	192	
Terrebonne Bay	Louisiana, USA	GMx	Huang et al. (2015)	–4	
			Mean	**222**	**6.8**
			Standard error	**85**	**2.6**
Atlantic Coast and Gulf of Mexico Totals					
			Mean		**9.9**
			Standard error		**2.8**

Notes

a) The Atlantic Coast is subdivided into three subregions: Gulf of Maine, Mid-Atlantic Bight, and South Atlantic Bight.

b) Positive values = atmospheric CO_2 source; negative values = atmospheric CO_2 sink. A spatially representative annual CO_2 flux integral is not calculated for the Pacific Coast due to the presence of only one study and limited seasonal sampling.

c) CO_2, carbon dioxide; g C, grams of carbon; Tg C, teragrams of carbon.

d) NA (or blank): Not assessed.